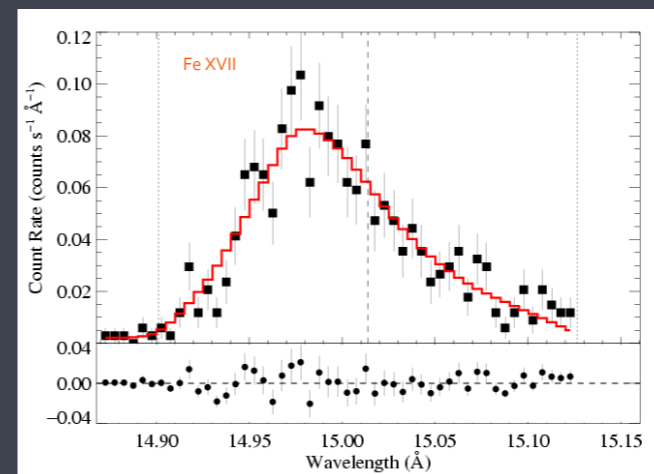
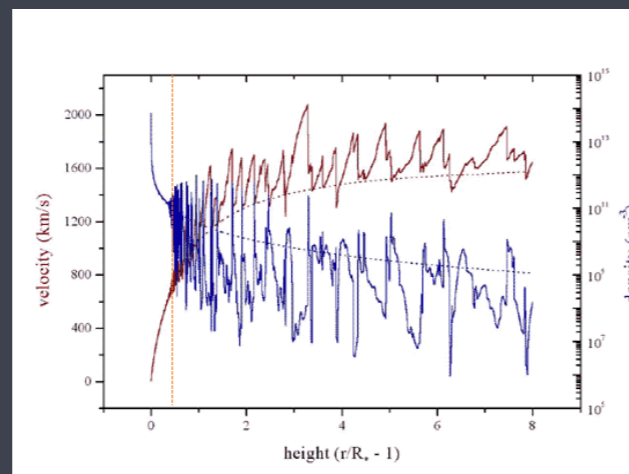


X-rays from the Winds of Massive Stars

David Cohen
Swarthmore College

with Stan Owocki (U. Delaware), Maurice Leutenegger (GSFC), Jon Sundqvist (Leuven),
Véronique Petit (Florida Tech), Gregg Wade (RMC), Marc Gagné (West Chester University)
and
Emma Wollman (Swarthmore '09; JPL), Roban Kramer (Swarthmore '03), James MacArthur
(Swarthmore '11; Stanford), Jackie Pezzato (Swarthmore '17)



Stellar surface temperatures range from
3000 to 50,000 K : red to blue



red stars are low mass and blue ones are massive



Basic properties of massive stars - O stars

mass $\sim 50 M_{\text{sun}}$

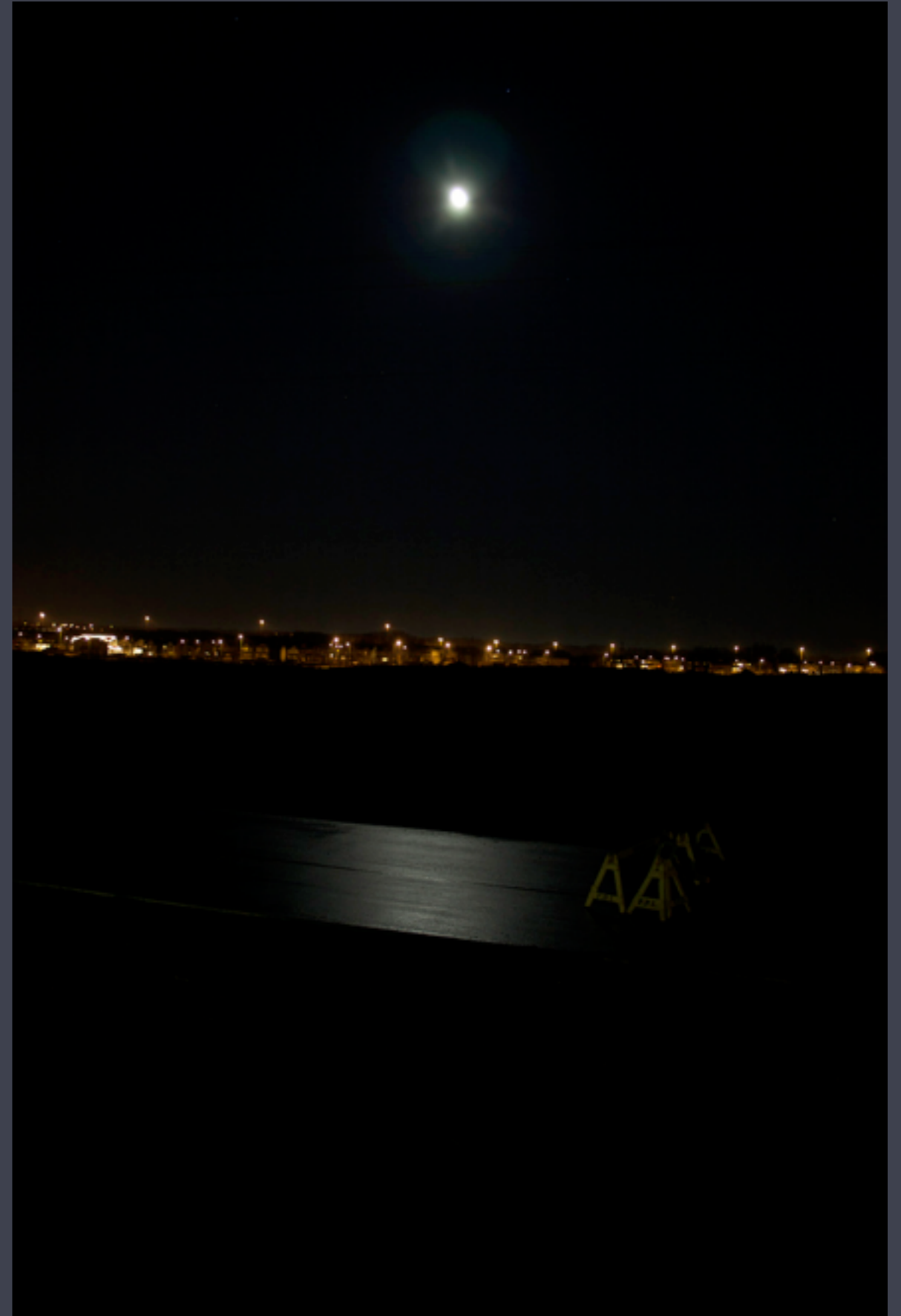
luminosity $\sim 10^6 L_{\text{sun}}$ (Watts of radiated power)

surface temperature $\sim 45,000 \text{ K} \sim 8 T_{\text{sun}}$

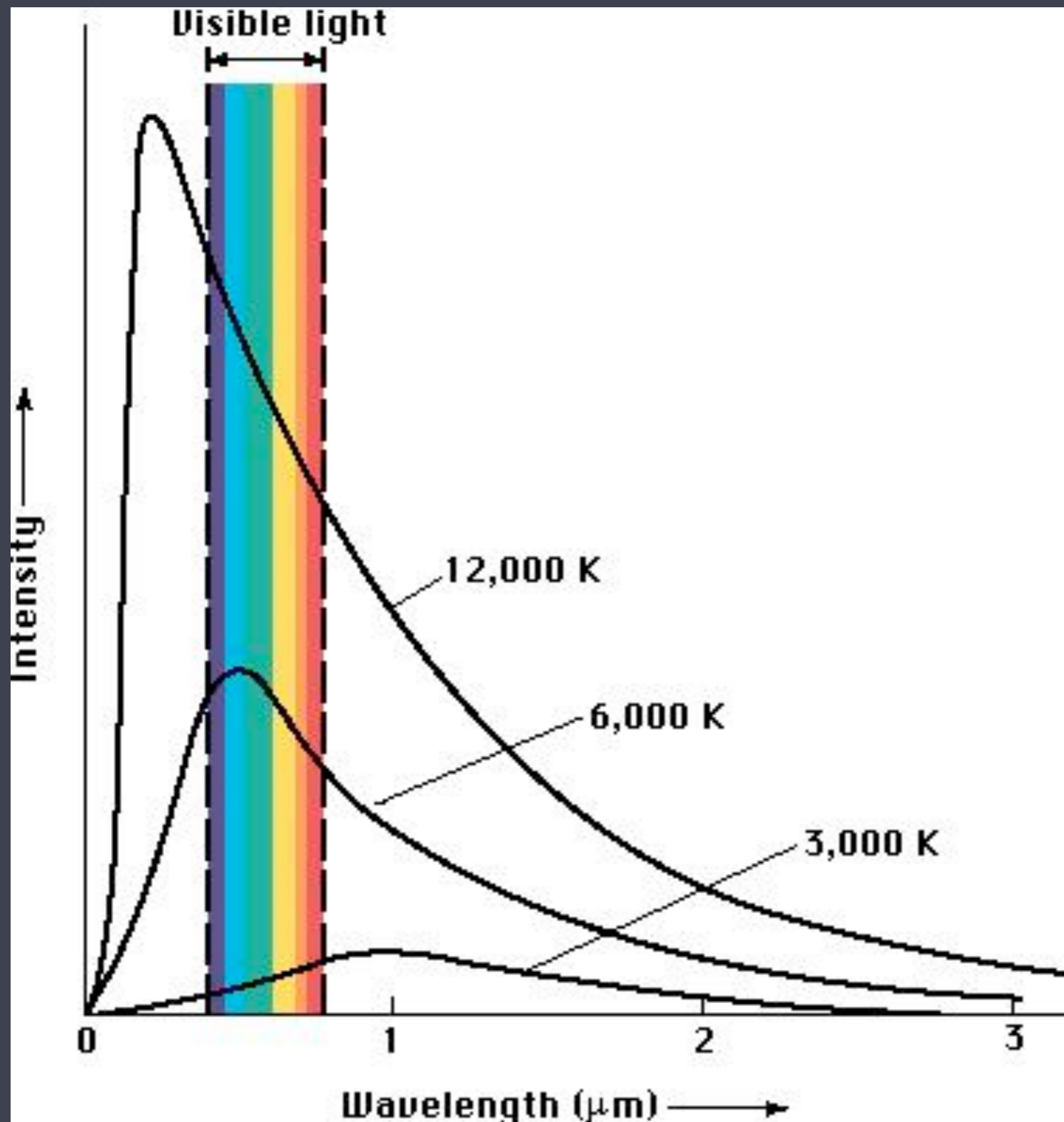
zeta Ori :
brightest O
star in the sky



Sun and full Moon - factor of a million (10^6) in brightness



Star's surface emission is basically blackbody



above $T \sim 10,000 \text{ K}$
most of a star's
emission is in the UV

O stars are even more
extreme: $T > 30,000 \text{ K}$

even so, no X-ray
emission from the
photospheres
(surfaces) of even the
hottest stars

cool stars

vs.

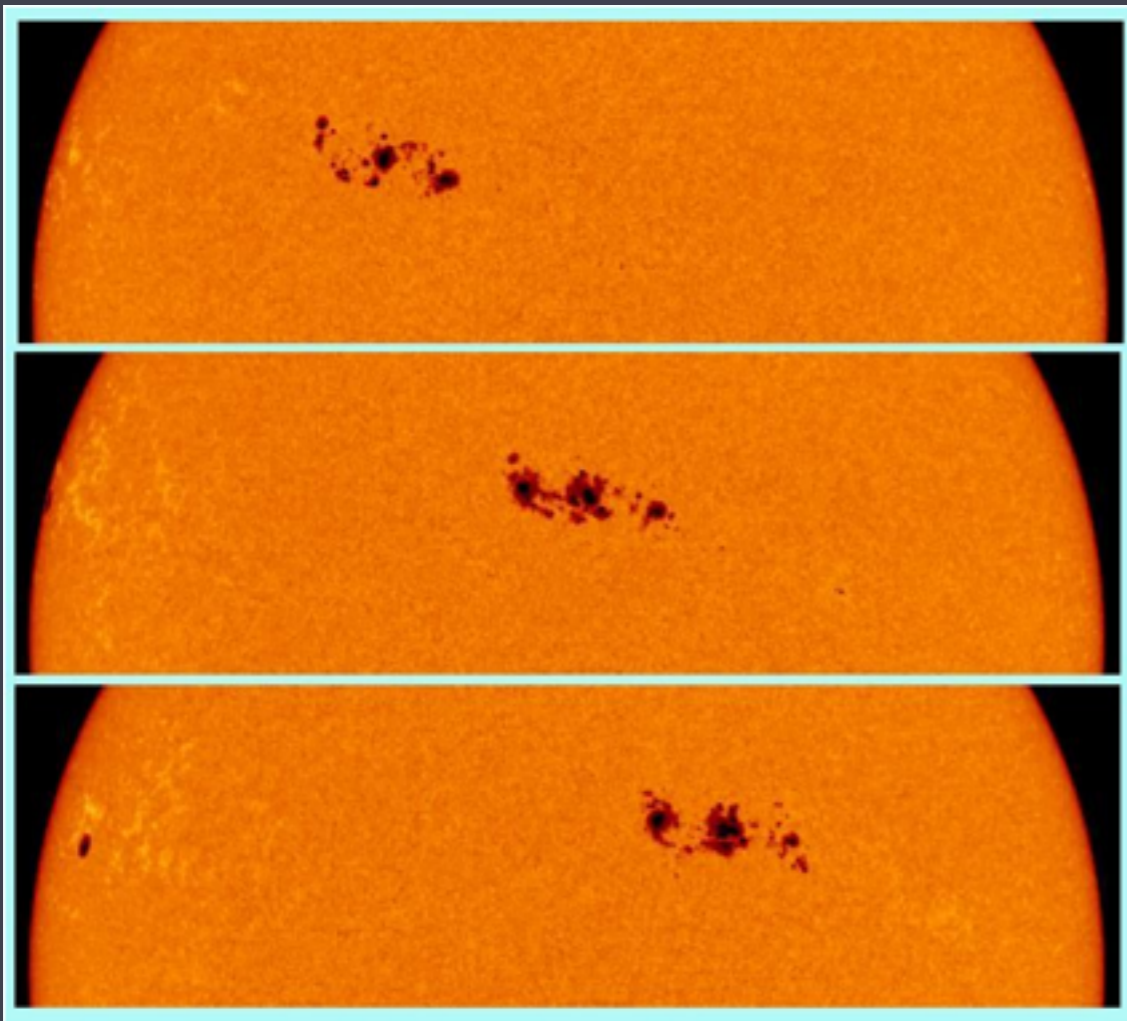
hot stars



starfish, *in situ*, at the Monterey (California) Aquarium

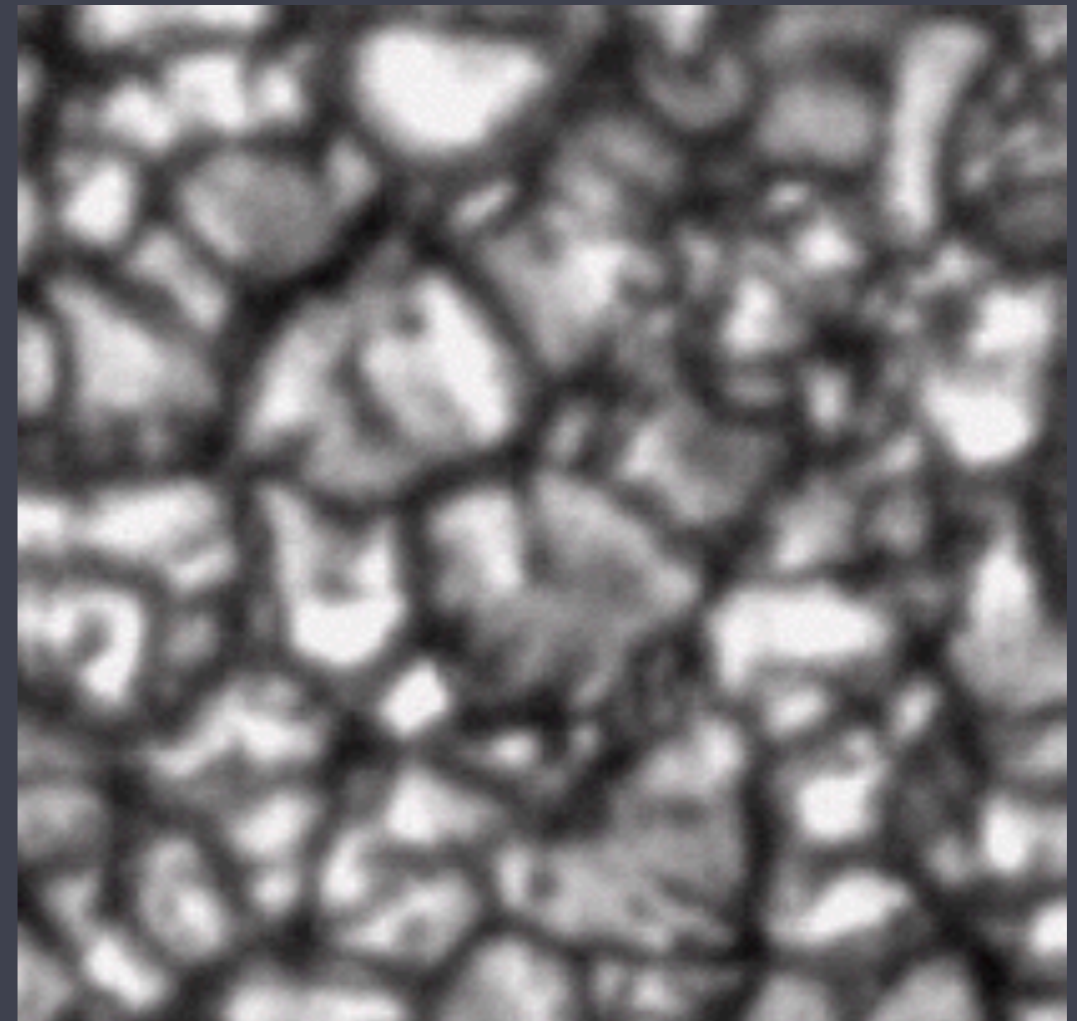
The Sun's **X-ray emission** is associated with its magnetic dynamo (rotation + convection are key ingredients)

rotation



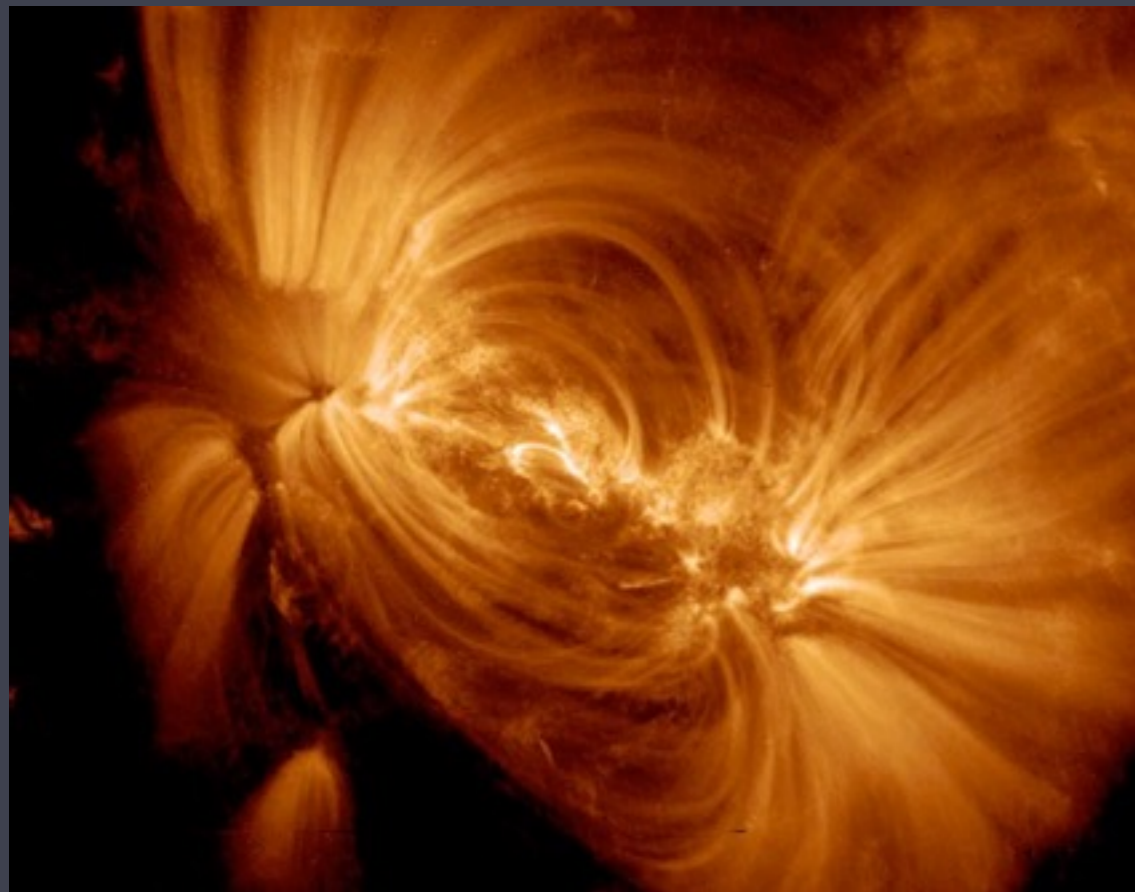
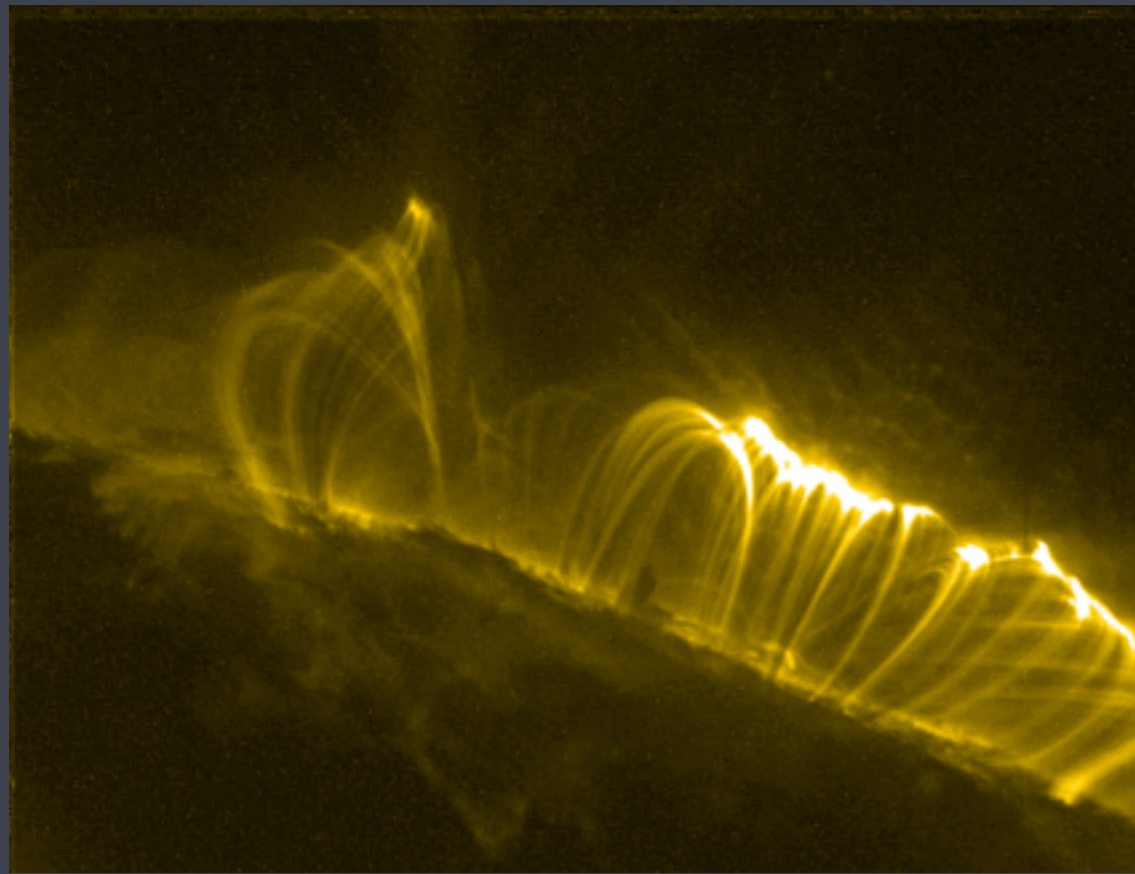
sunspots rotate across our field of view in a few days

convection



area roughly the size of the Earth

The Sun in the extreme ultraviolet

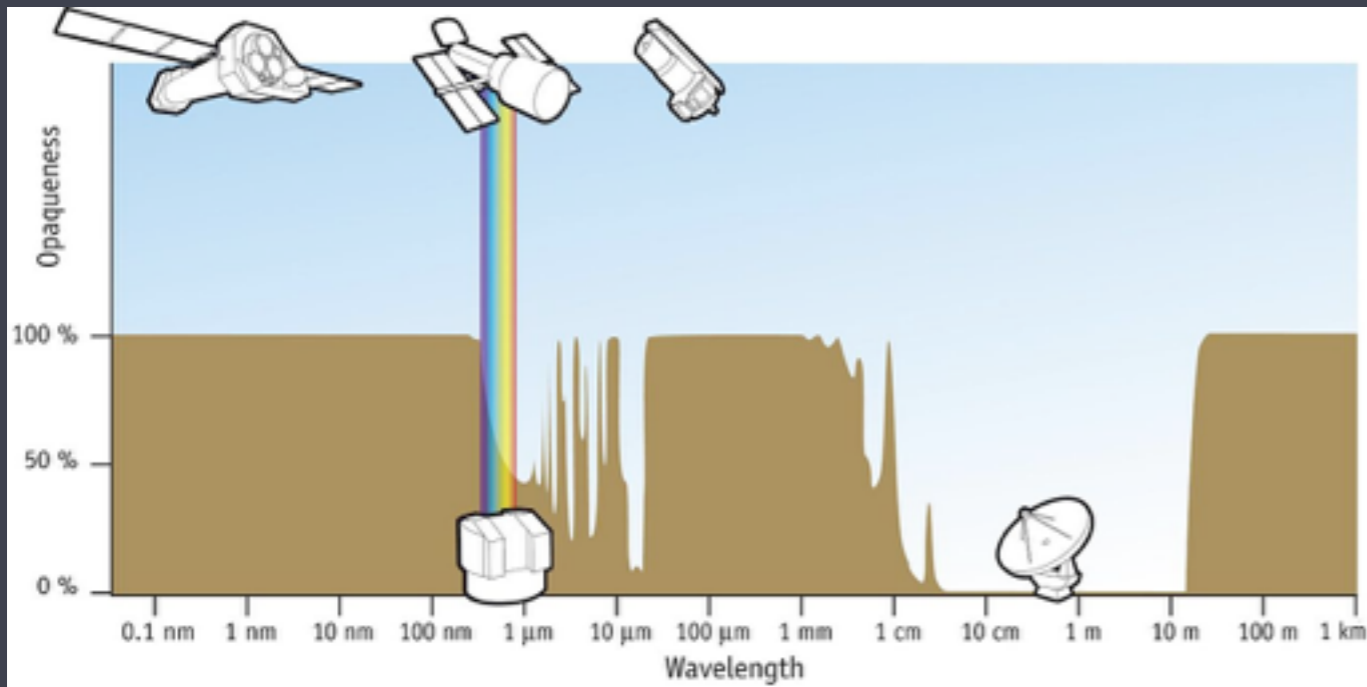


NASA:TRACE

X-ray Astronomy was born in the 1960-70's

state of knowledge in the mid-70s:

Massive stars don't have convective surfaces
And they don't have magnetic fields (with a few notable exceptions)



F. Granato (ESA/Hubble) - ESA/Hubble

Einstein X-ray Observatory launched 1978



unexpected discovery of massive star X-ray emission in 1979

THE ASTROPHYSICAL JOURNAL, 234:L51-54, 1979 November 15
© 1979. The American Astronomical Society. All rights reserved. Printed in U.S.A.

DISCOVERY OF AN X-RAY STAR ASSOCIATION IN VI CYGNI (CYG OB2)

F. R. HARNDEN, JR., G. BRANDUARDI, M. ELVIS,¹ P. GORENSTEIN, J. GRINDLAY,
J. P. PYE,¹ R. ROSNER, K. TOPKA, AND G. S. VAIANA²

Harvard-Smithsonian Center for Astrophysics, Cambridge, Massachusetts

Received 1979 June 26; accepted 1979 July 26

ABSTRACT

A group of six X-ray sources located within $0^{\circ}.4$ of Cygnus X-3 has been discovered with the *Einstein* Observatory. These sources have been positively identified and five of them correspond to stars in the heavily obscured OB association VI Cygni. The optical counterparts include four of the most luminous O stars within the field of view and a B5 supergiant. These sources are found to have typical X-ray luminosities L_x (0.2–4.0 keV) $\sim 5 \times 10^{33}$ ergs s⁻¹, with temperatures $T \sim 10^{6.8}$ K and hydrogen column densities $N_H \sim 10^{22}$ cm⁻², and therefore comprise a new class of low-luminosity galactic X-ray sources associated with early-type stars.

Massive star X-ray emission is different from low-mass stellar X-ray emission

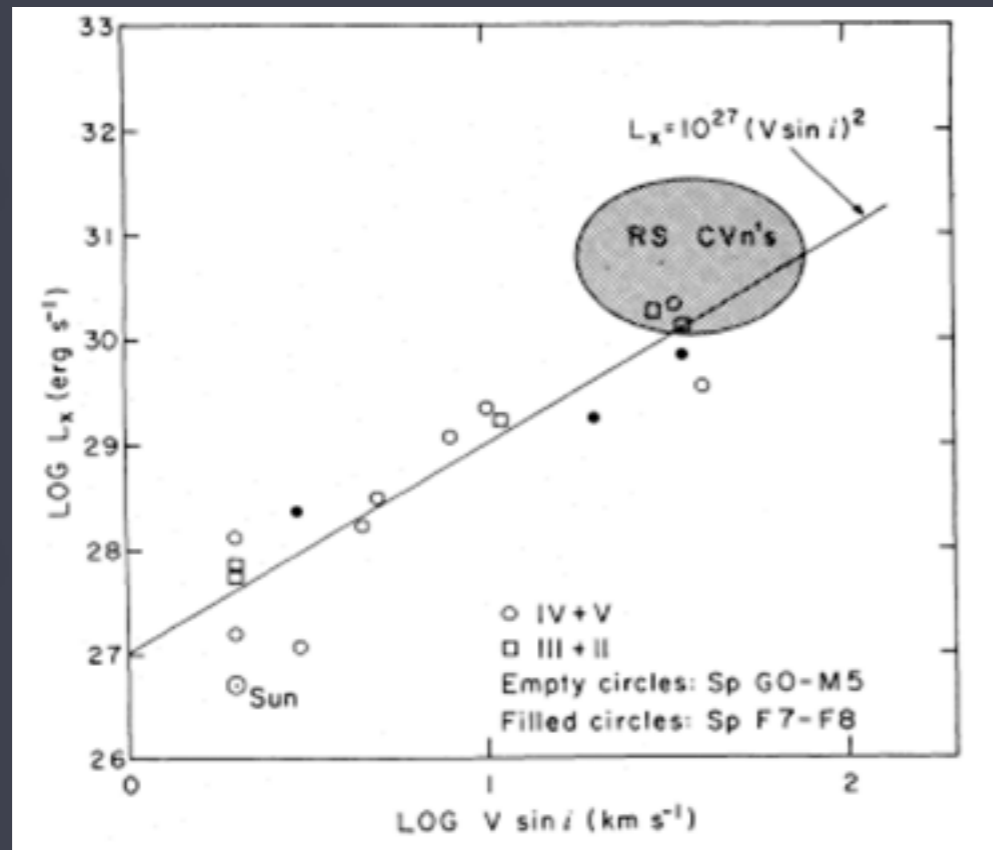


No observed correlation between rotation and X-rays for the massive stars

low mass

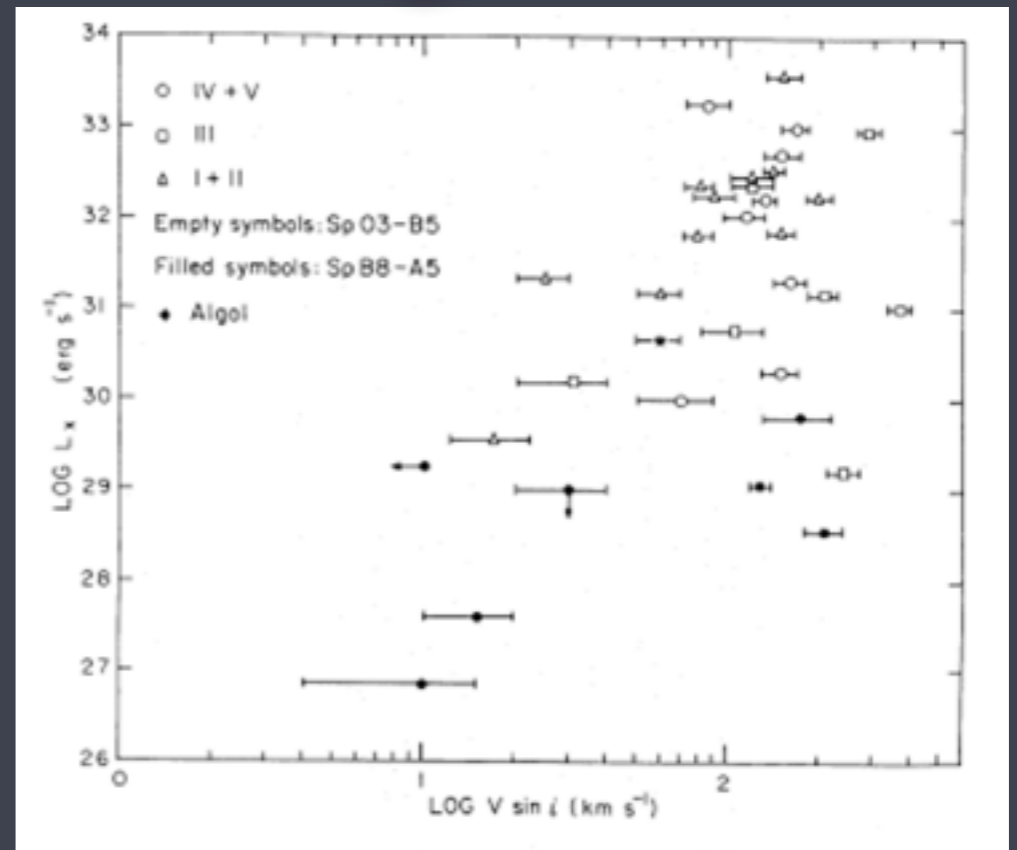
high mass

X-ray luminosity



rotation

X-ray luminosity



rotation

X-ray properties of bright OB-type stars detected in the ROSAT all-sky survey

T.W. Berghöfer^{1,2*}, J.H.M.M. Schmitt¹, R. Danner^{1,3}, and J.P. Cassinelli⁴

¹ Max-Planck-Institut für Extraterrestrische Physik, Giessenbachstr, 1, D-85740 Garching, Germany

² Center for EUV Astrophysics, 2150 Kittredge Street, University of California, Berkeley, CA 94720, USA

³ Division of Physics, Mathematics, and Astronomy, Caltech 105-24, Pasadena, CA 91125, USA

⁴ University of Wisconsin - Madison, Department of Astronomy, 475 North Charter Street, Madison, WI 53706-1582, USA

Received 17 July 1996 / Accepted 26 November 1996

Abstract. The ROSAT all-sky survey has been used to study the X-ray properties for all OB-type stars listed in the Yale Bright Star Catalogue. Here we present a detailed astrophysical discussion of our analysis of the X-ray properties of our complete sample of OB-type stars; a compilation of the X-ray data is provided in an accompanying paper (Berghöfer, Schmitt & Cassinelli 1996).

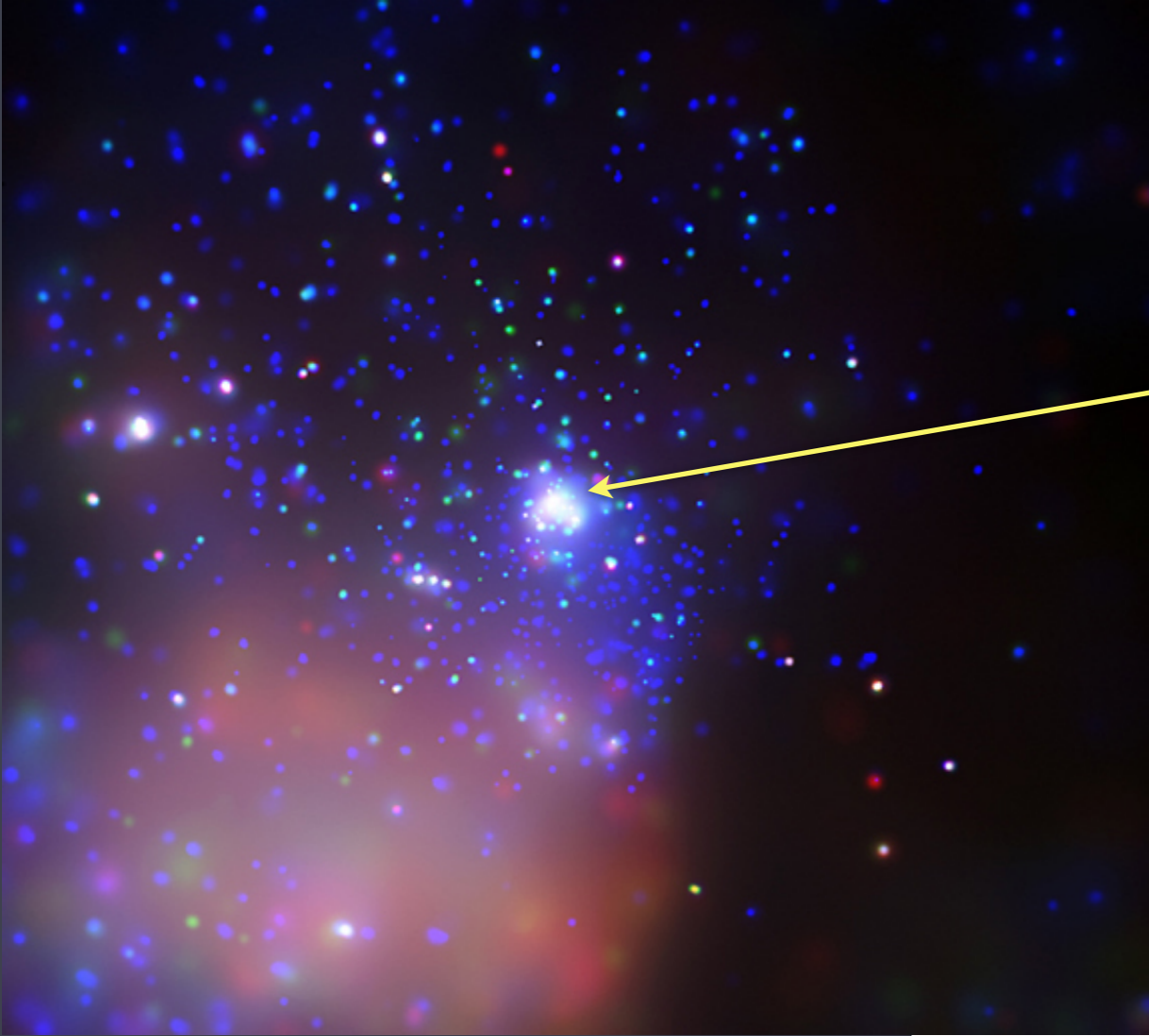
We demonstrate that the “canonical” relation between X-ray and total luminosity of $L_x/L_{\text{Bol}} \approx 10^{-7}$ valid for O-type stars extends among the early B-type stars down to a spectral type B1–B1.5; for stars of luminosity classes I and II the spectral type B1 defines a dividing line for early-type star X-ray emission.

1979, Pallavicini *et al.* 1981, Chlebowski *et al.* 1989, Sciortino *et al.* 1990). However, the scatter for values of individual stars, 2 orders of magnitude, around the mean value is quite large. The widely accepted model for the X-ray emission from O stars assumes that it is produced by shock-heated gas propagating in the strong winds of these stars. In a phenomenological model Lucy & White (1980) and Lucy (1982) postulate the existence of shocks in the radiation driven winds of hot stars which are formed as a consequence of a strong hydrodynamic instability (e.g., Lucy & Solomon 1980). Hydrodynamical calculations for hot star winds (e.g., Owocki, Castor & Rybicki 1988) provide strong support for such a model. The base corona source of X-

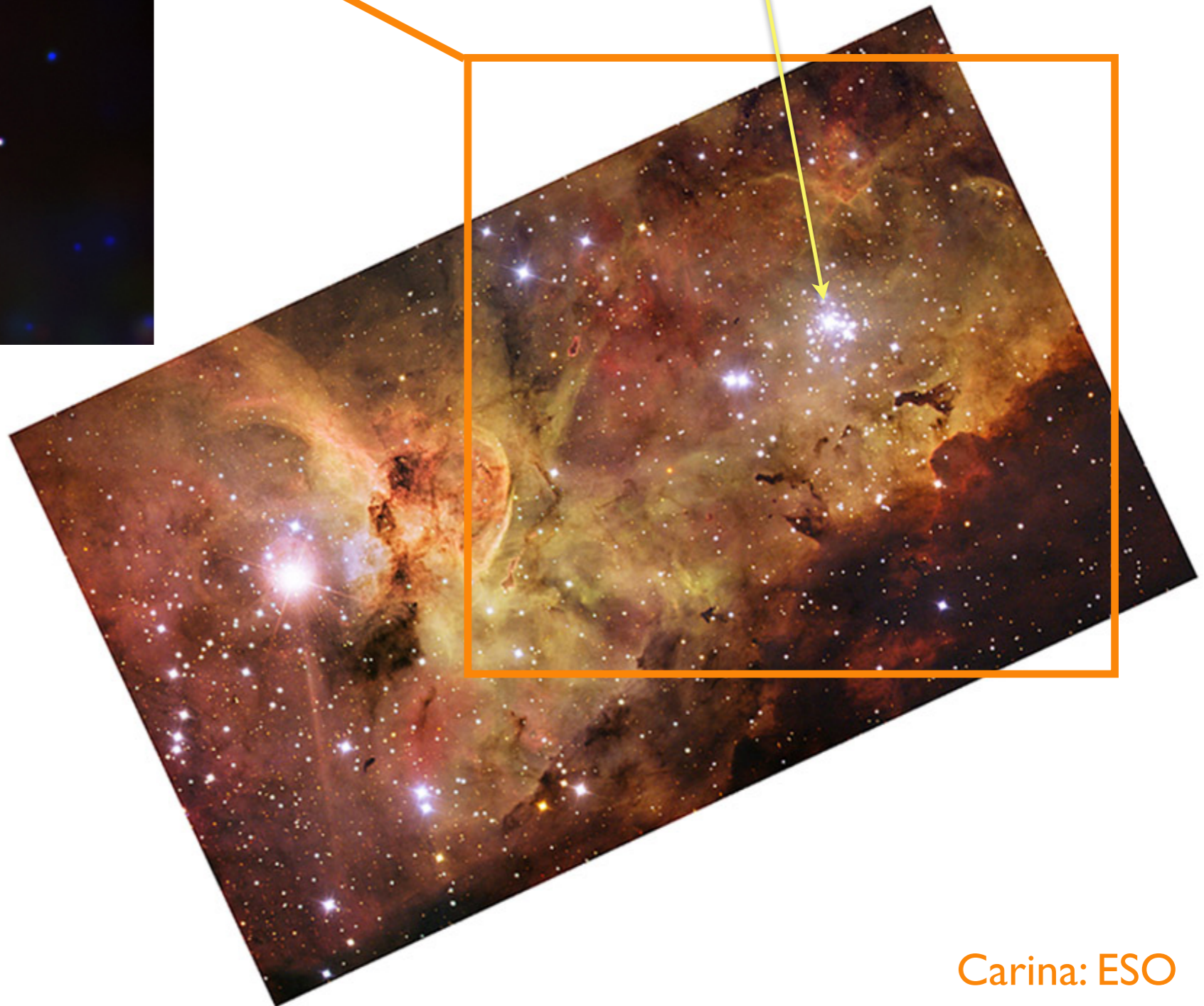
The Carina Complex

X-ray image to the left

HD 93129A (O2If*)



Tr 14 in Carina: Chandra



Carina: ESO

○ Stars are characterized by their dense stellar winds

Prodigious matter, momentum, and kinetic energy input into the cluster environment via these winds



Carina (Hubble Space Telescope)

These winds are the site and energy source of the X-ray emission



Carina (Hubble Space Telescope)

wind-blown bubble around a massive star

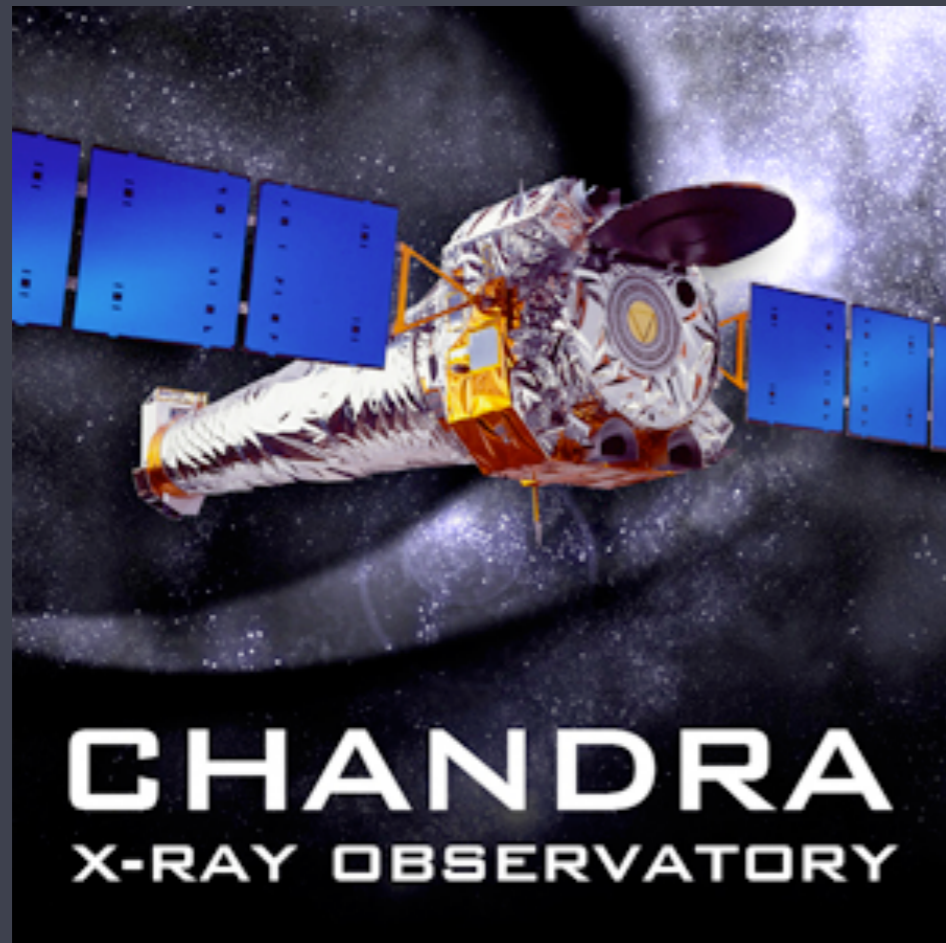


NGC 6888 Crescent Nebula - Tony Hallas

In general, X-ray imaging of massive stars is not so useful

...use **spectroscopy** as a proxy for imaging

Chandra launched in 1999 -
first high-resolution X-ray spectrograph

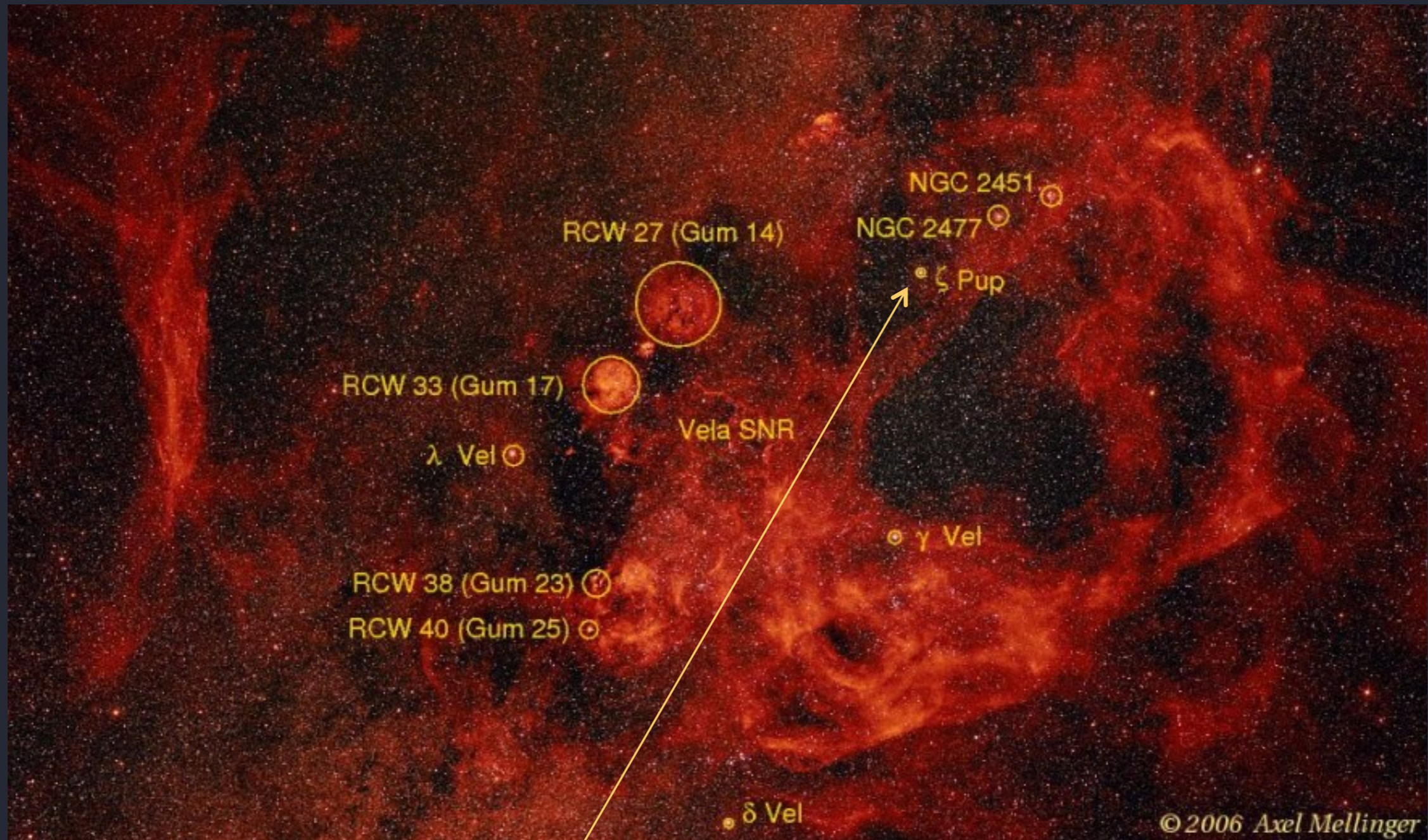


response to photons with
 $h\nu \sim 0.5 \text{ keV}$ up to a few
 keV (corresp. $\sim 5\text{\AA}$ to 24\AA)

X-ray imaging? $> 0.5 \text{ arc sec}$, at best (100s of AU)
spectroscopy ($\lambda/\Delta\lambda < 1000$ corresp. $v > 300 \text{ km/s}$)

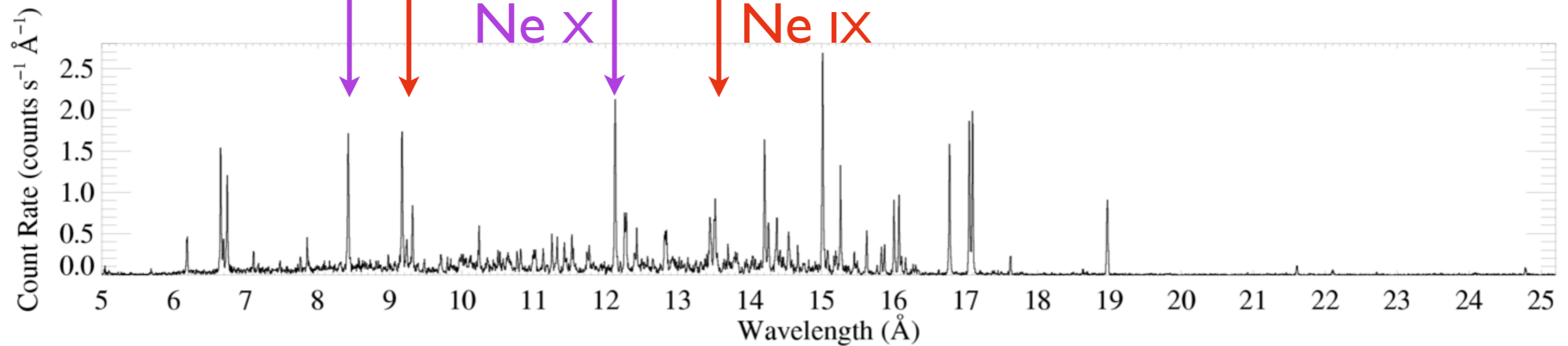
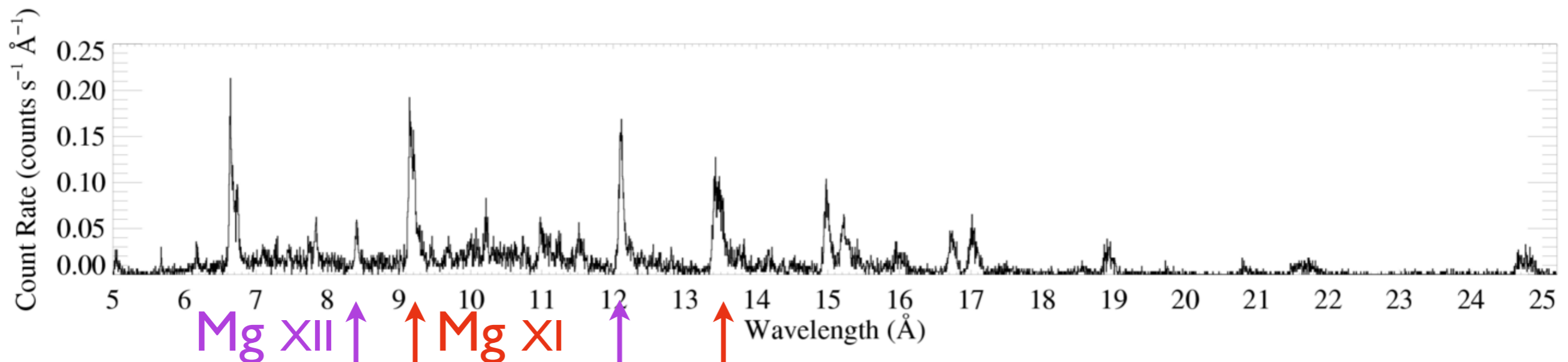
Chandra grating spectroscopy

ζ Pup (O4 If)



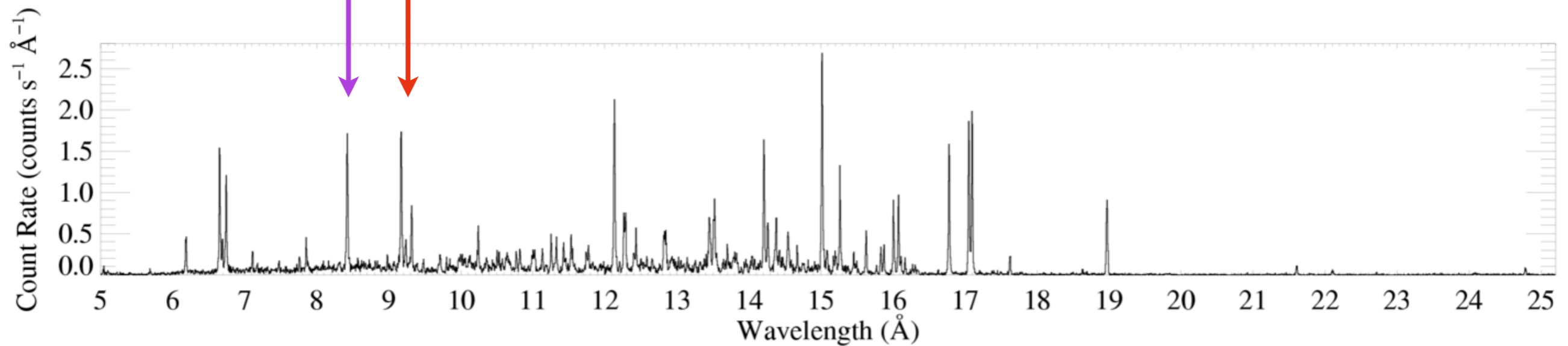
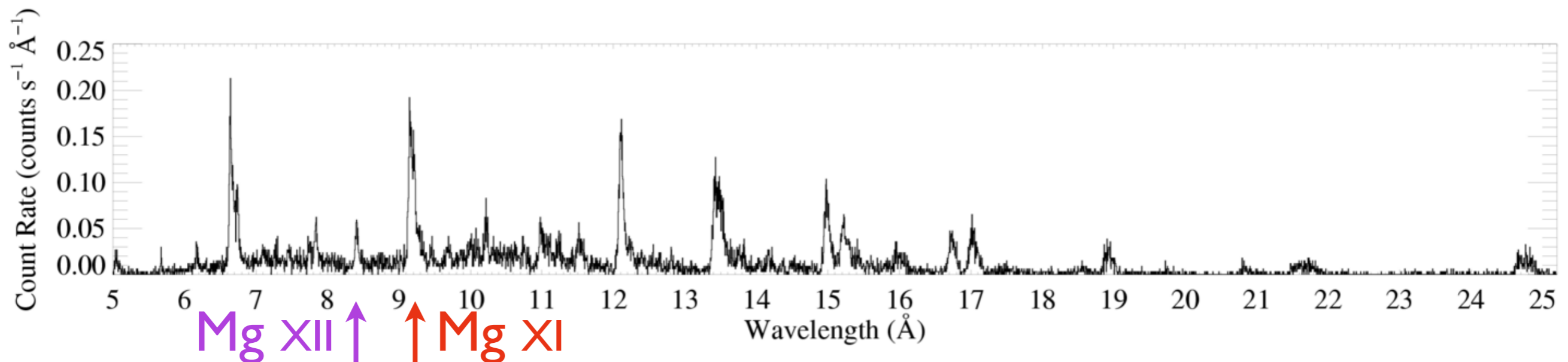
Chandra grating (HETGS/MEG) spectra

ζ Pup (O4 If)



Capella (G5 III)

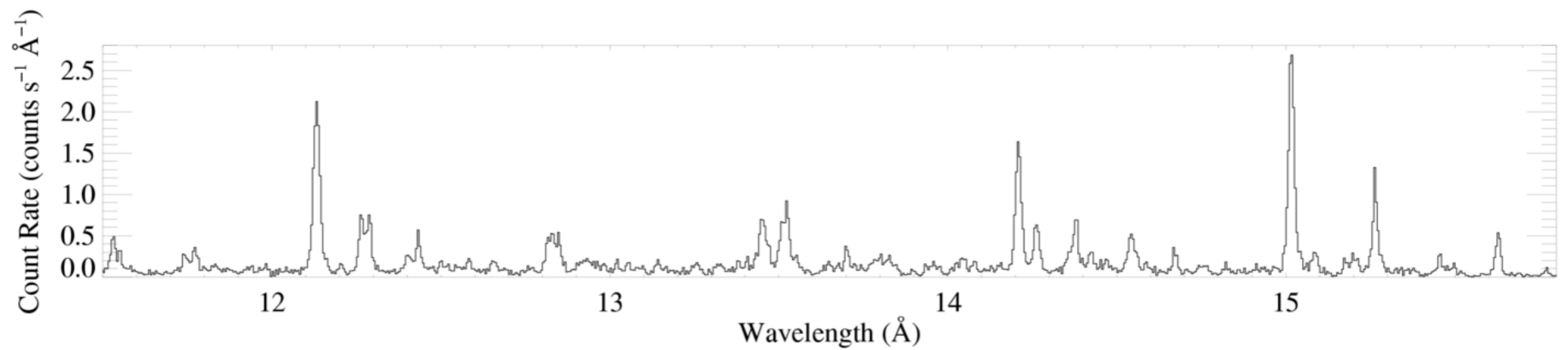
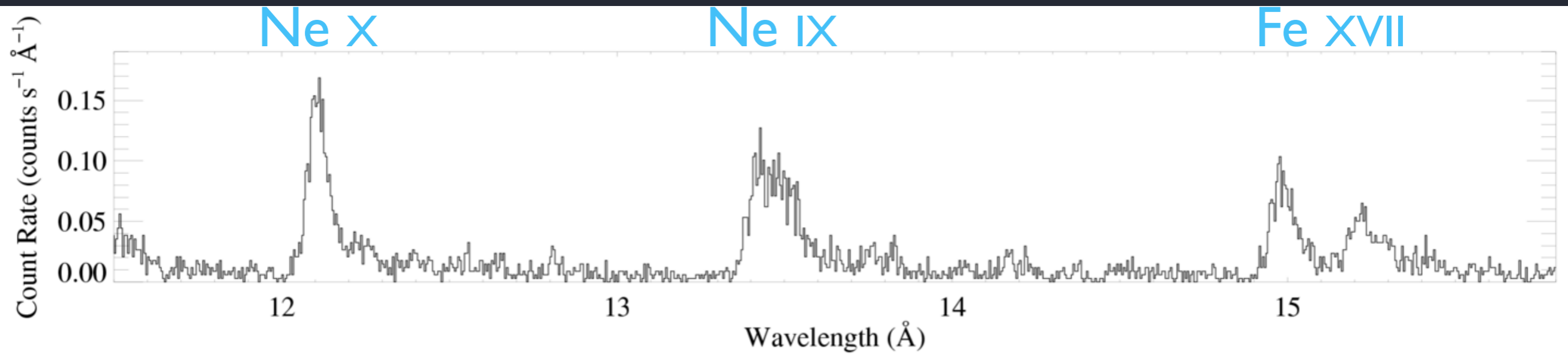
typical temperatures $T \sim \text{few } 10^6 \text{ K}$
(low-mass stars' coronae tend to be hotter) $\zeta \text{ Pup (O4 If)}$



Capella (G5 III)

Zoom in

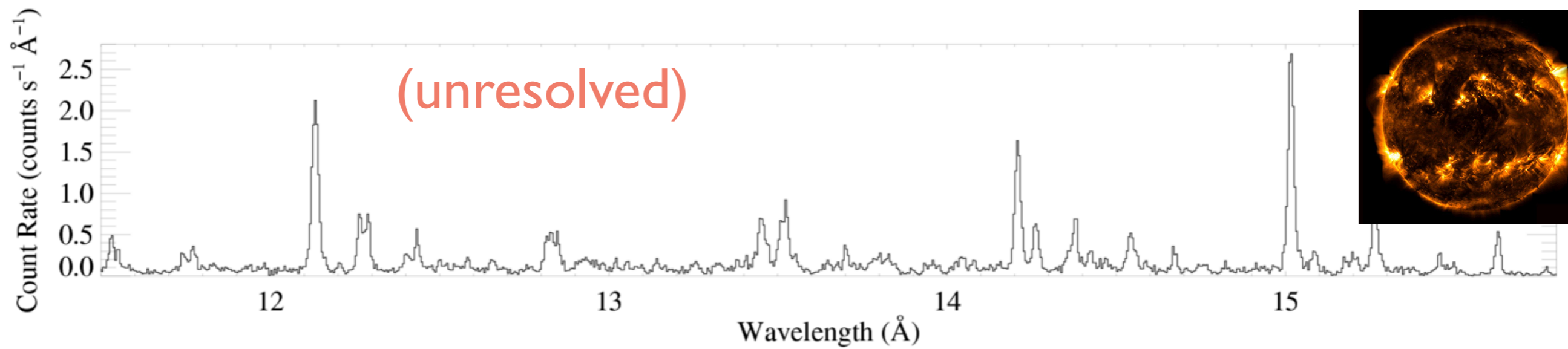
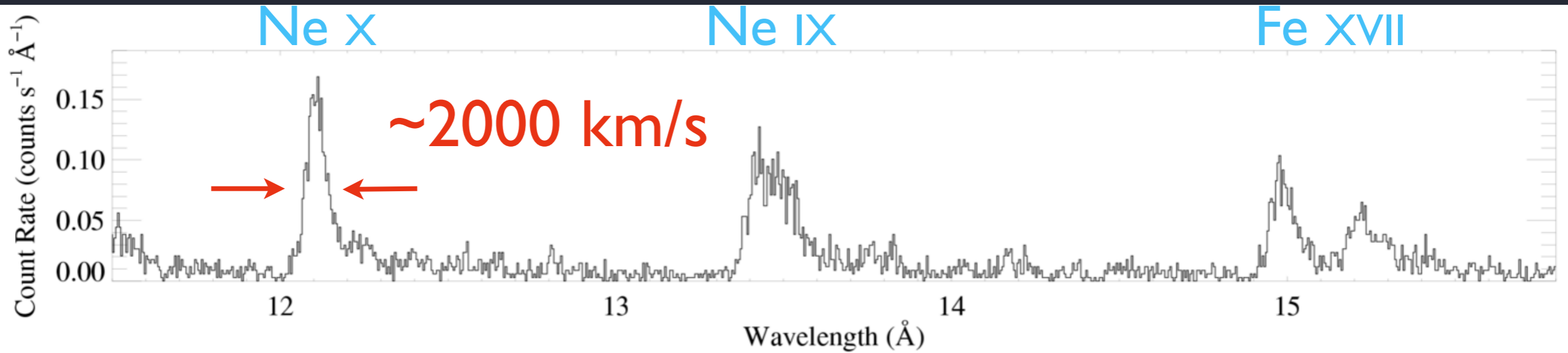
ζ Pup (O4 If)



Capella (G5 III)

Zoom in

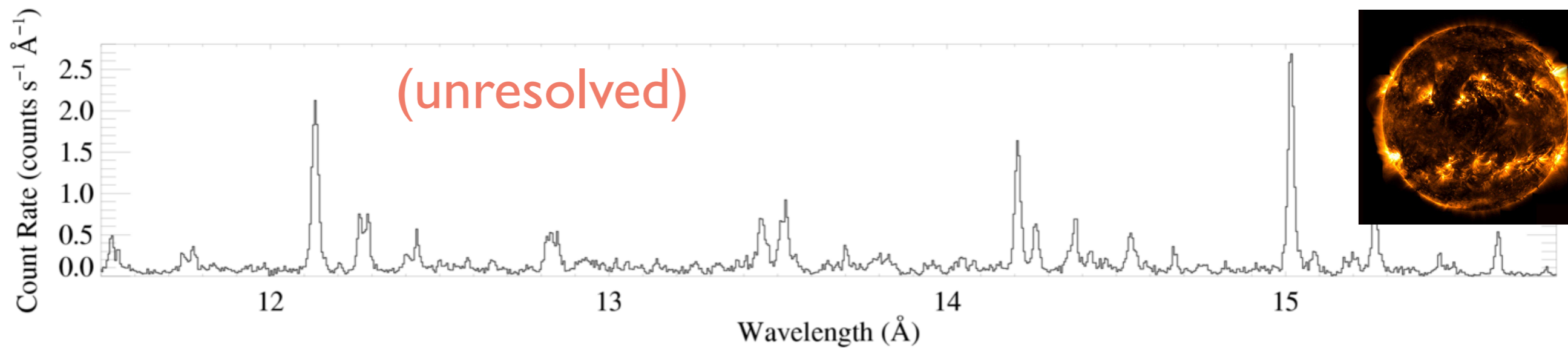
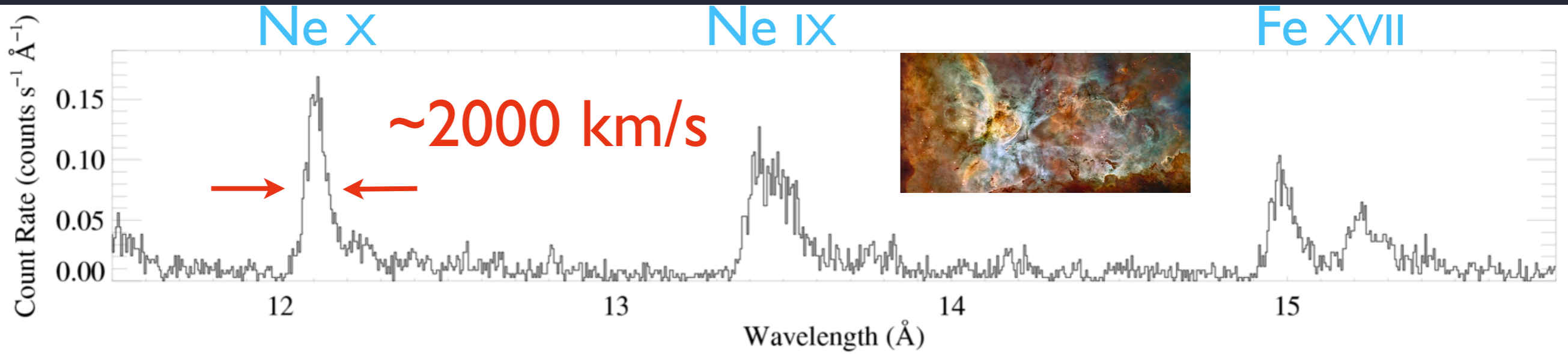
ζ Pup (O4 If)



Capella (G5 III)

conclusive evidence that the X-ray plasma is in the stellar wind

ζ Pup (O4 If)



Capella (G5 III)

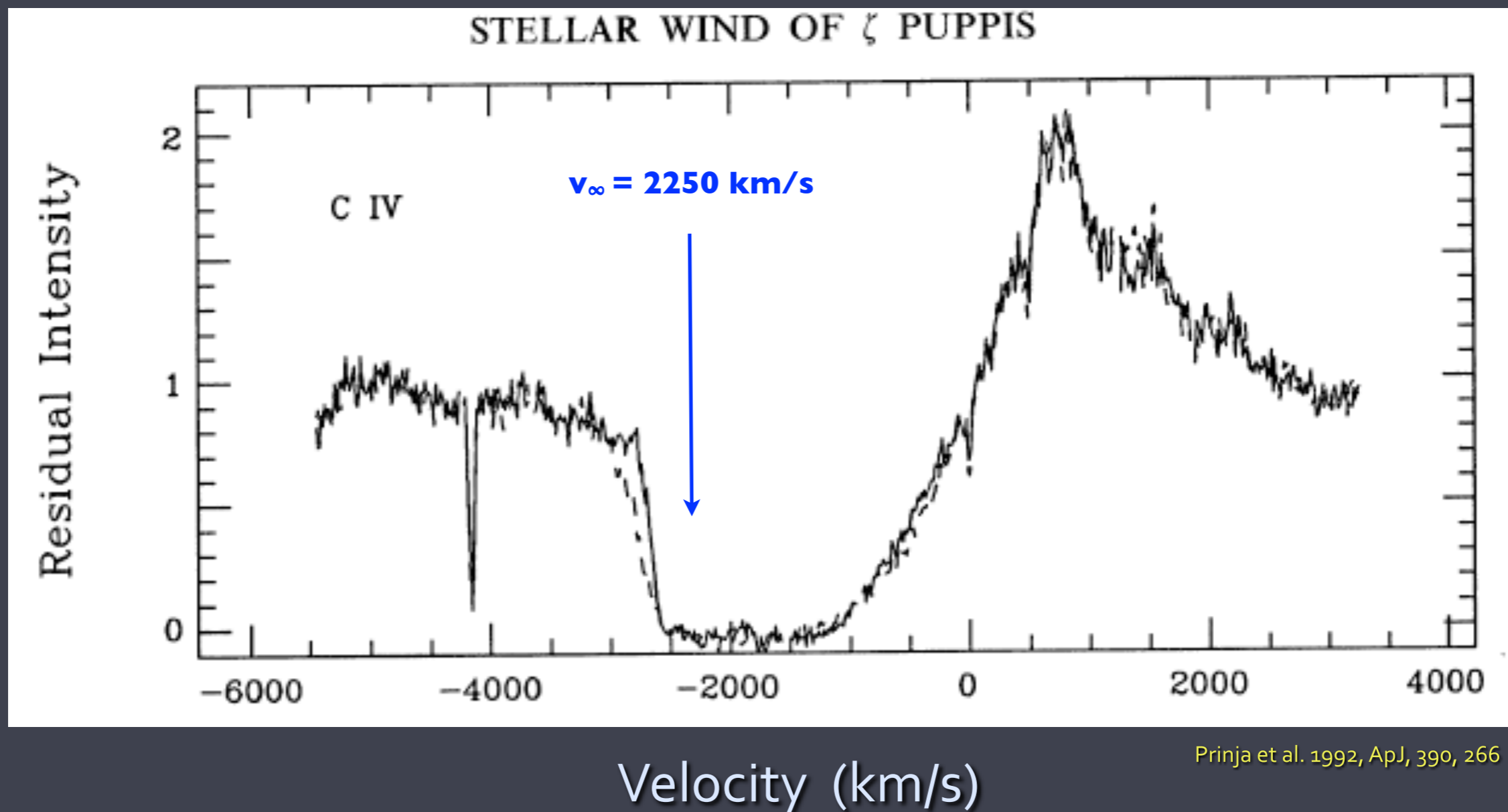
radiation-driven winds



Ultraviolet spectral line: wind signature “P Cygni profile”

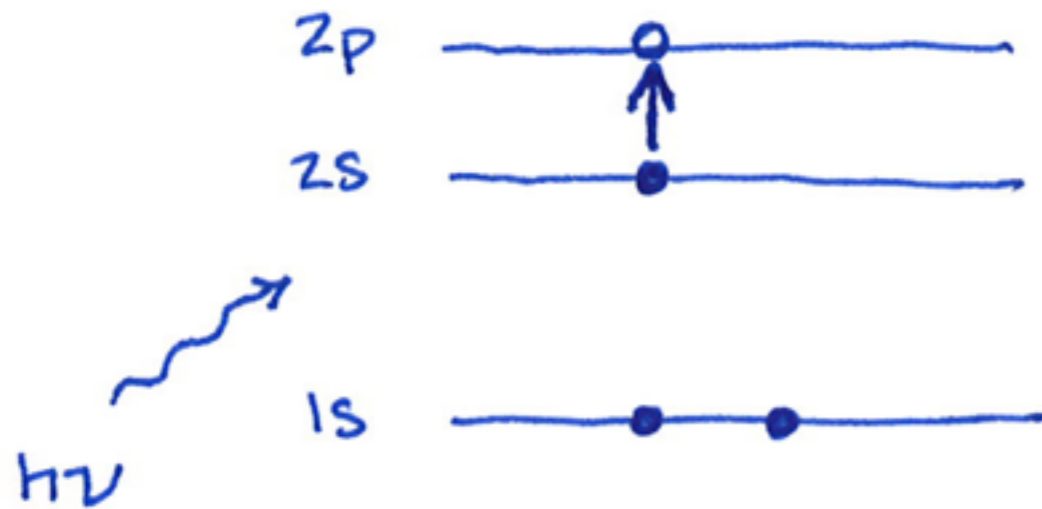
ζ Pup (O4 supergiant): $\dot{M} \sim \text{few } 10^{-6} M_{\text{sun}}/\text{yr}$

UV spectrum: C IV 1548, 1551 Å

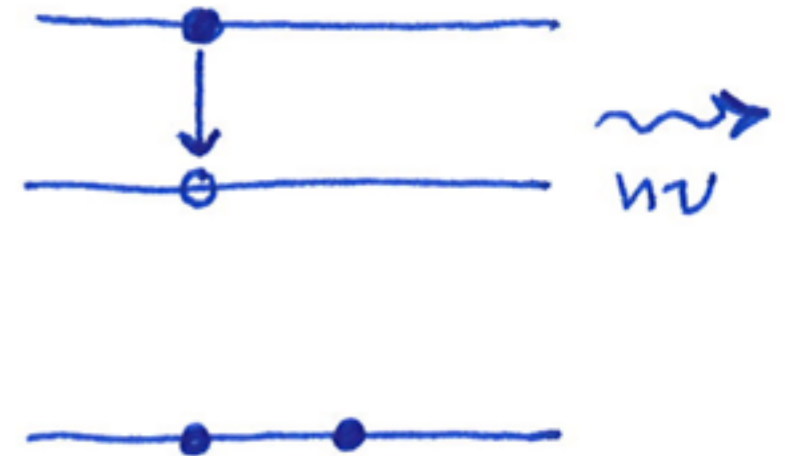


absorption and emission: atomic energy level diagrams

C^{+3} is lithium-like

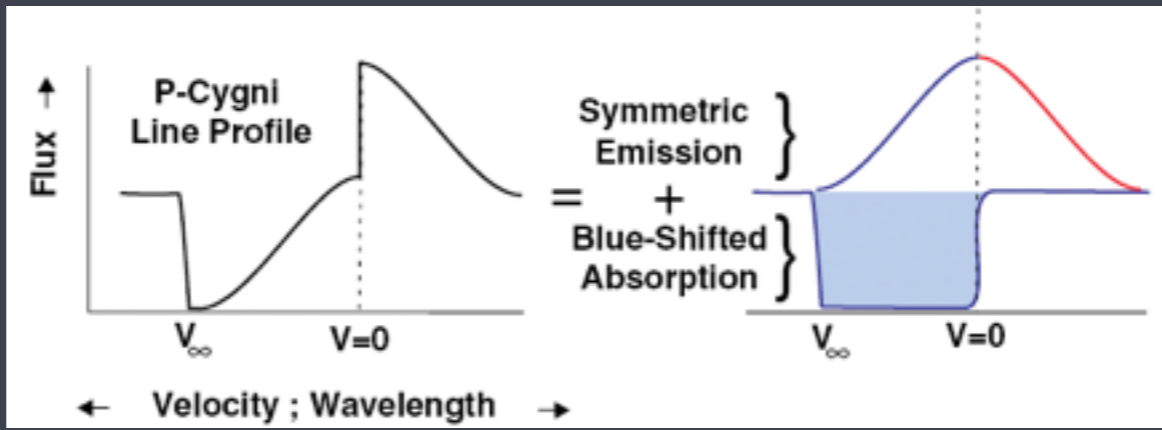
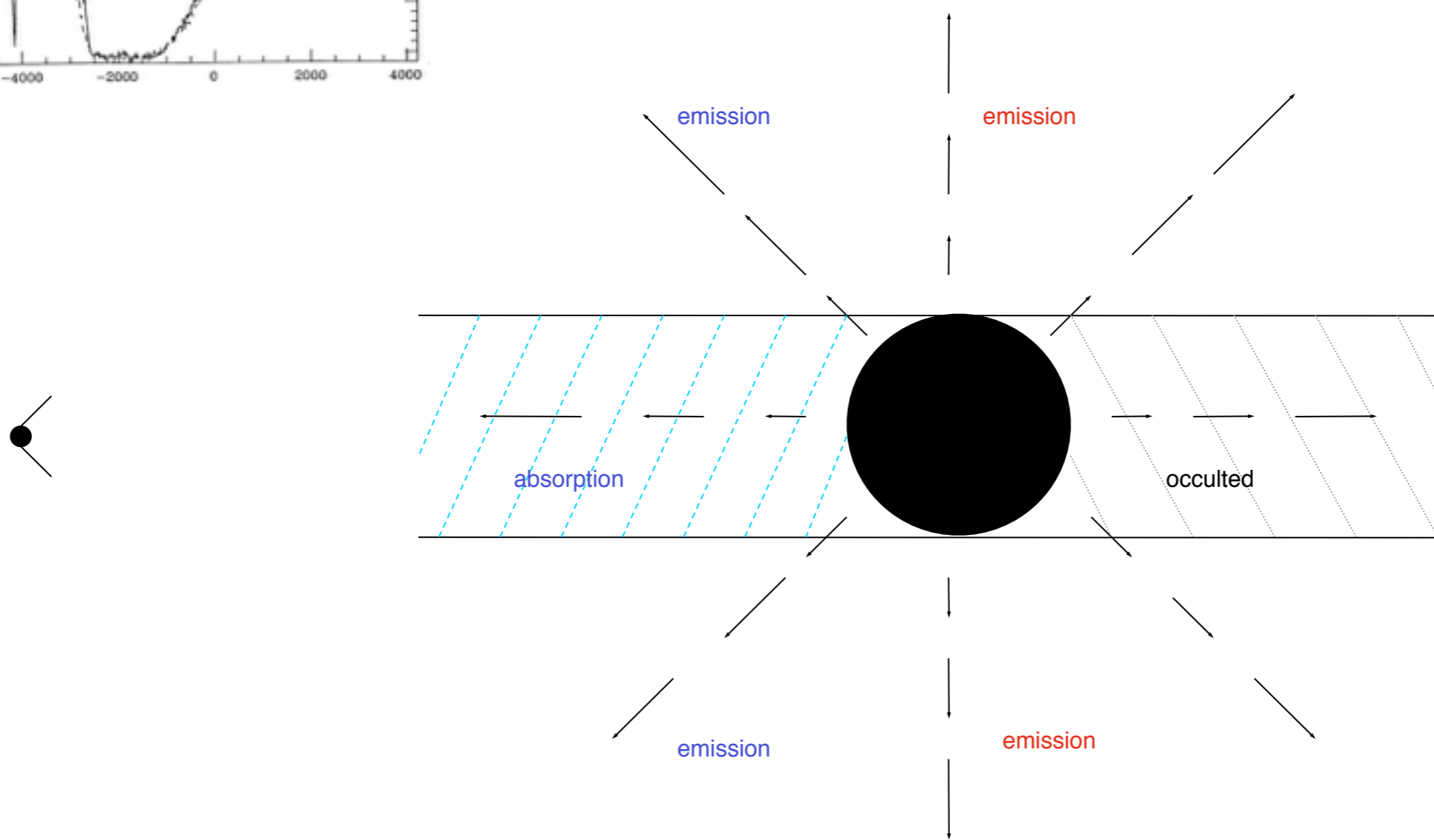
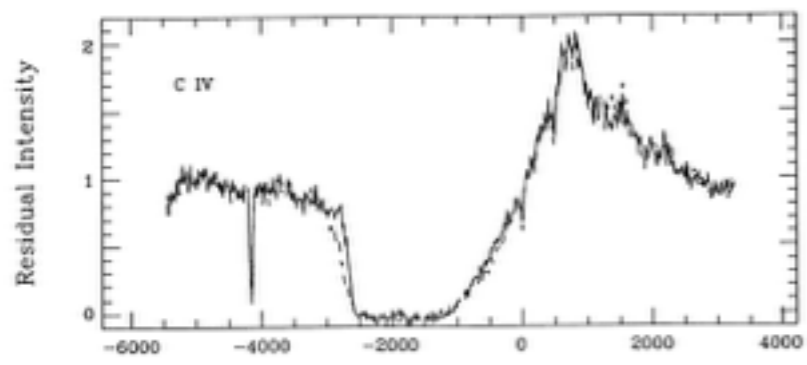


Absorption



Emission

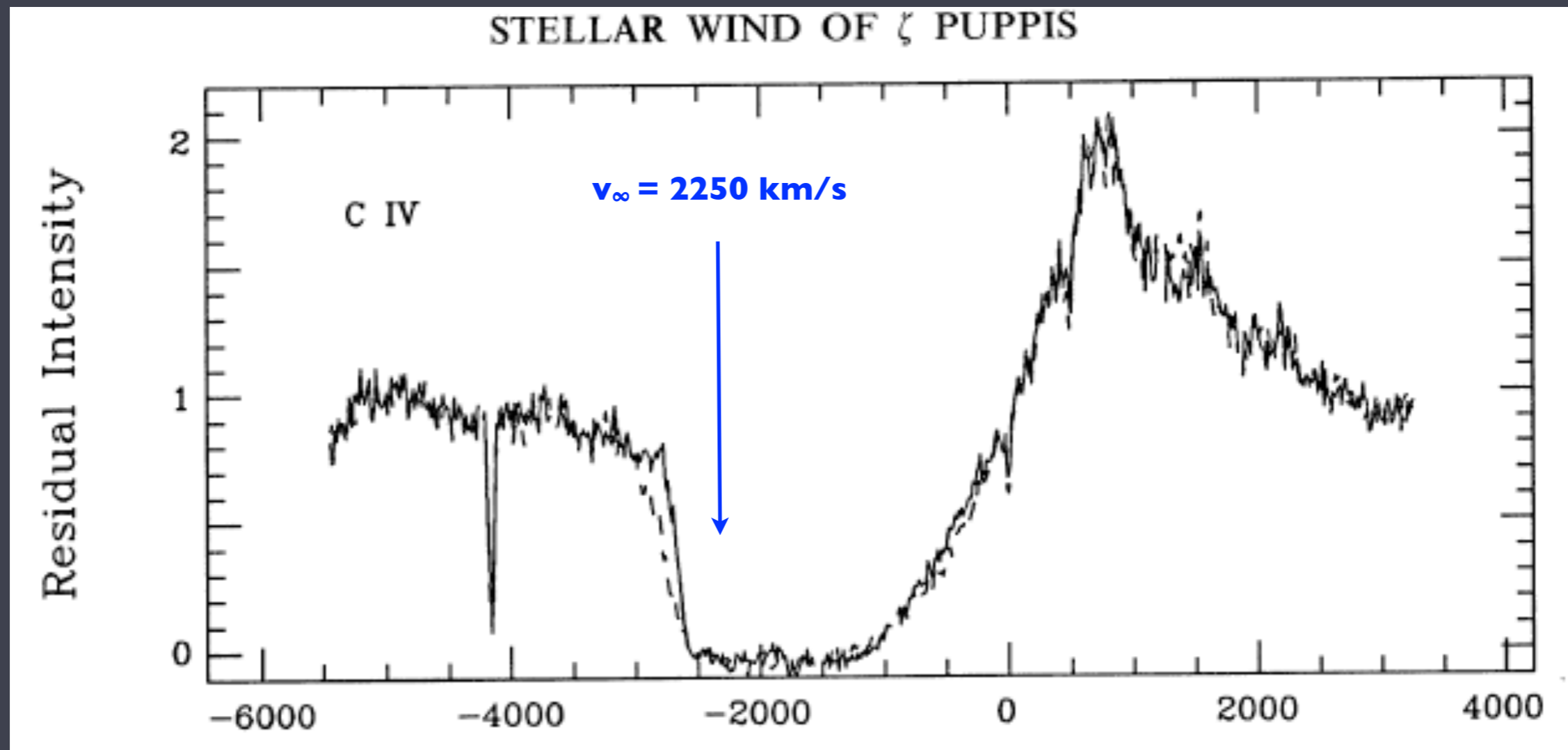
STELLAR WIND OF ζ PUPPIS



Terminal (asymptotic) wind velocity

ζ Pup (O4 supergiant): $\dot{M} \sim \text{few } 10^{-6} M_{\text{sun}}/\text{yr}$

UV spectrum: C IV 1548, 1551 Å



Velocity (km/s)

Physics of line-driven winds

radiation couples the momentum in the starlight to the matter in the wind via resonance line scattering in C, N, O, Fe,....

$\dot{M} \sim 10^{-6} M_{\text{sun}}/\text{yr}$ (10^8 times the Sun's value)

kinetic power in the wind = $1/2 \dot{M} v_{\infty}^2$ ($\sim 10^{-3} L_{\text{star}}$)

Radiation Force on an atom



$h\nu$ (energy)

$\frac{h\nu}{c}$ (momentum, p)

rate at which atom
absorbs momentum

$$\frac{dp}{dt} = F_{\text{rad}}$$

$$F_{\text{rad}} = \frac{L\sigma}{4\pi r^2 c}$$

luminosity, star's power output (watts)

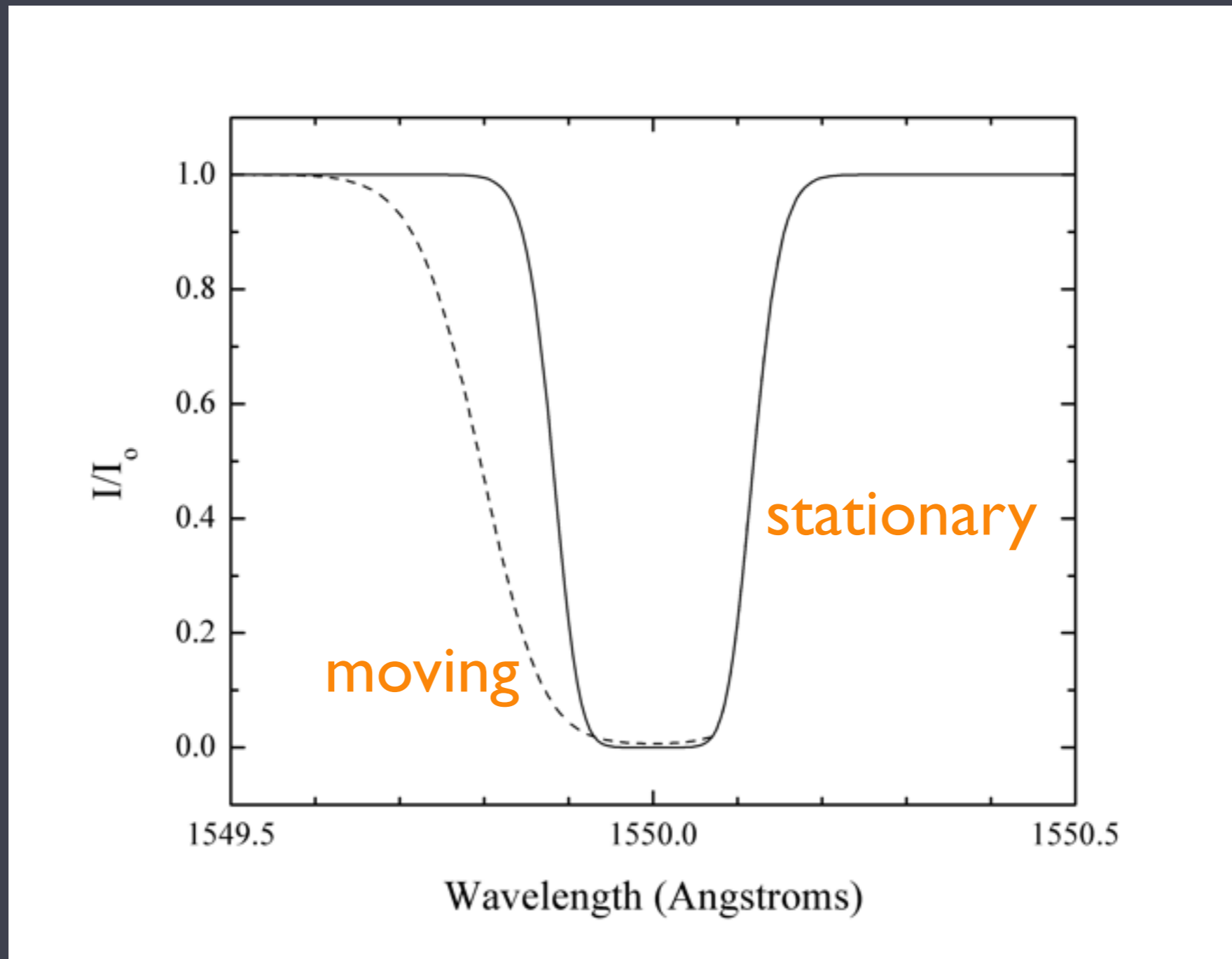
absorption cross section of atom (m^2)

Three things to consider when we consider *line-driven winds*

1. Bound electrons (10^7 times as efficient as free electrons)
2. But strong lines are saturated
3. Doppler shift will *desaturate* them

Doppler desaturation is key to line-driven winds

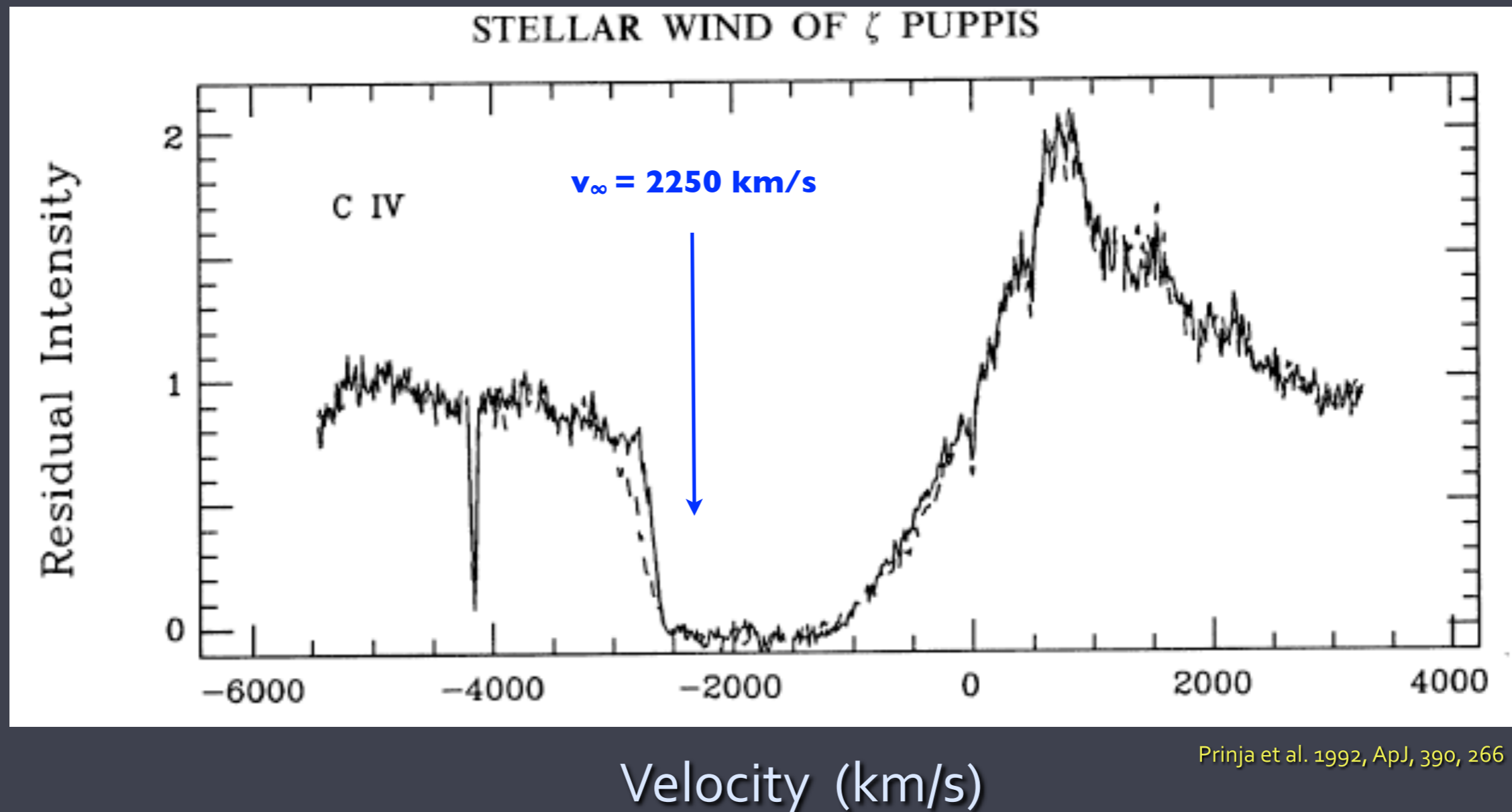
line strength increases in a moving medium



$\sim 10^{-3}$ of the radiative power of the star goes into
the wind

ζ Pup (O4 supergiant): $\dot{M} \sim \text{few } 10^{-6} M_{\text{sun}}/\text{yr}$

UV spectrum: C IV 1548, 1551 Å



$\sim 10^{-4}$ of the wind power is converted to X-rays

X-ray properties of bright OB-type stars detected in the ROSAT all-sky survey

T.W. Berghöfer^{1,2*}, J.H.M.M. Schmitt¹, R. Danner^{1,3}, and J.P. Cassinelli⁴

¹ Max-Planck-Institut für Extraterrestrische Physik, Giessenbachstr, 1, D-85740 Garching, Germany

² Center for EUV Astrophysics, 2150 Kittredge Street, University of California, Berkeley, CA 94720, USA

³ Division of Physics, Mathematics, and Astronomy, Caltech 105-24, Pasadena, CA 91125, USA

⁴ University of Wisconsin - Madison, Department of Astronomy, 475 North Charter Street, Madison, WI 53706-1582, USA

Received 17 July 1996 / Accepted 26 November 1996

Abstract. The ROSAT all-sky survey has been used to study the X-ray properties for all OB-type stars listed in the Yale Bright Star Catalogue. Here we present a detailed astrophysical discussion of our analysis of the X-ray properties of our complete sample of OB-type stars; a compilation of the X-ray data is provided in an accompanying paper (Berghöfer, Schmitt & Cassinelli 1996).

We demonstrate that the “canonical” relation between X-ray and total luminosity of $L_x/L_{\text{Bol}} \approx 10^{-7}$ valid for O-type stars extends among the early B-type stars down to a spectral type B1–B1.5; for stars of luminosity classes I and II the spectral type B1 defines a dividing line for early-type star X-ray emission.

1979, Pallavicini *et al.* 1981, Chlebowski *et al.* 1989, Sciortino *et al.* 1990). However, the scatter for values of individual stars, 2 orders of magnitude, around the mean value is quite large. The widely accepted model for the X-ray emission from O stars assumes that it is produced by shock-heated gas propagating in the strong winds of these stars. In a phenomenological model Lucy & White (1980) and Lucy (1982) postulate the existence of shocks in the radiation driven winds of hot stars which are formed as a consequence of a strong hydrodynamic instability (e.g., Lucy & Solomon 1980). Hydrodynamical calculations for hot star winds (e.g., Owocki, Castor & Rybicki 1988) provide strong support for such a model. The base corona source of X-

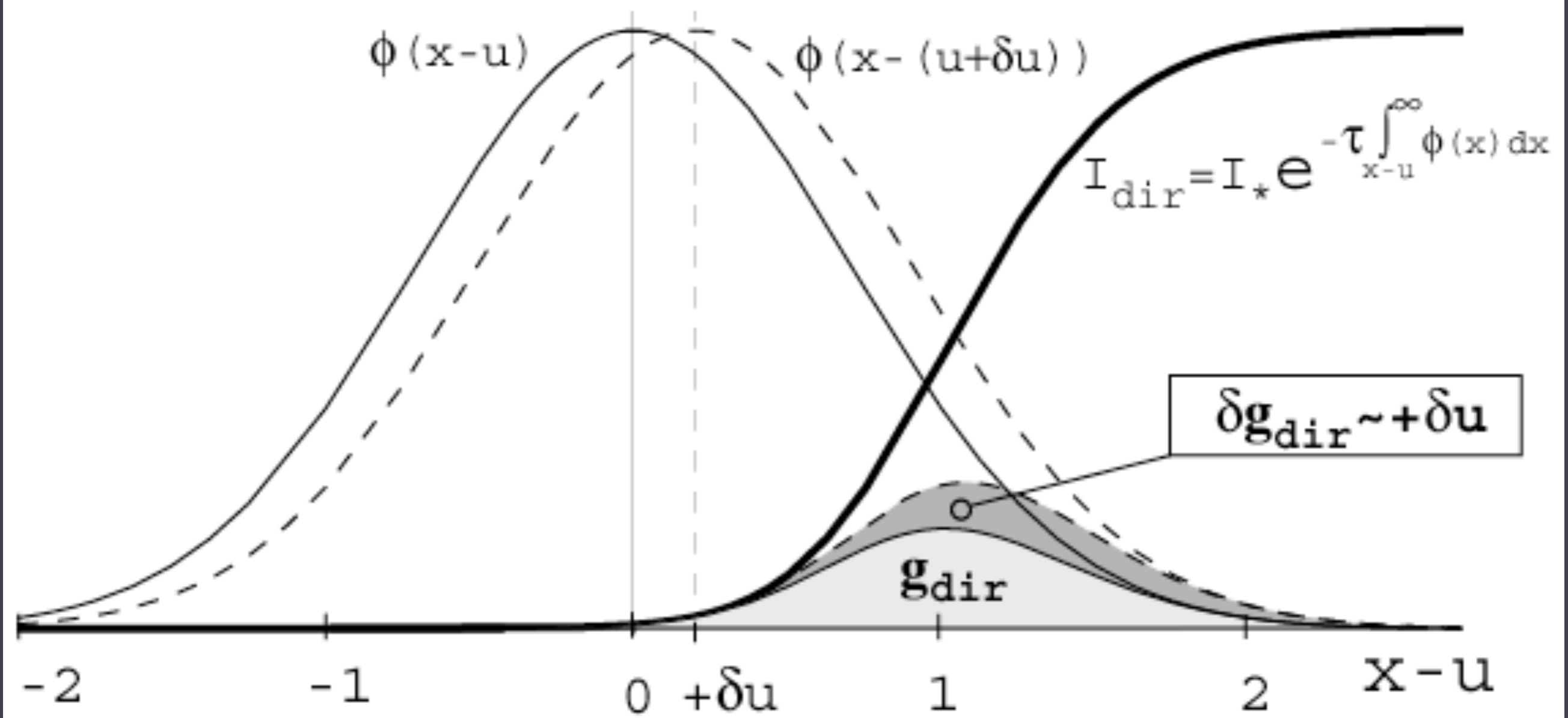
The line-deshadowing instability (LDI)

causes fast, rarefied wind plasma to slam into slower, denser wind plasma

the resulting shocks heat the wind plasma

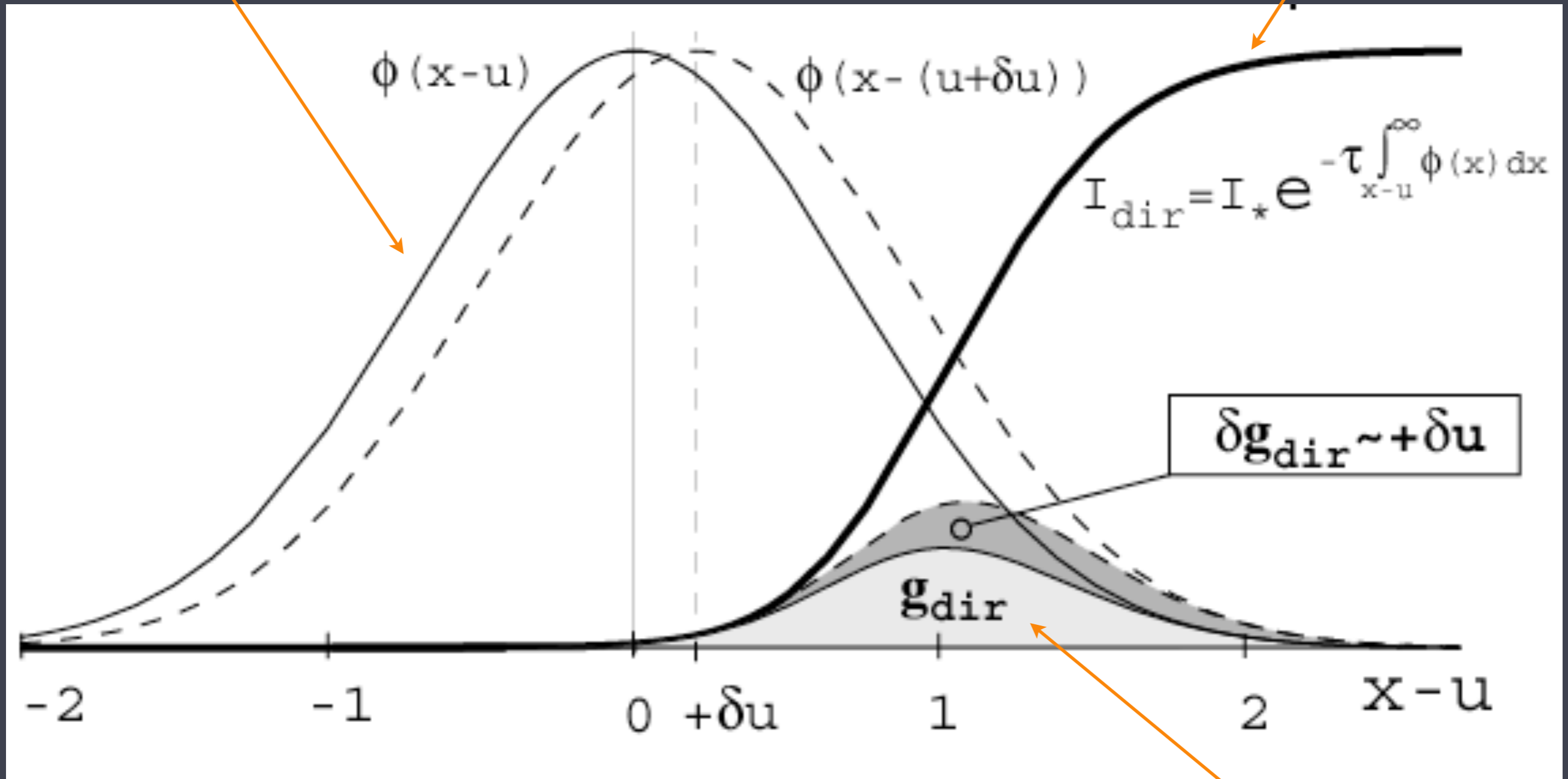
general result from shock theory:

$$T \sim 10^6 (\Delta v_{\text{shock}} / 300 \text{ km/s})^2$$



line profile

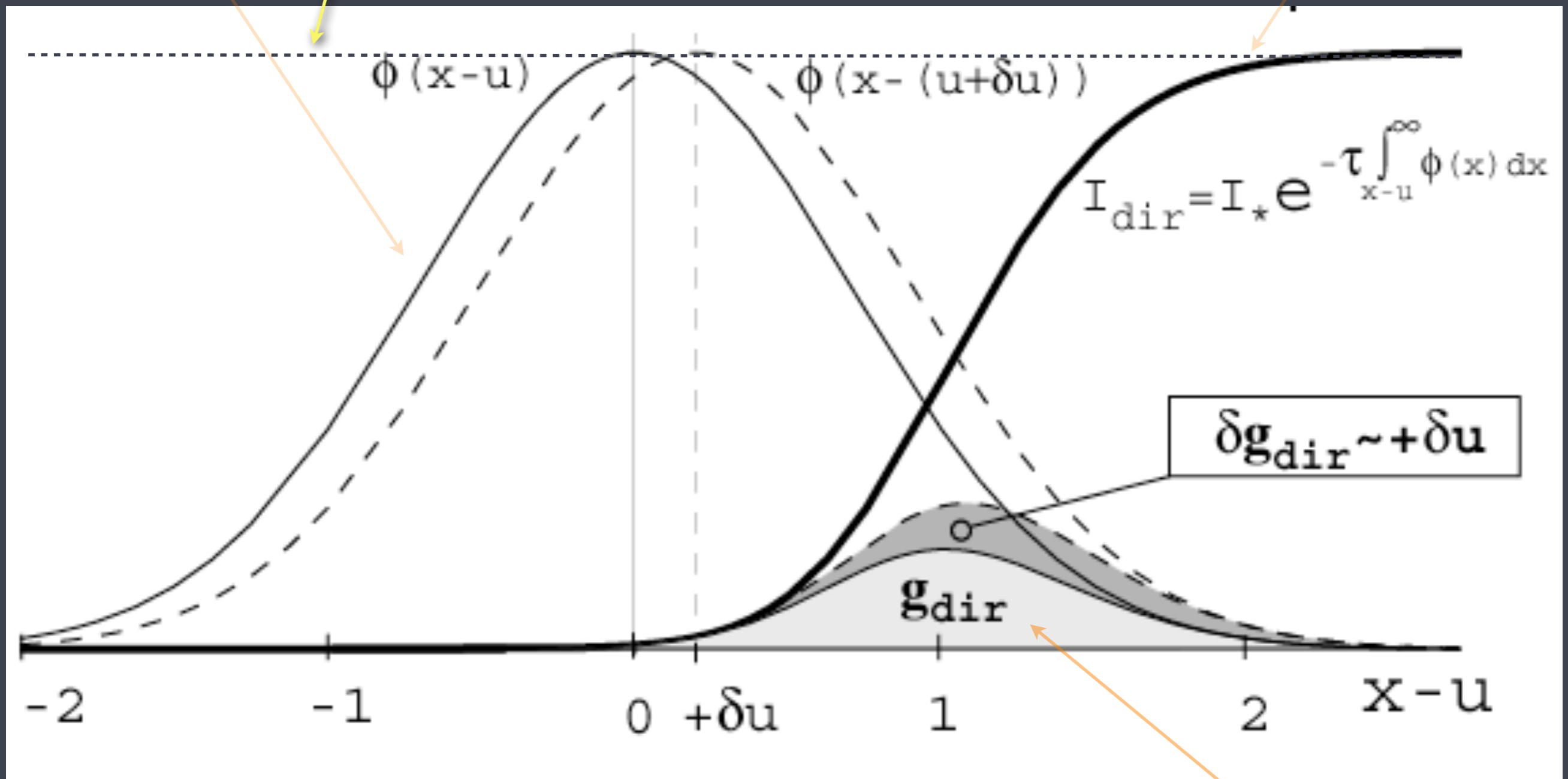
photospheric radiation



frequency

radiation force

photospheric radiation if there were no absorption by slower-moving parts of the lower portion of the wind

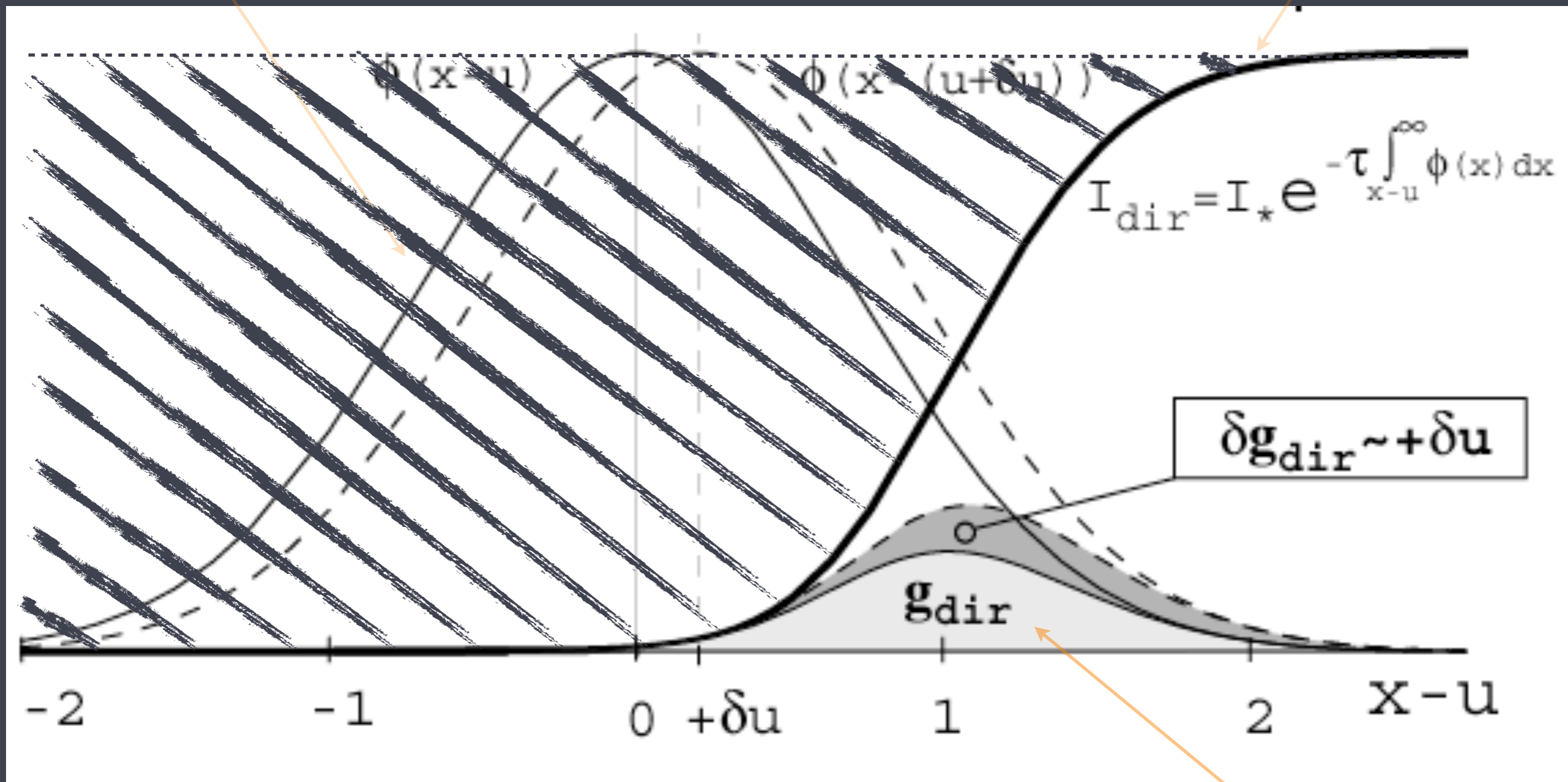


frequency

radiation force

line profile the Doppler shadow

photospheric radiation

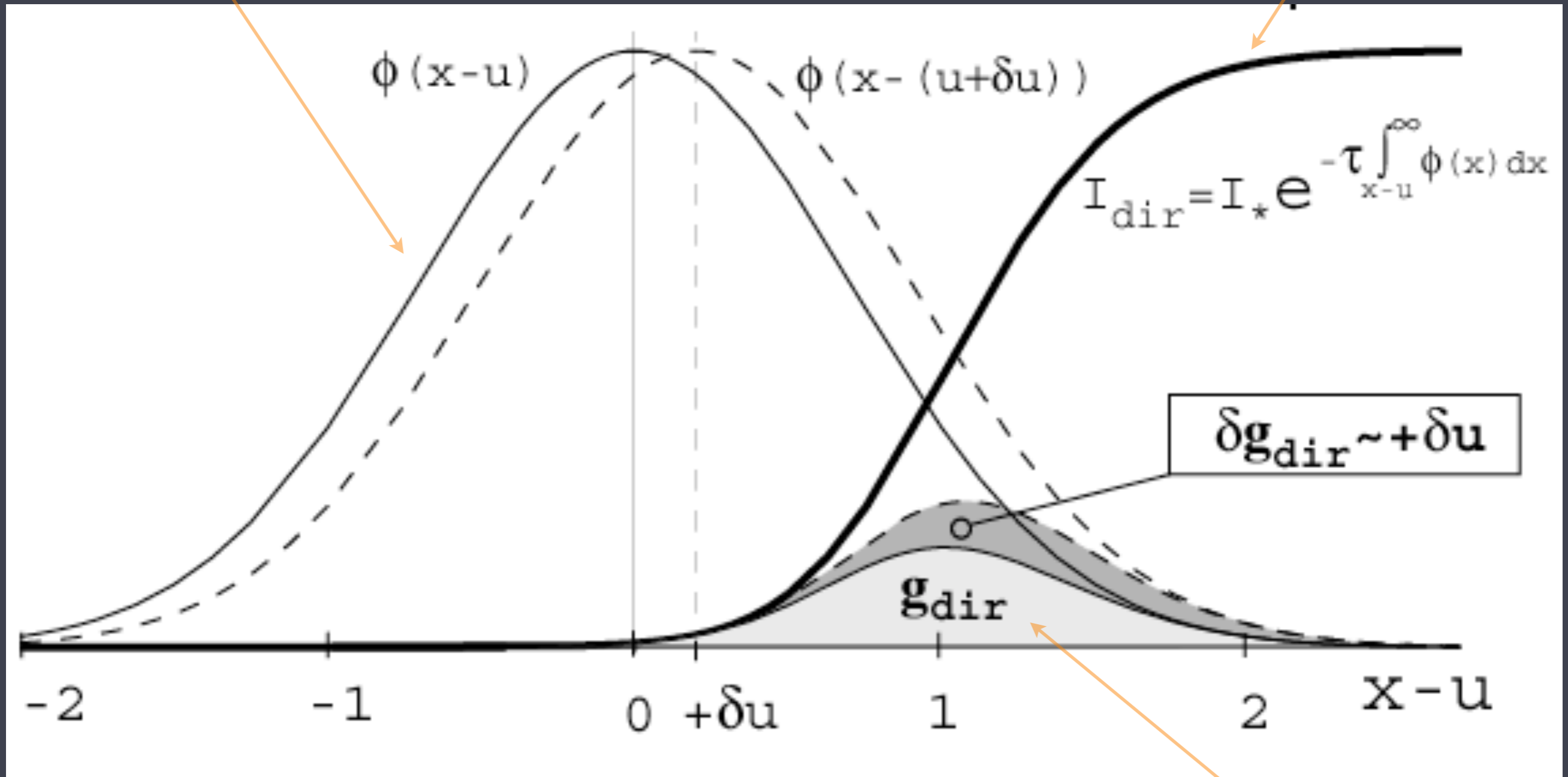


frequency

radiation force

positive velocity perturbation
line profile

photospheric radiation

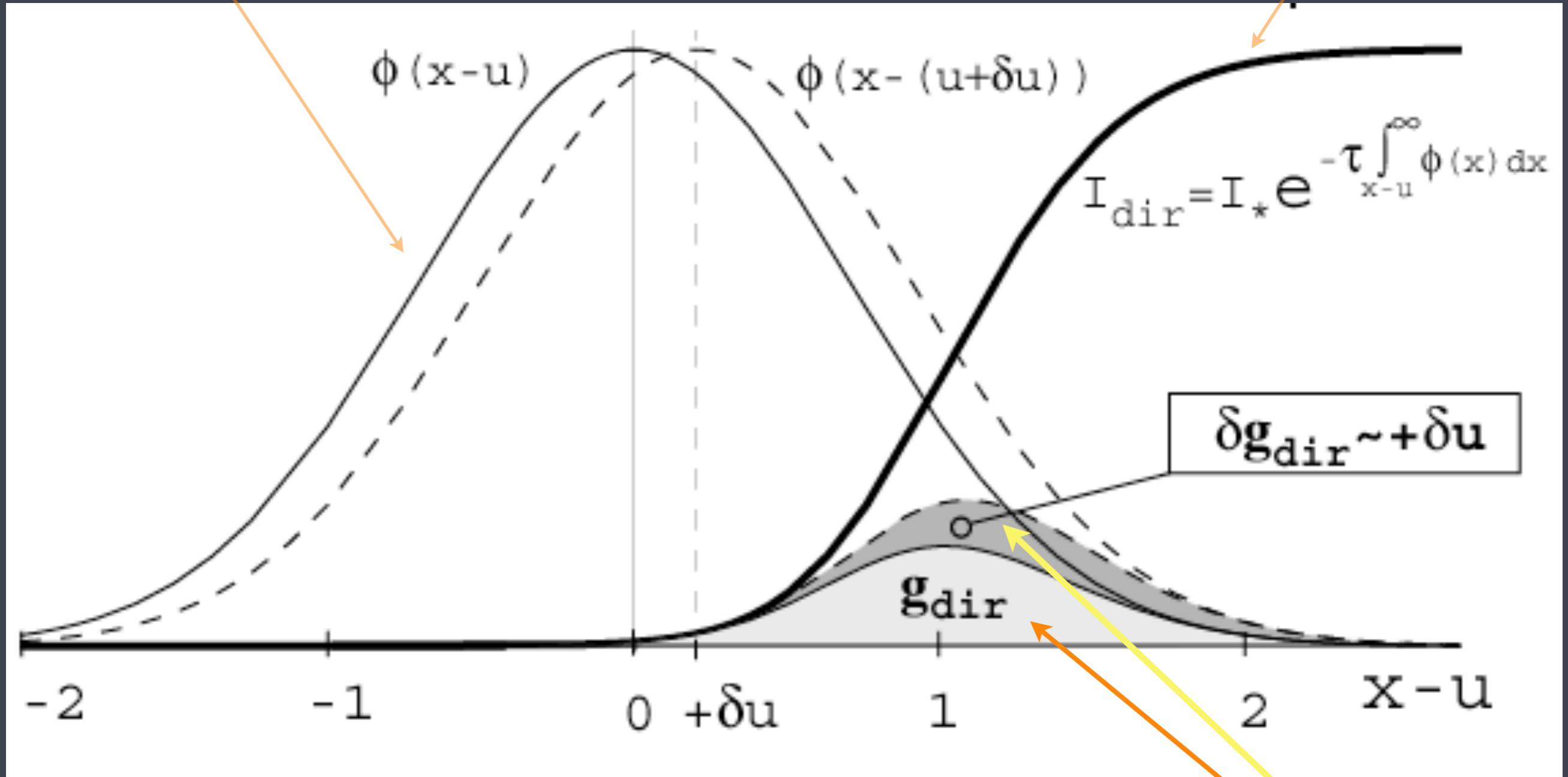


frequency

radiation force

positive velocity perturbation
line profile

photospheric radiation



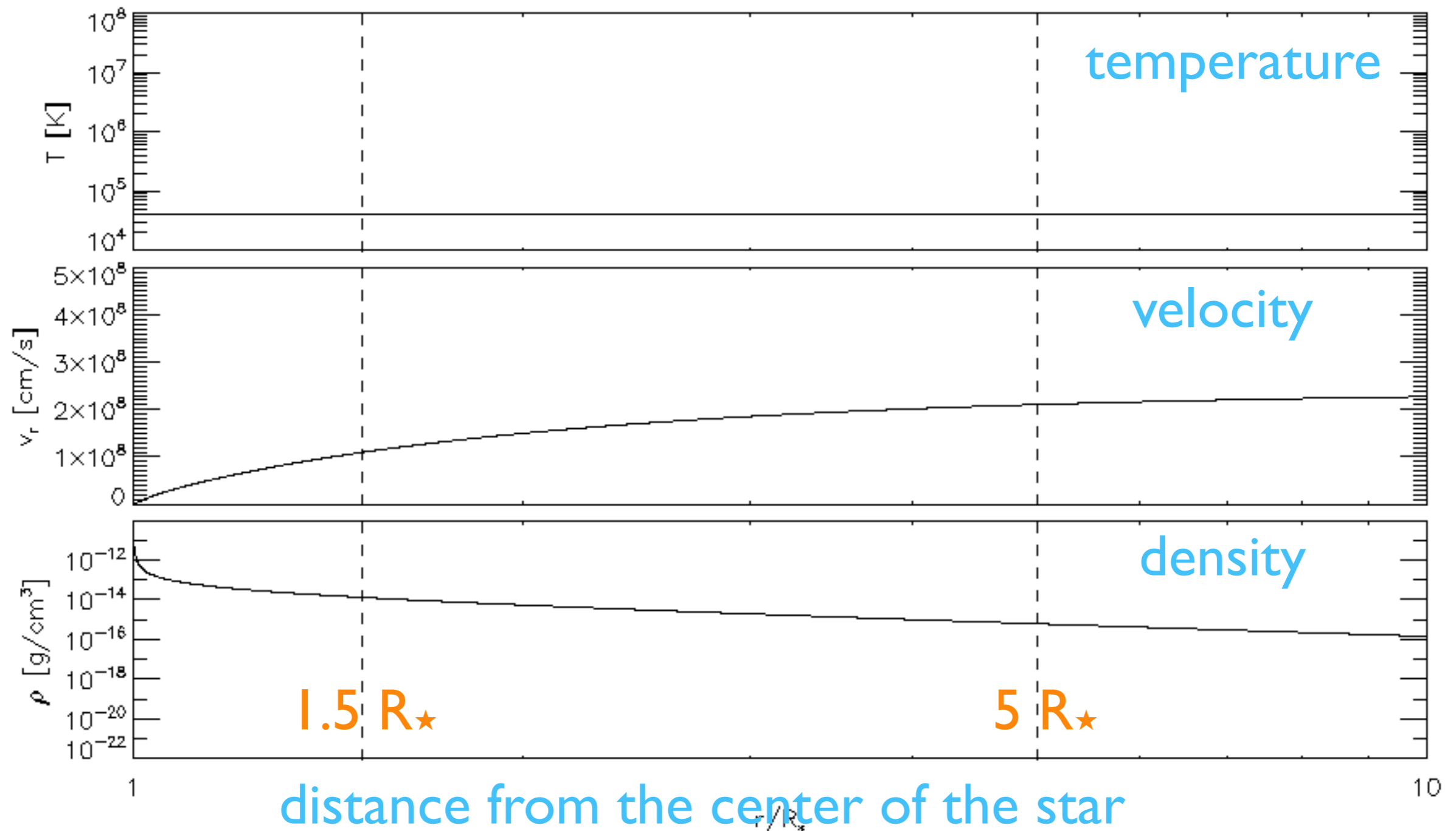
frequency

radiation force
increases

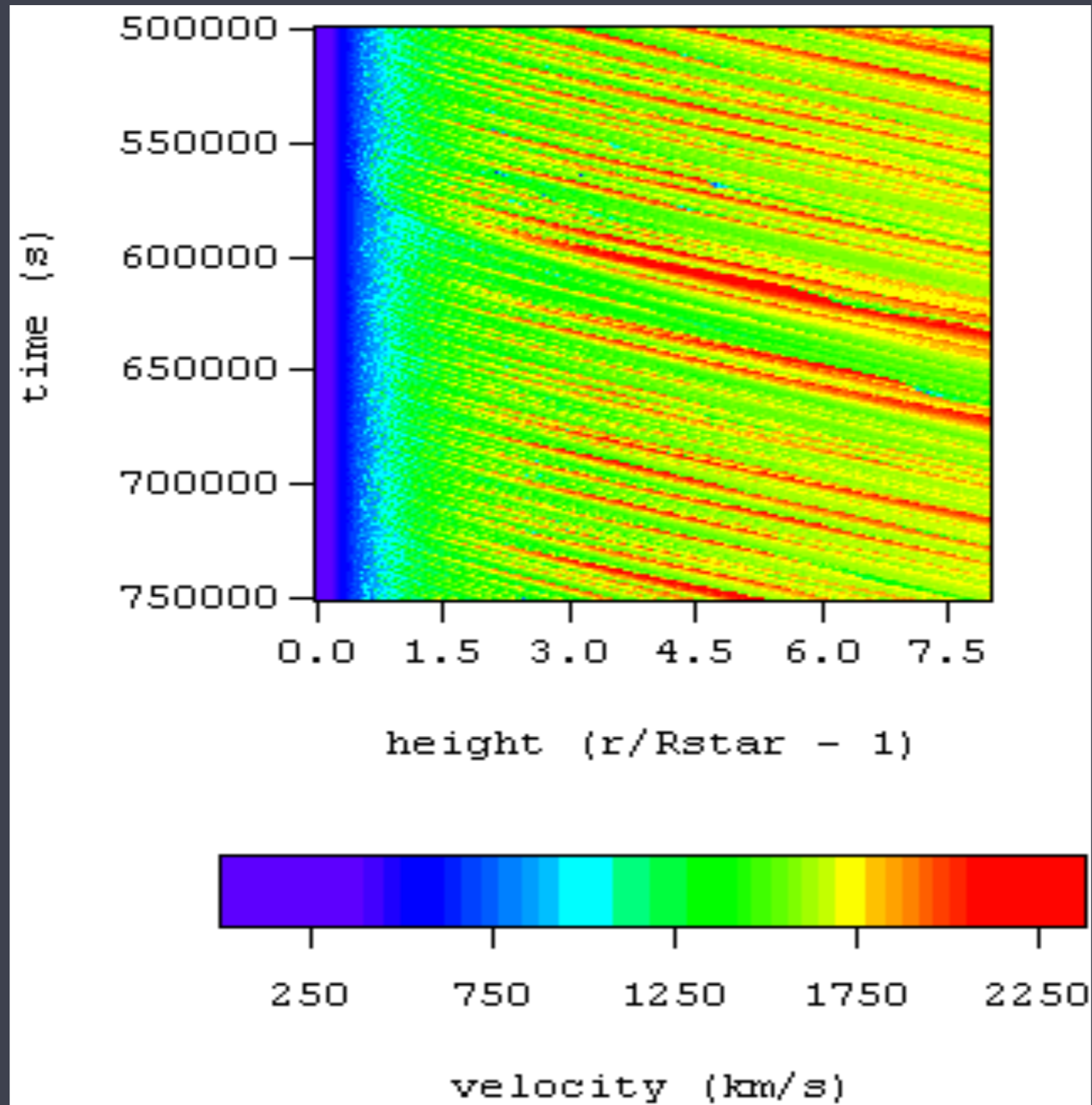
X-ray emitting plasma is embedded in the wind

intrinsic instability of radiative driving, Line Deshadowing Instability (LDI), leads to shock-heating of the wind

http://astro.swarthmore.edu/~cohen/projects/ldi/ifrc3_abbott0.65_xkovbc350_xmbko1.e-2_epsabs-1.e-20.gif



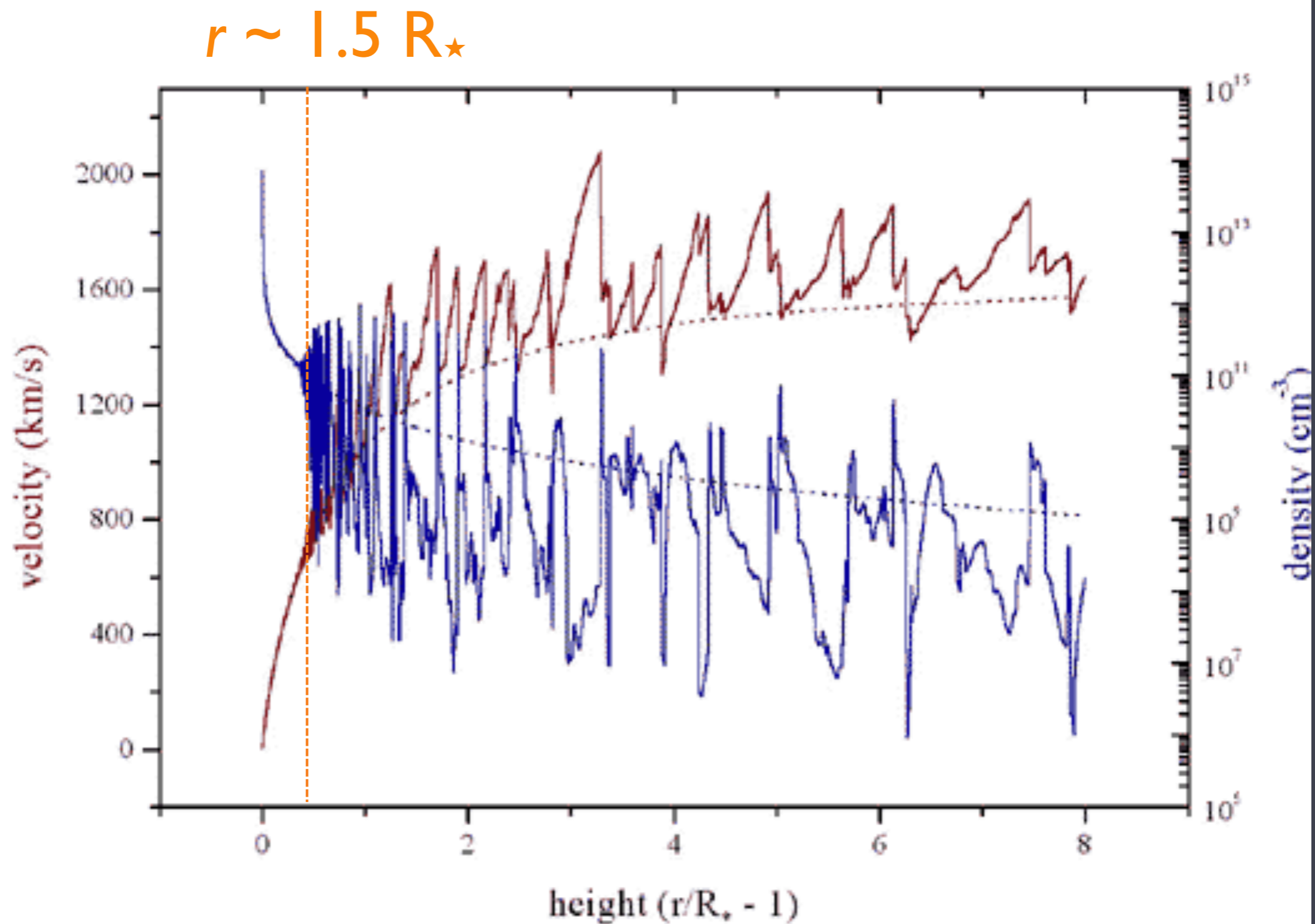
Numerical simulations of the line-deshadowing instability (LDI)



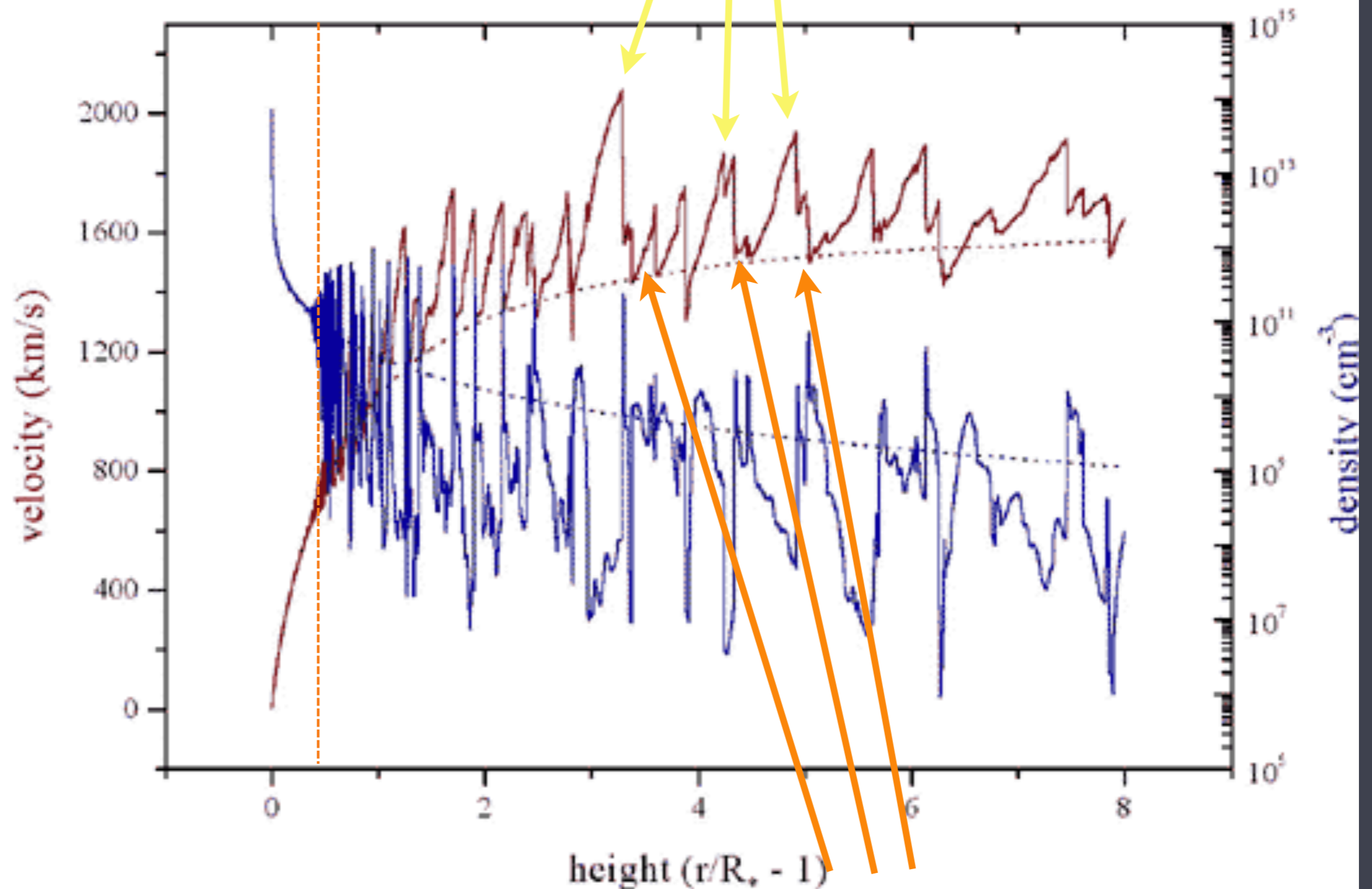
Owocki, Cooper, Cohen 1999

shock jump **velocities** ~ few 100 km/s

Numerous shock structures distributed above $r \sim 1.5 R_{\star}$

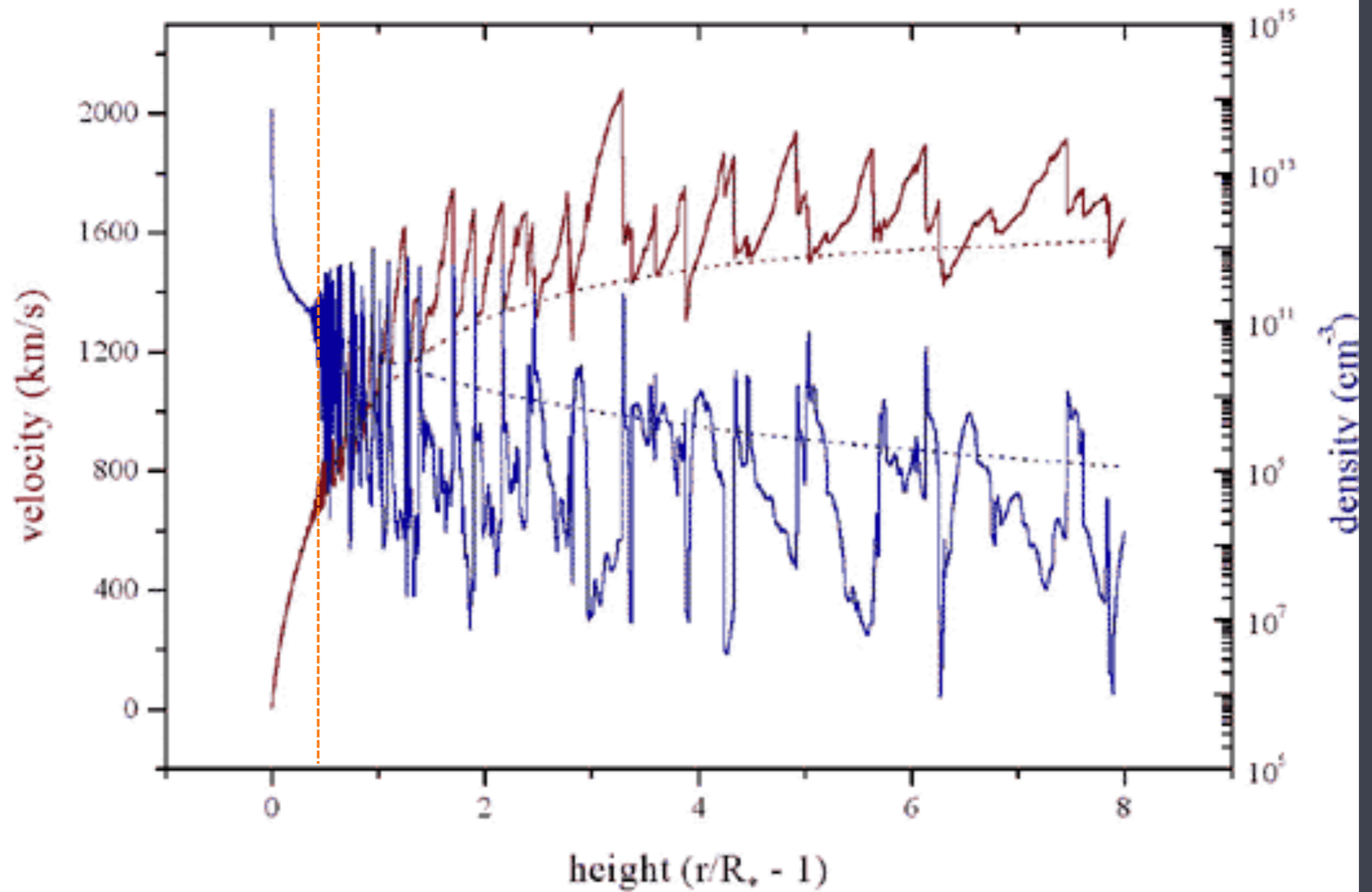


$V_{\text{shock}} \sim 300 \text{ km/s} : T \sim 10^6 \text{ K}$

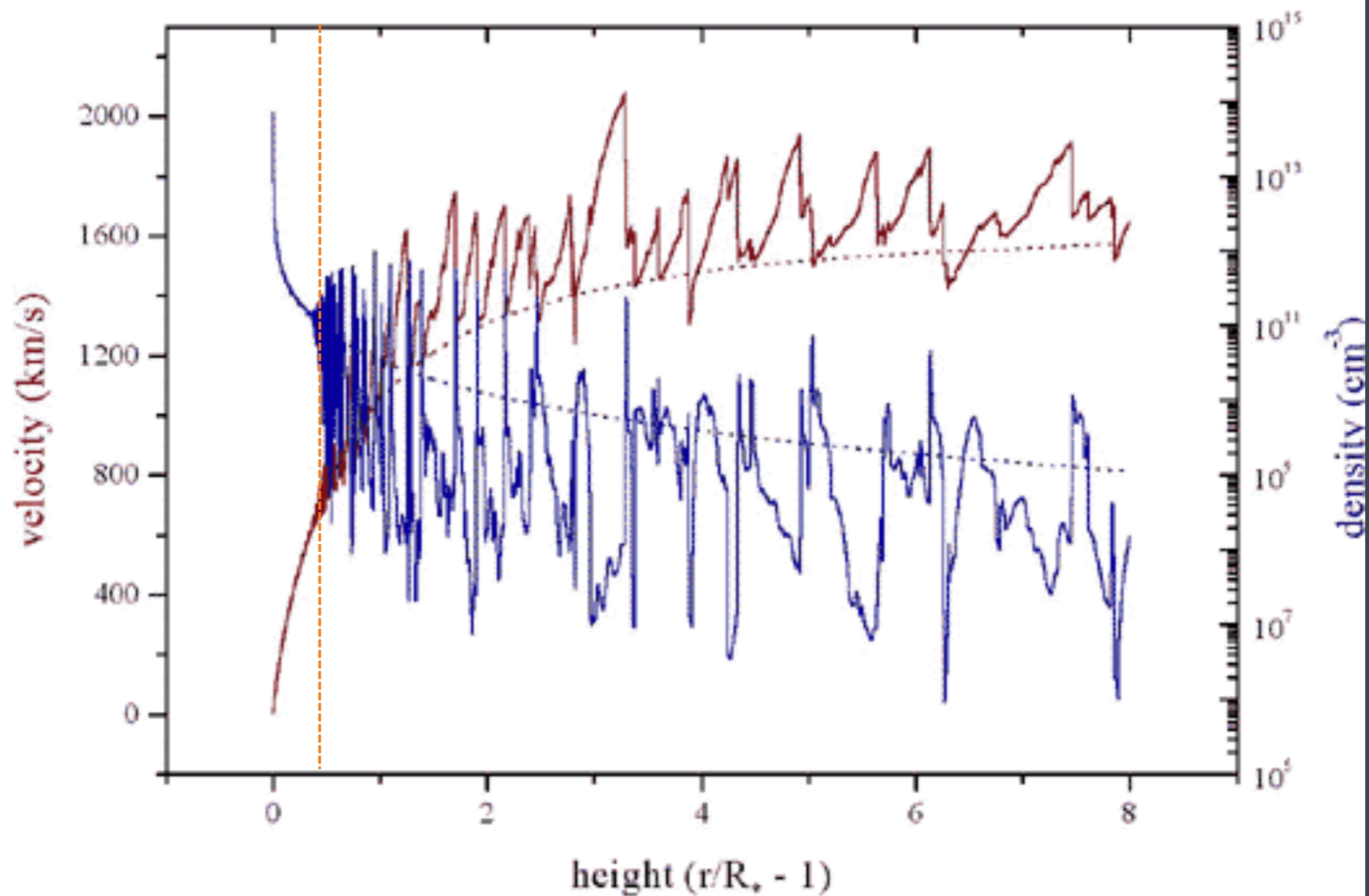


shocked wind plasma is decelerated back down to the local CAK wind velocity

Shocked plasma is moving at $v \sim 1000$ km/s

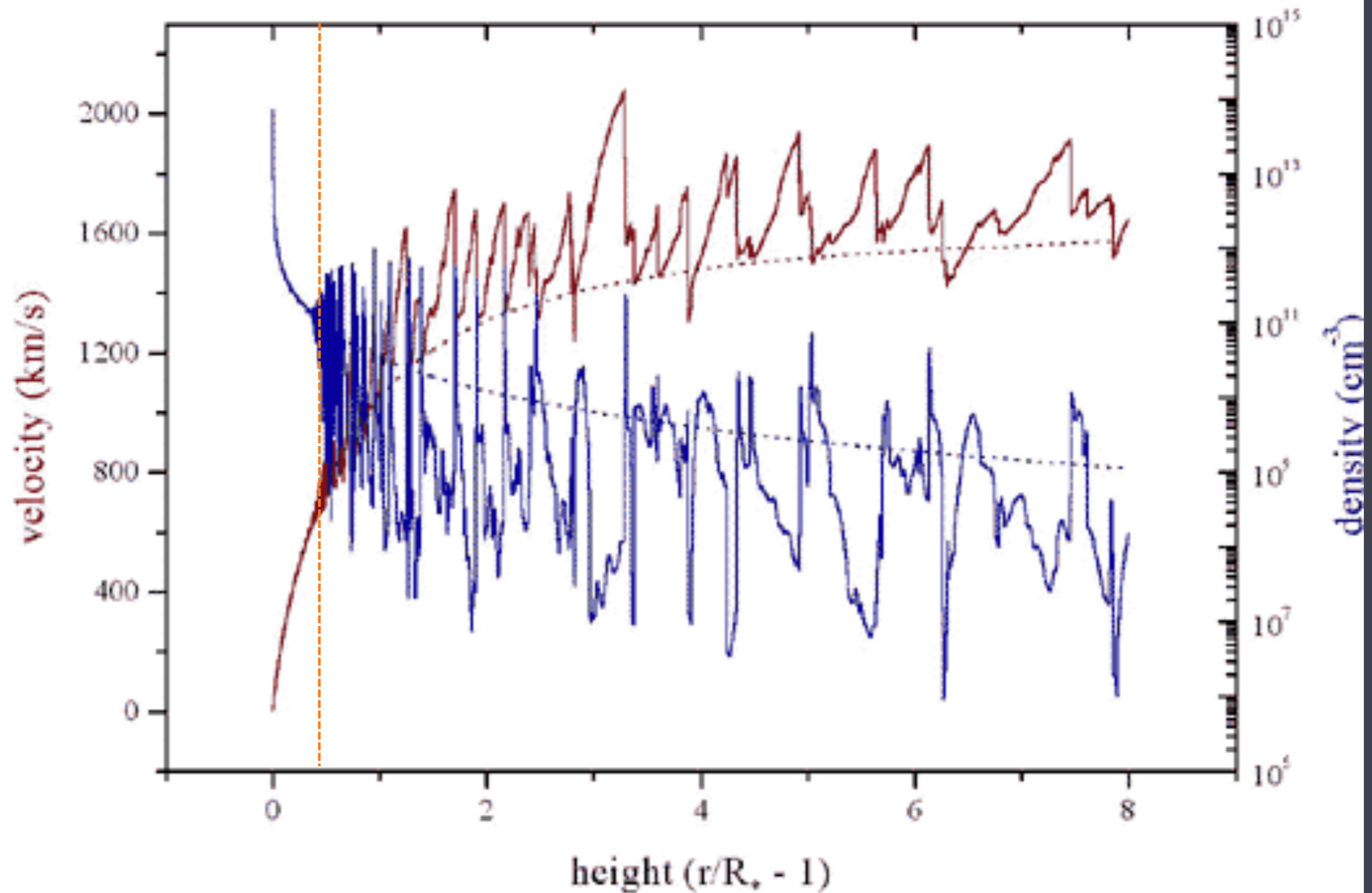


X-ray emission lines should be Doppler broadened



Less than 1% of the wind is emitting X-rays

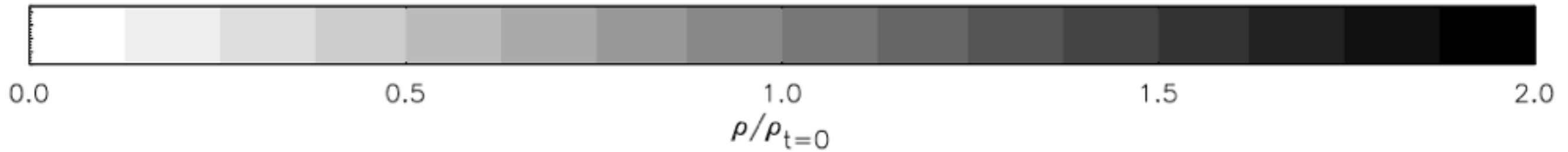
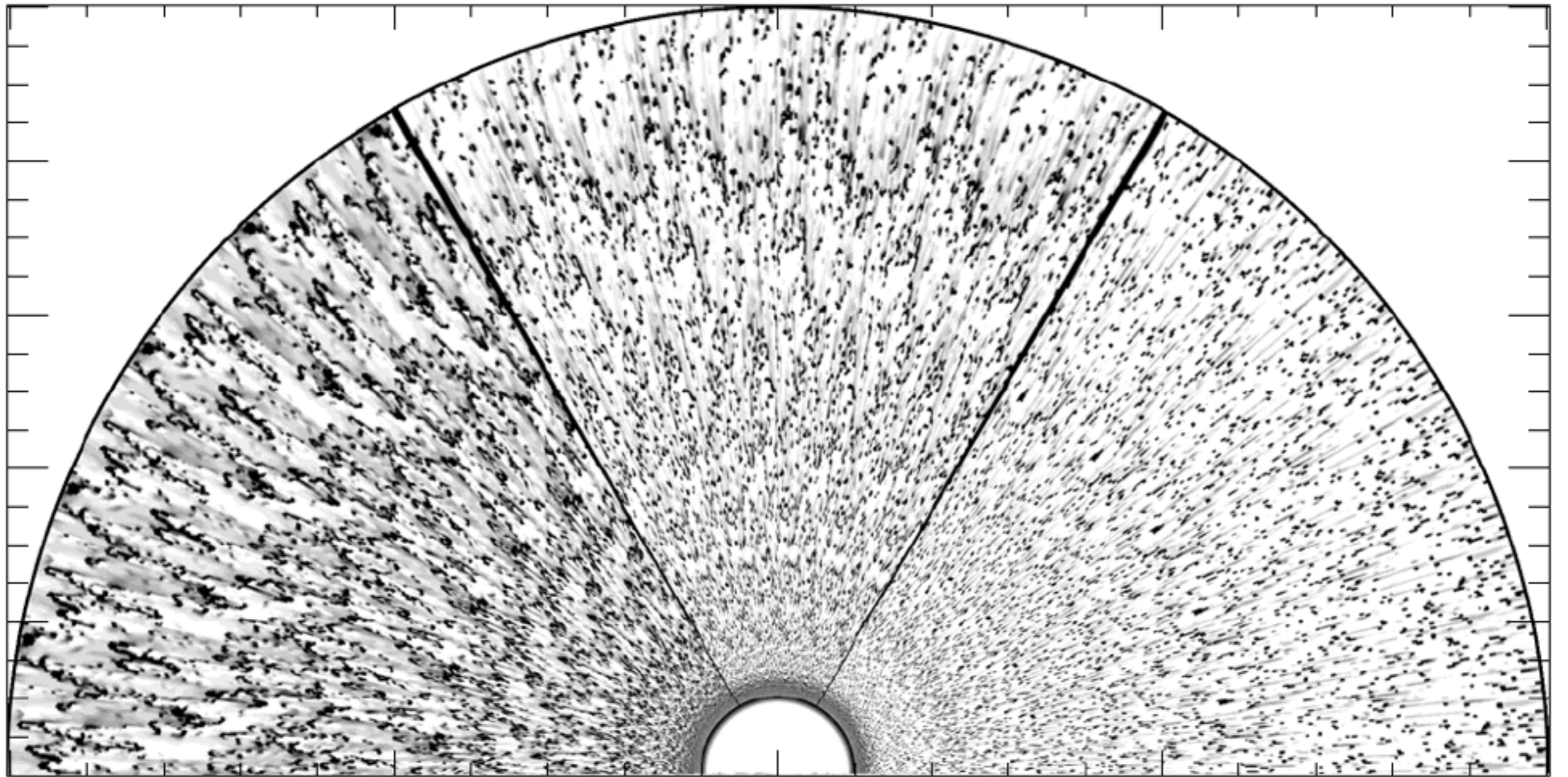
>99% of the wind is cold and X-ray absorbing



I-D is a severe limitation

lack of observed time variability suggests
numerous (> 100) individual post-shock cooling
volumes in the wind

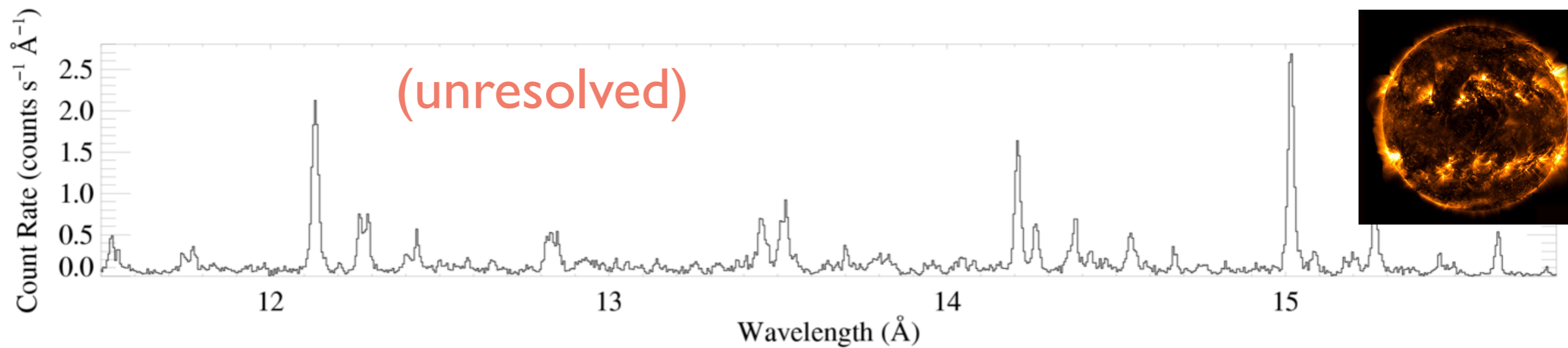
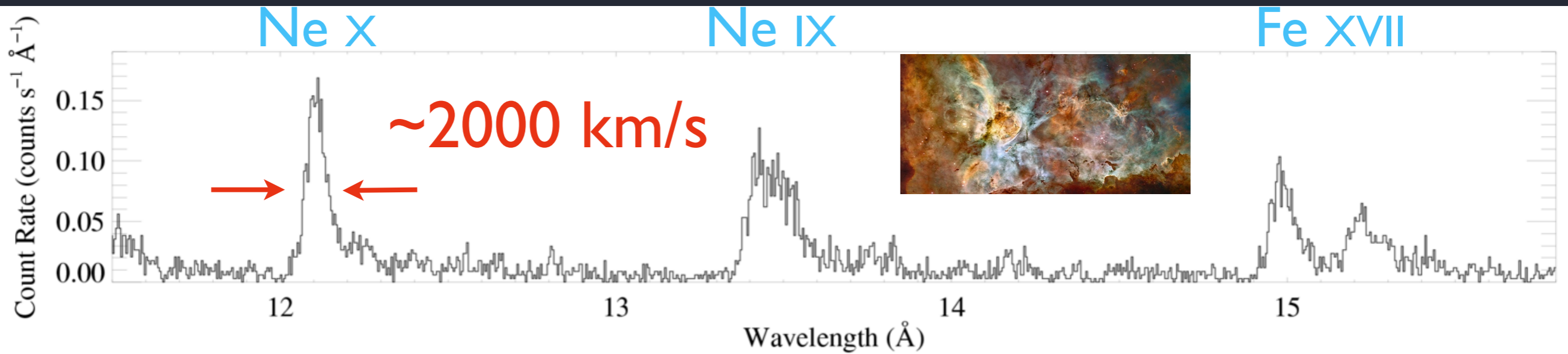
2-D simulations



Quantitative modeling of the X-ray spectrum based on
these LDI numerical hydro simulations

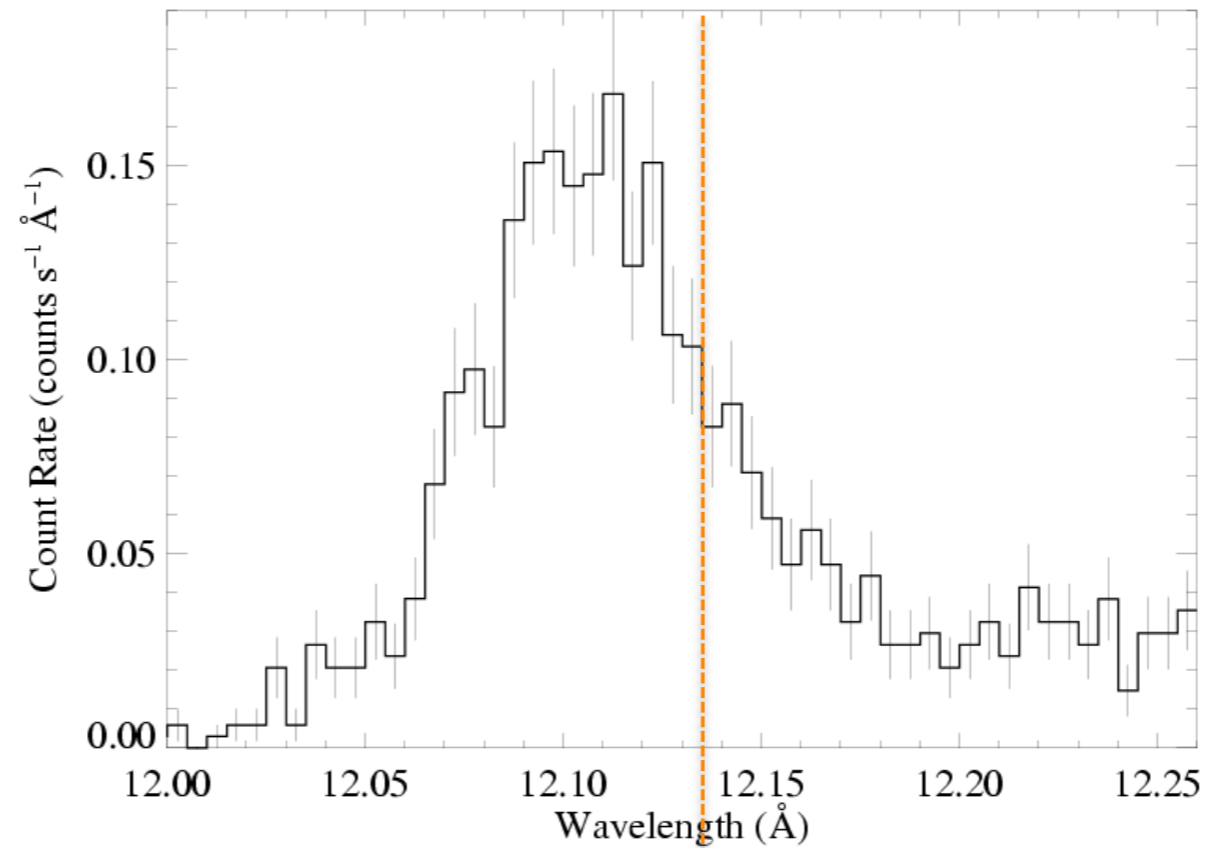
conclusive evidence that the X-ray plasma is in the stellar wind

ζ Pup (O4 If)

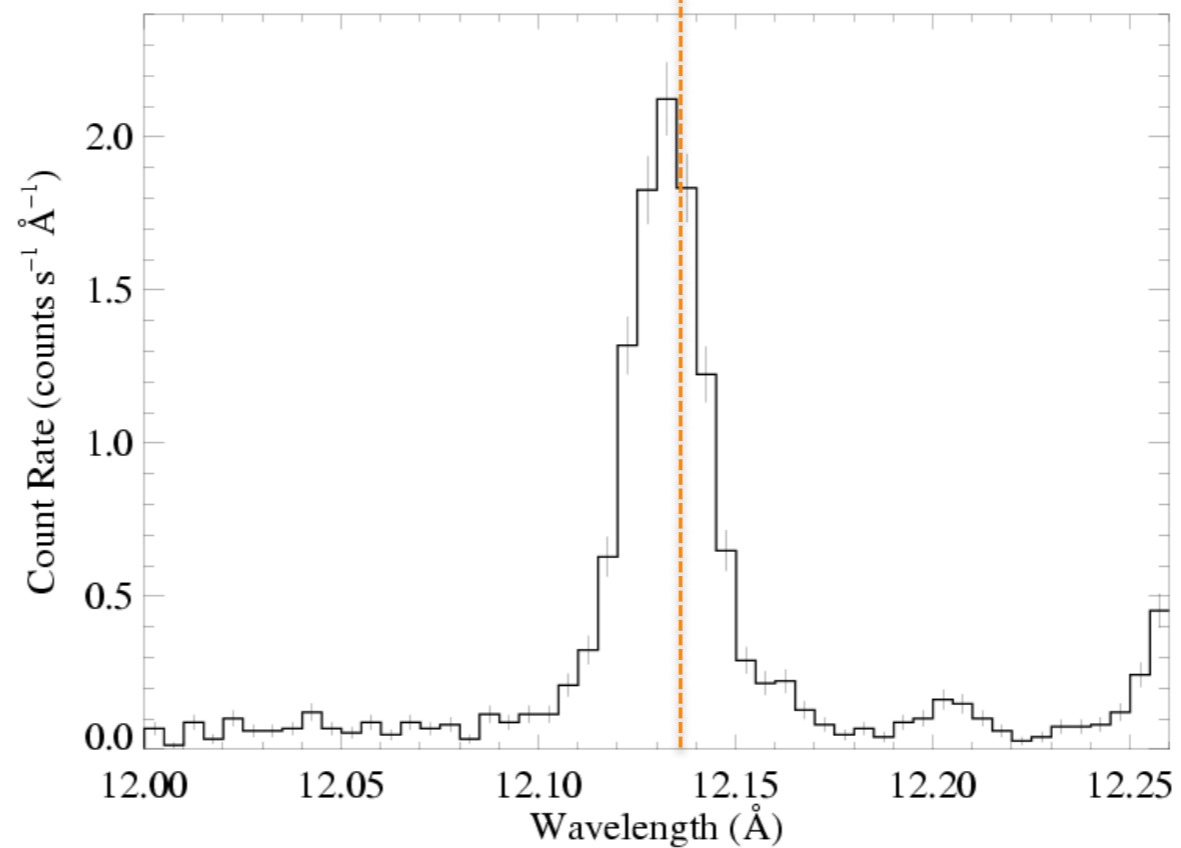


Capella (G5 III)

lines are
asymmetric

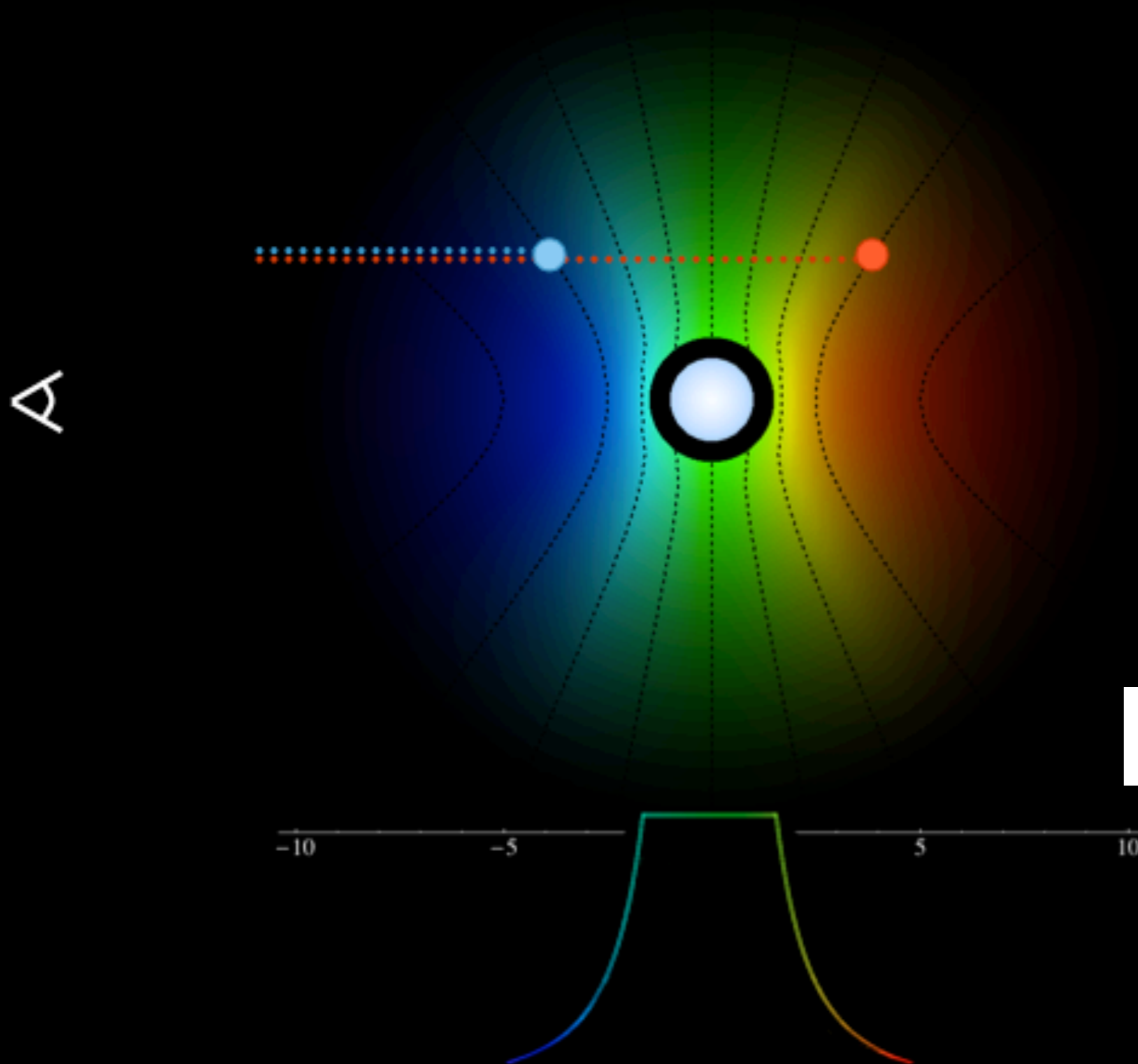


ζ Pup (O4If)

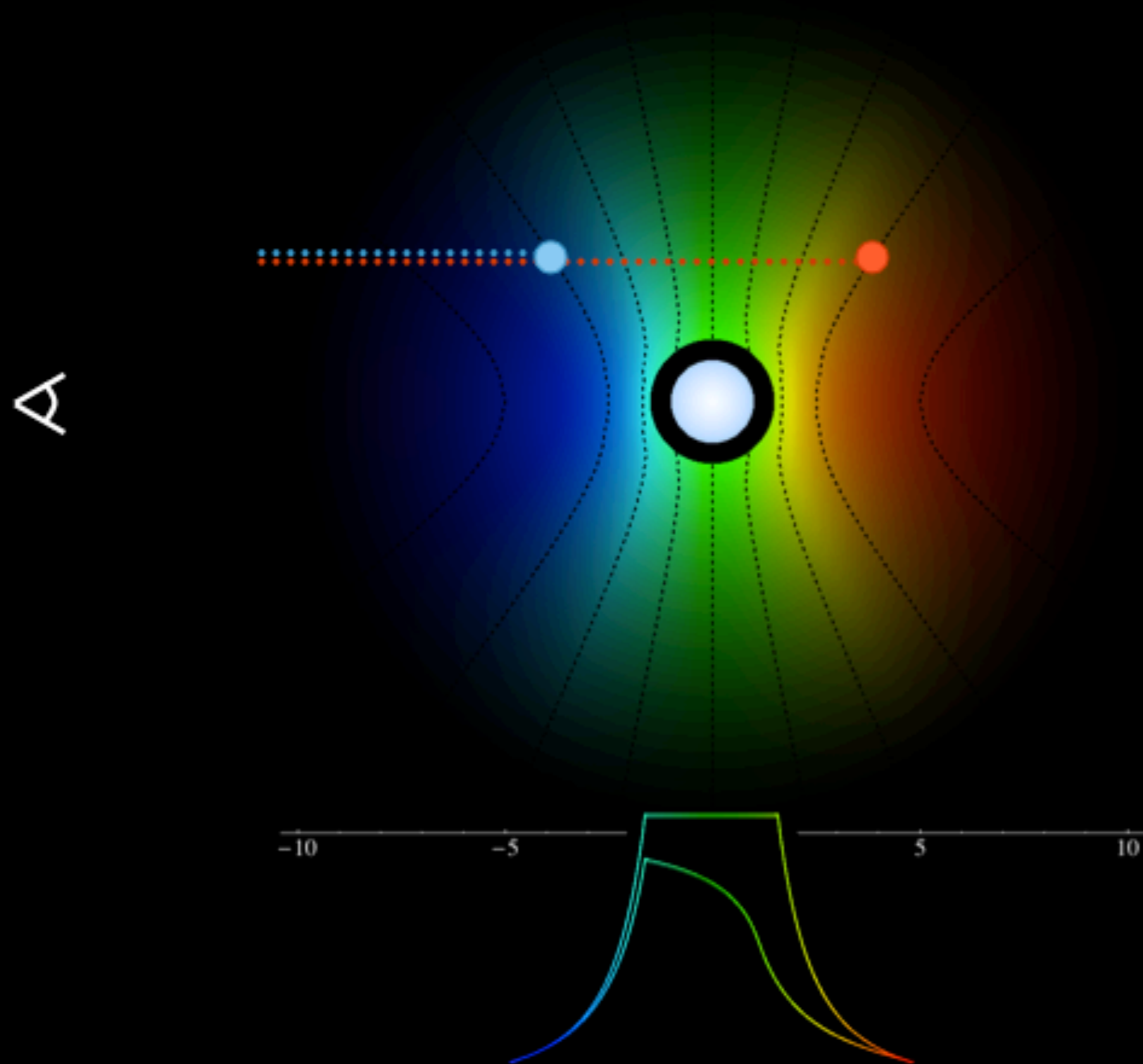


Capella (G5 III)

Line Asymmetry



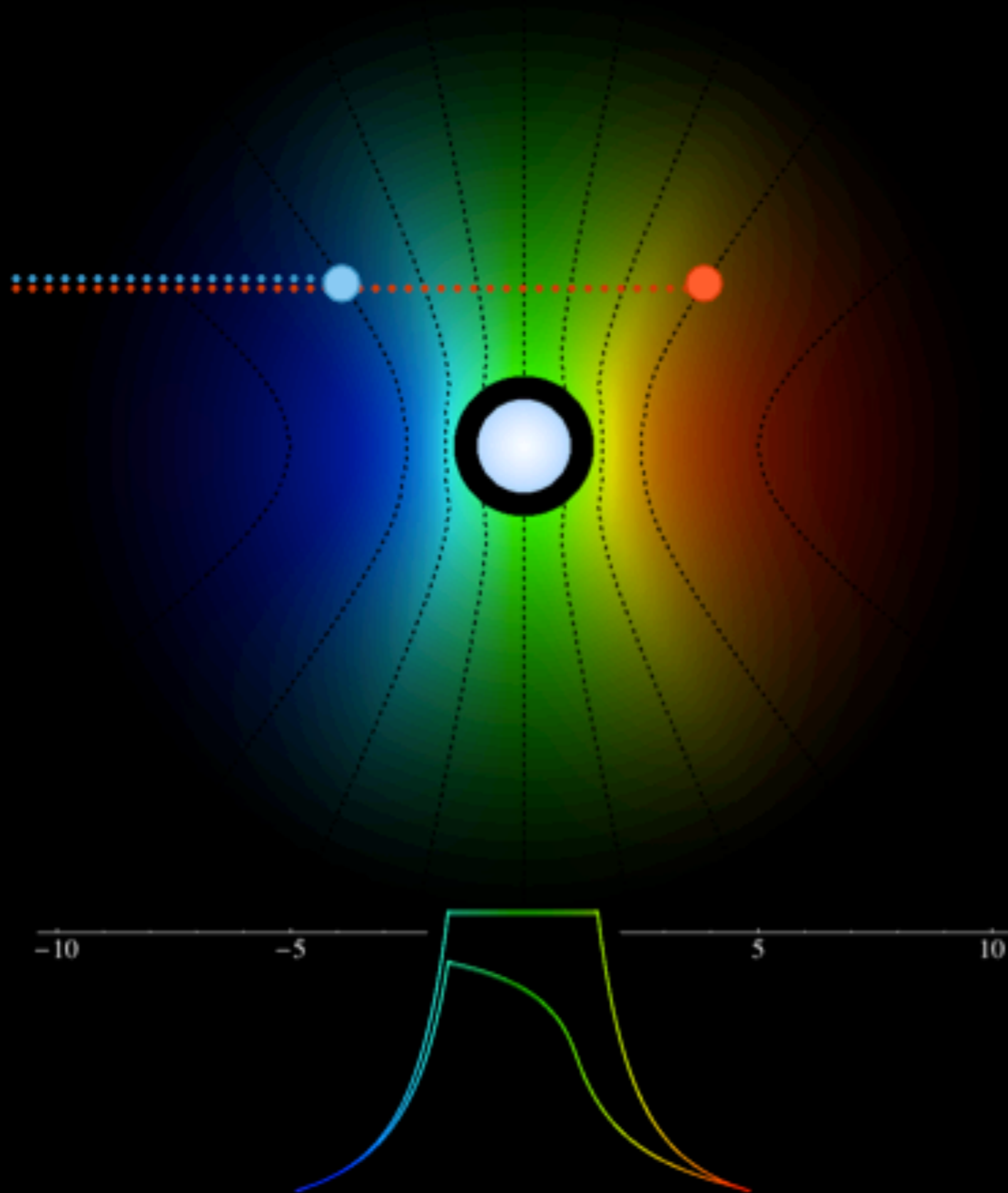
Line Asymmetry



Line Asymmetry

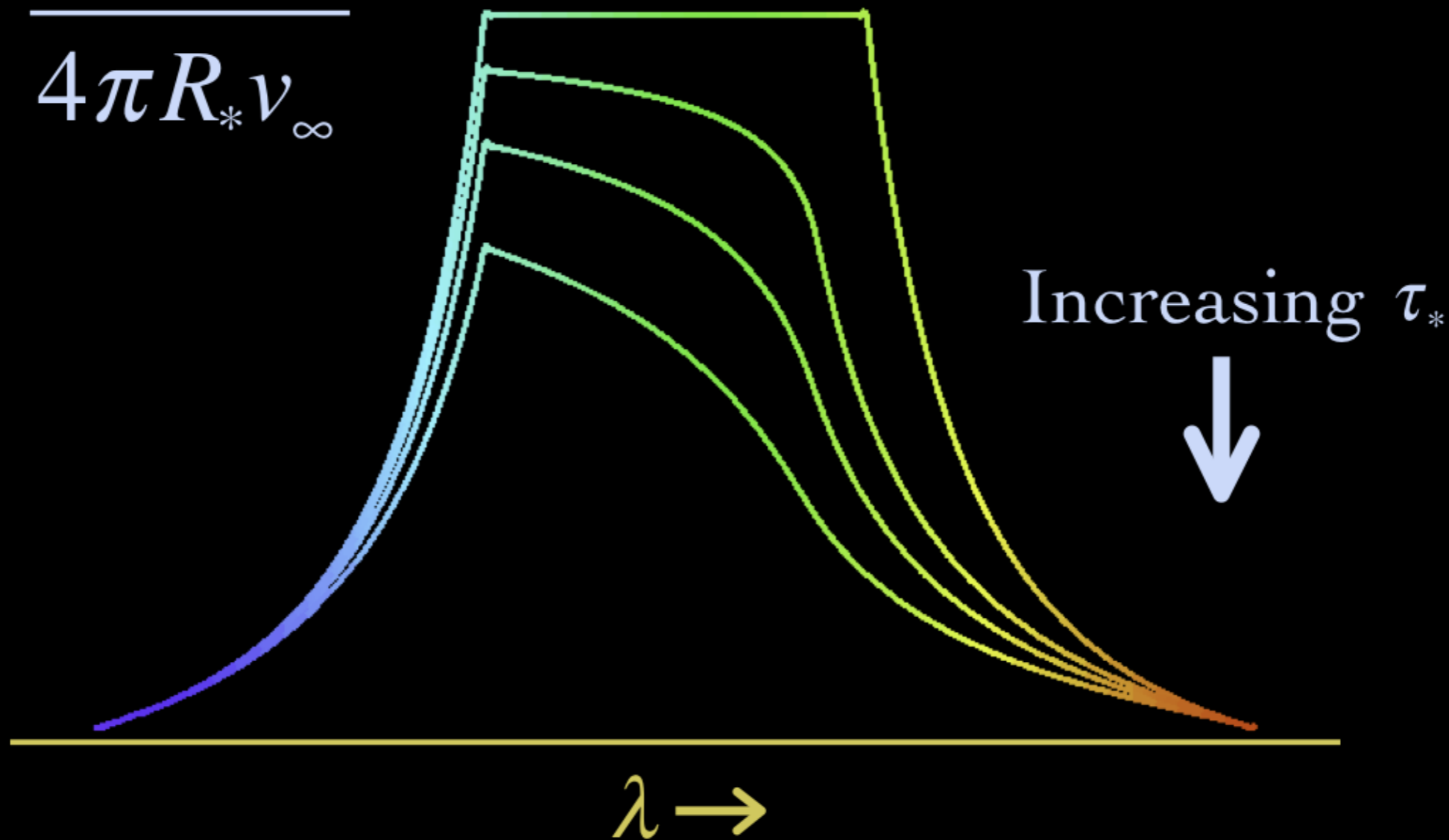
$$\tau = \tau_* \int_z^\infty \frac{R_* dz'}{r'^2 (1 - R_*/r')^\beta}$$

A

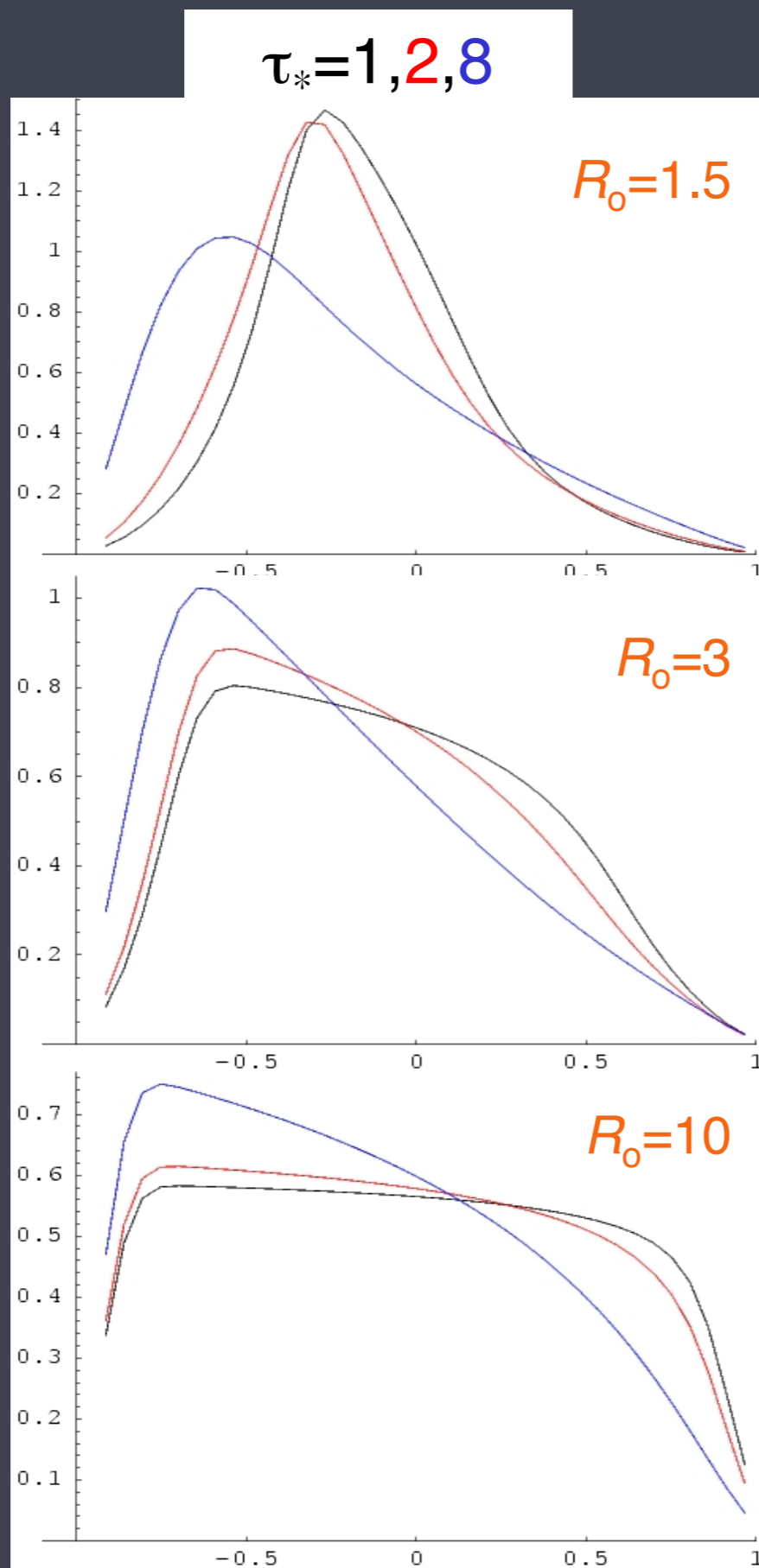
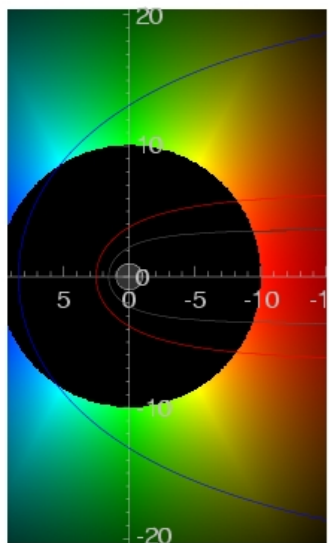
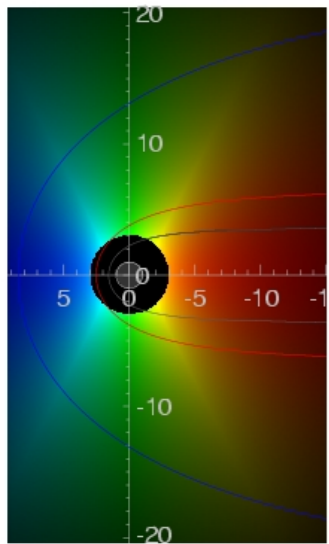
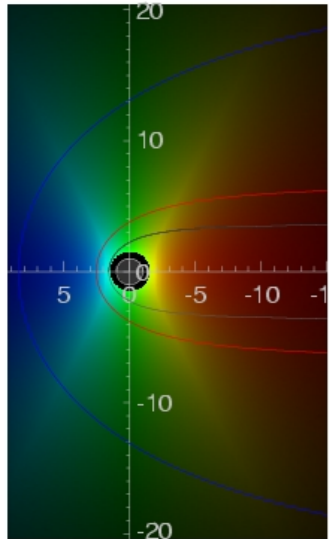


Wind Profile Model

$$\tau_* = \frac{\kappa \dot{M}}{4\pi R_* v_\infty}$$



Line profile shapes



key parameters: R_0 & τ_*

$$v = v_\infty (1 - r/R_*)^\beta$$

$$j \sim \rho^2 \text{ for } r/R_* > R_0, \\ = 0 \text{ otherwise}$$

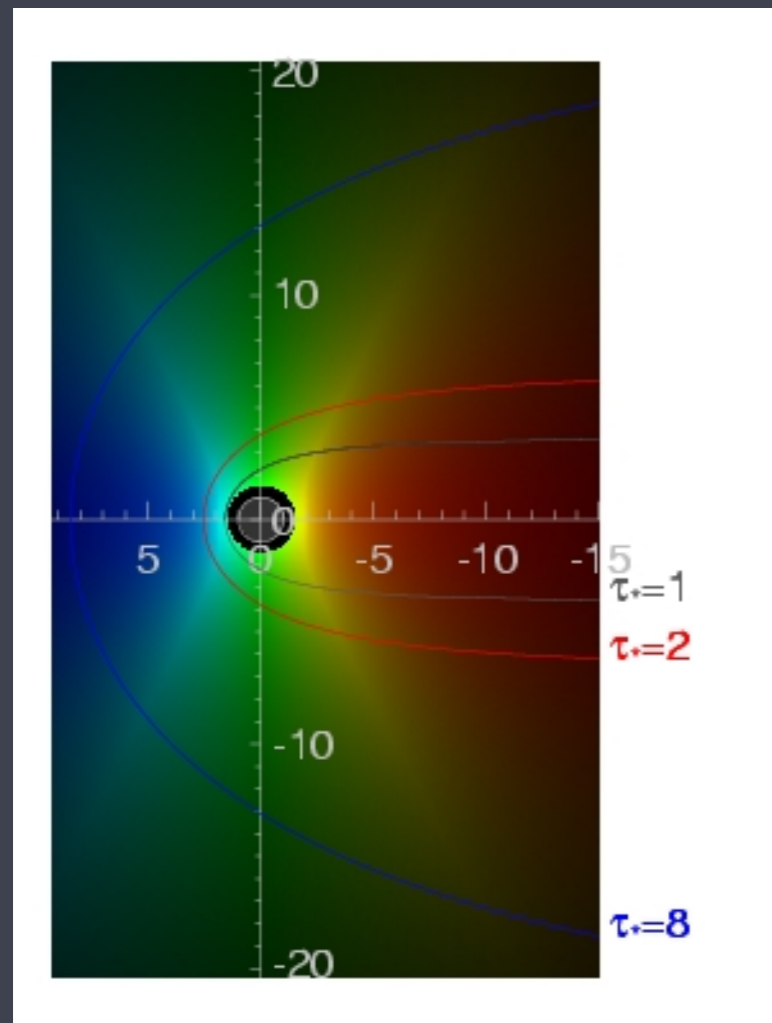
$$\tau = \tau_* \int_z^\infty \frac{R_* dz'}{r'^2 (1 - R_*/r')^\beta}$$

$$\tau_* \equiv \frac{\kappa \dot{M}}{4\pi R_* v_\infty}$$

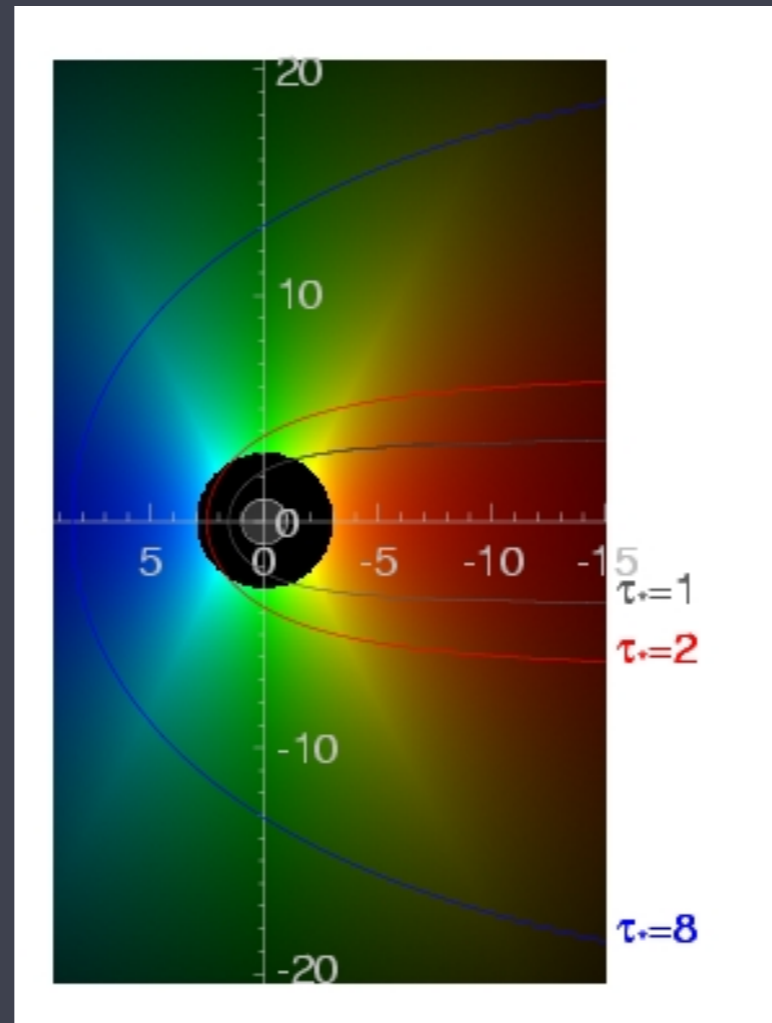
Hot plasma kinematics and location

R_o controls the line width via $v(r)$

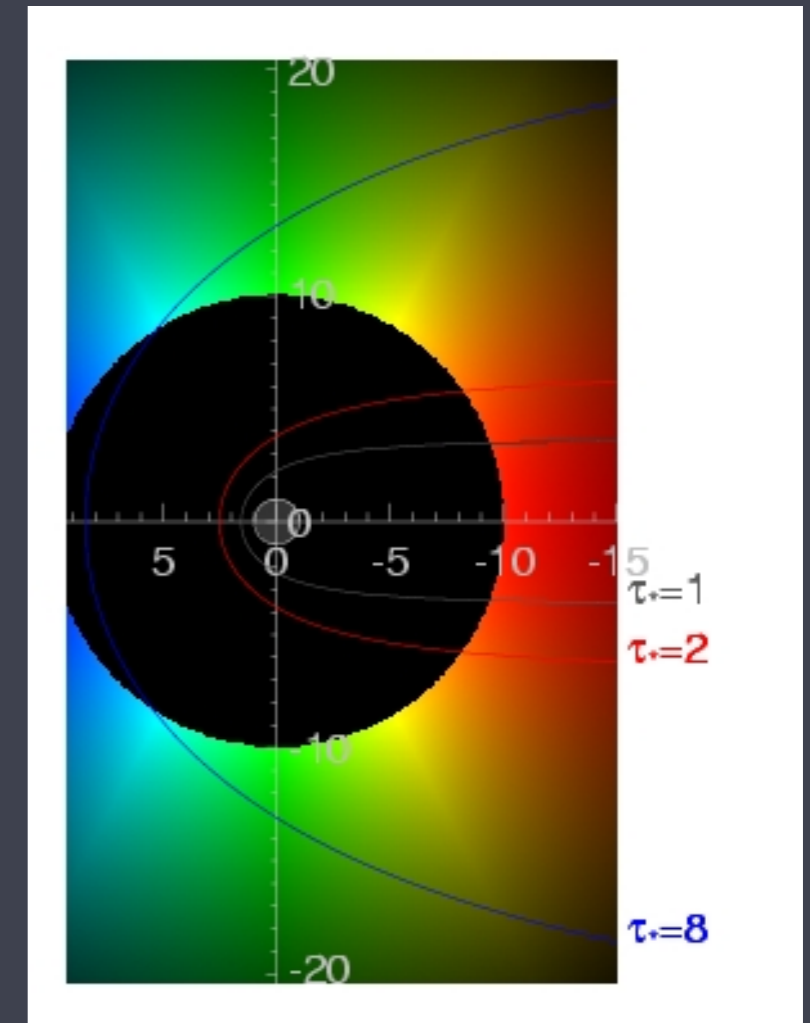
$R_o = 1.5 R_\star$



$R_o = 3 R_\star$

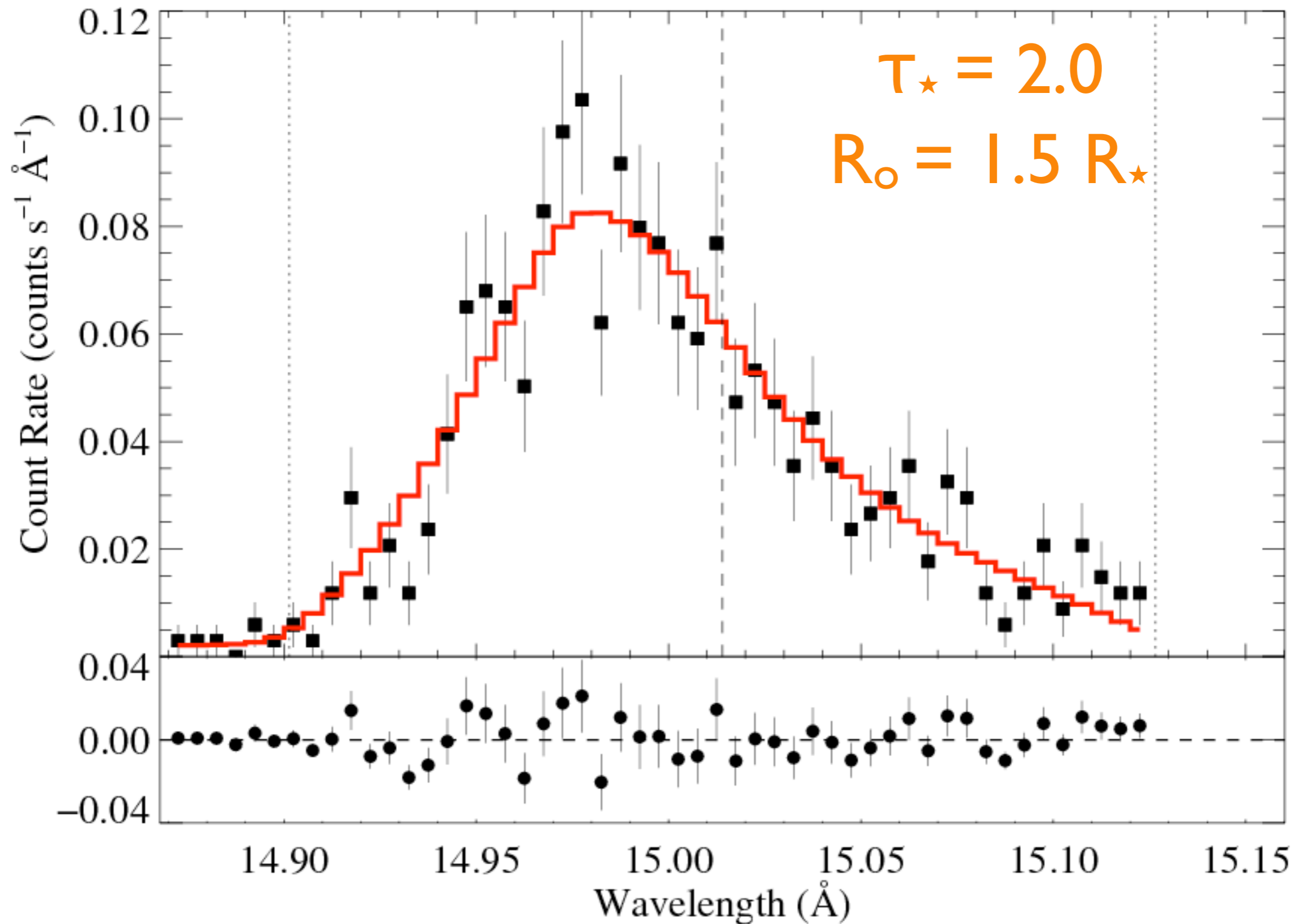


$R_o = 10 R_\star$



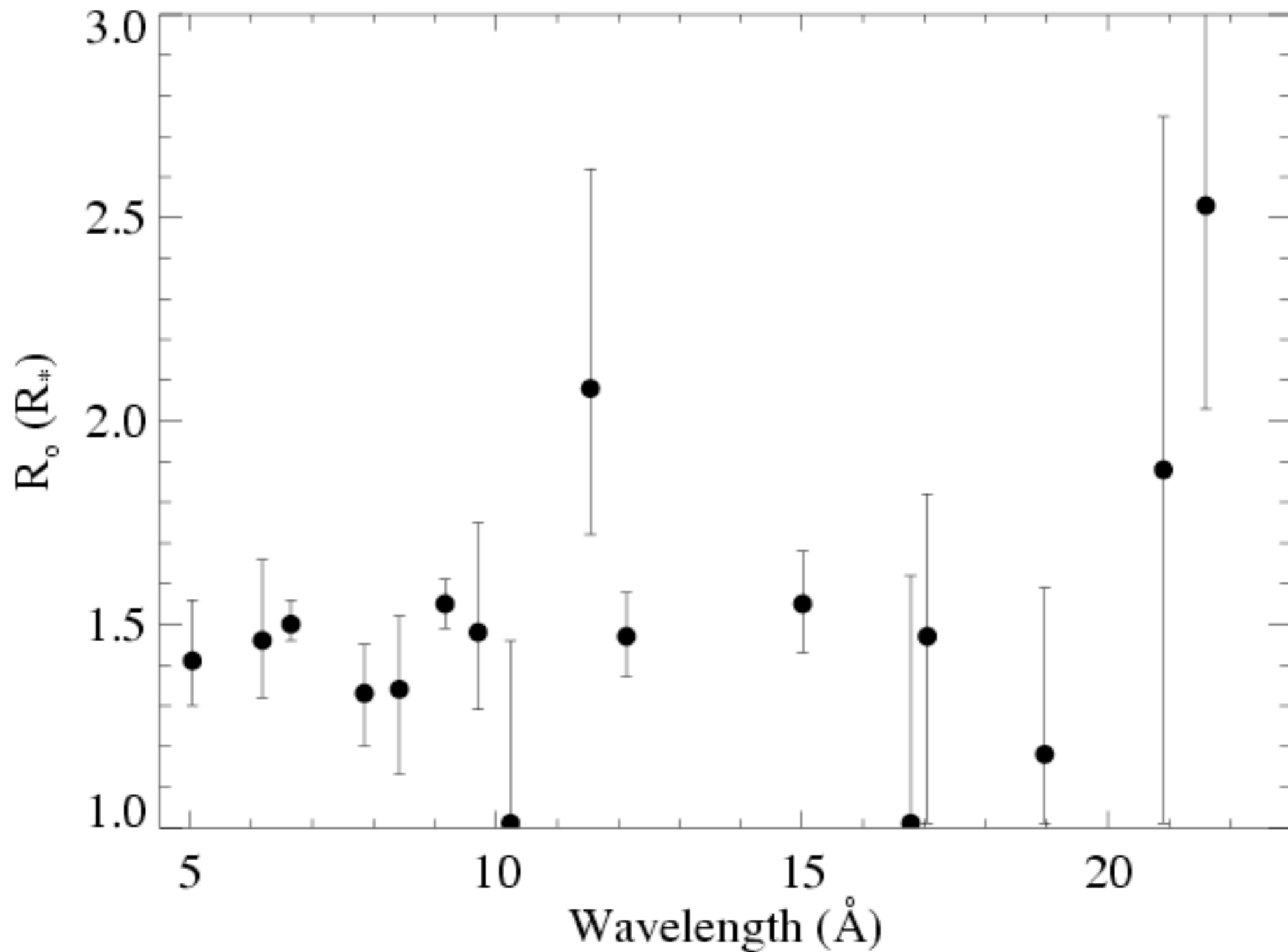
ζ Pup: Chandra MEG

Fe XVII

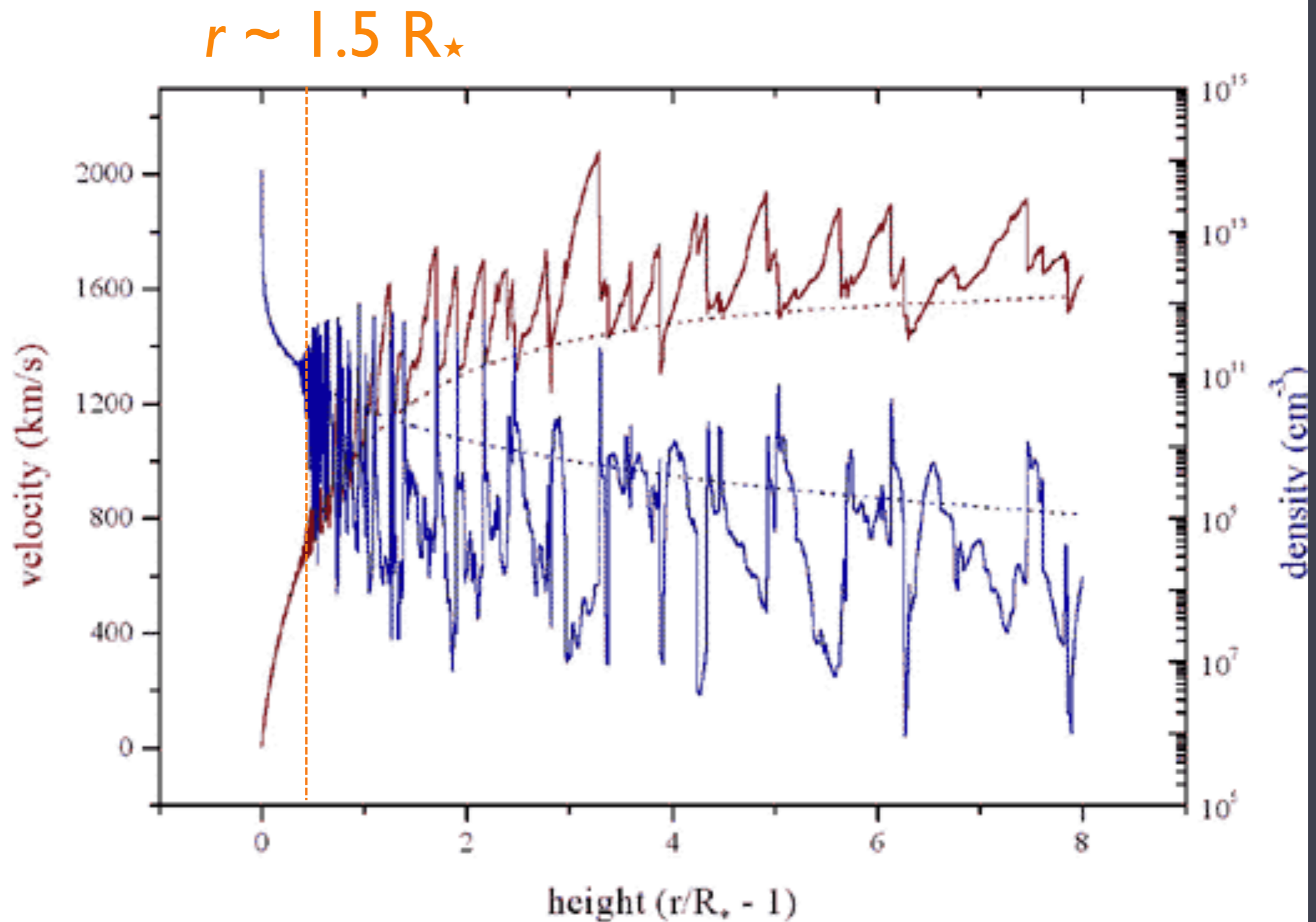


Distribution of R_o values for ζ Pup

consistent with a global value of $R_o = 1.5 R_\star$



Numerous shock structures distributed above $r \sim 1.5 R_{\star}$

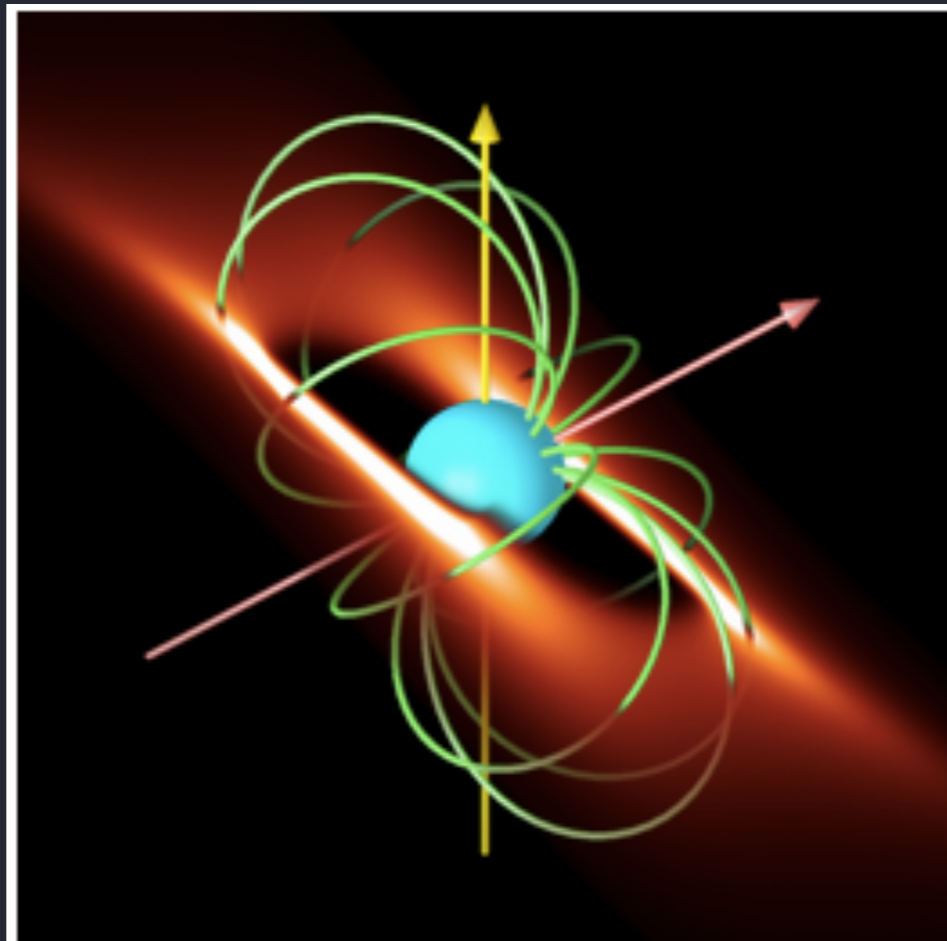


A subset of massive stars have large-scale
magnetic fields

this provides a variation on the wind-shock mechanism...

the Magnetically Channeled Wind Shock
mechanism (MCWS)

~10% of massive stars are magnetic
unlike solar type magnetism, though:
time-constant, not dynamo generated, often
large-scale dipole



A simulation of the circumstellar
matter distribution of σ Ori E, as
predicted by the Rigidly Rotating
Magnetosphere mode

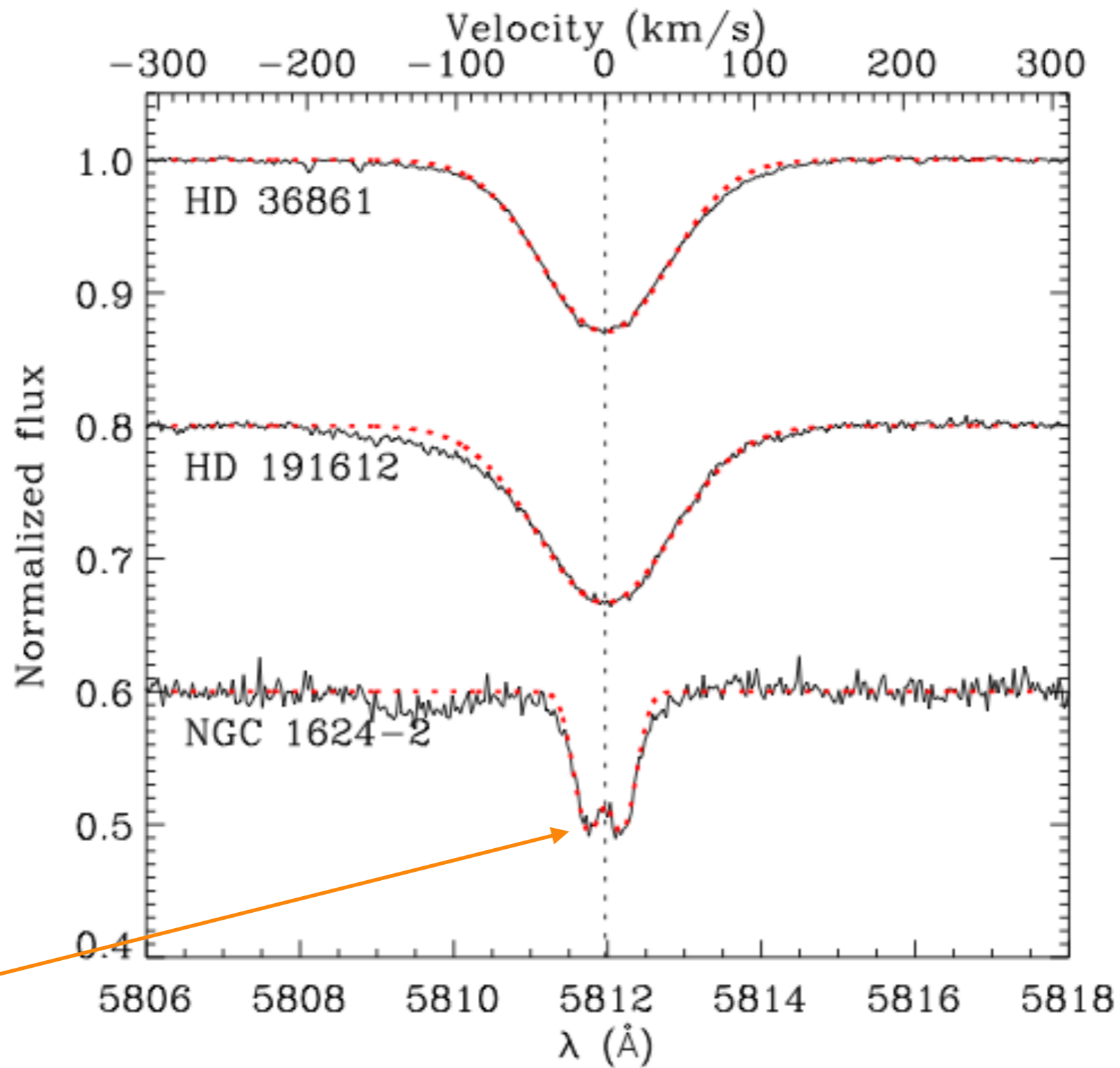
The MiMeS project: overview and current status

Gregg A. Wade¹, Evelyne Alecian², David A. Bohlender³,
Jean-Claude Bouret⁴, David H. Cohen⁵, Vincent Duez⁶, Marc
Gagné⁷, Jason H. Grunhut¹, Huib F. Henrichs⁸, Nick R. Hill⁹, Oleg
Kochukhov¹⁰, Stéphane Mathis¹¹, Coralie Neiner¹², Mary E. Oksala¹³,
Stan Owocki¹³, Véronique Petit⁷, Matthew Shultz¹, Thomas
Rivinius¹⁴, Richard H. D. Townsend⁹, Jorick S. Vink¹⁵
and the MiMeS collaboration†

¹Kingston, Canada, ²LOAG, France, ³HIA, Canada, ⁴LAM, France, ⁵Swarthmore, USA,
⁶Argelander, Germany, ⁷West Chester, USA, ⁸Amsterdam, Netherlands, ⁹Madison, USA,
¹⁰Uppsala, Sweden, ¹¹CEA, France, ¹²Paris Observatory, France, ¹³Delaware, USA, ¹⁴ESO,
Chile, ¹⁵Armagh, UK

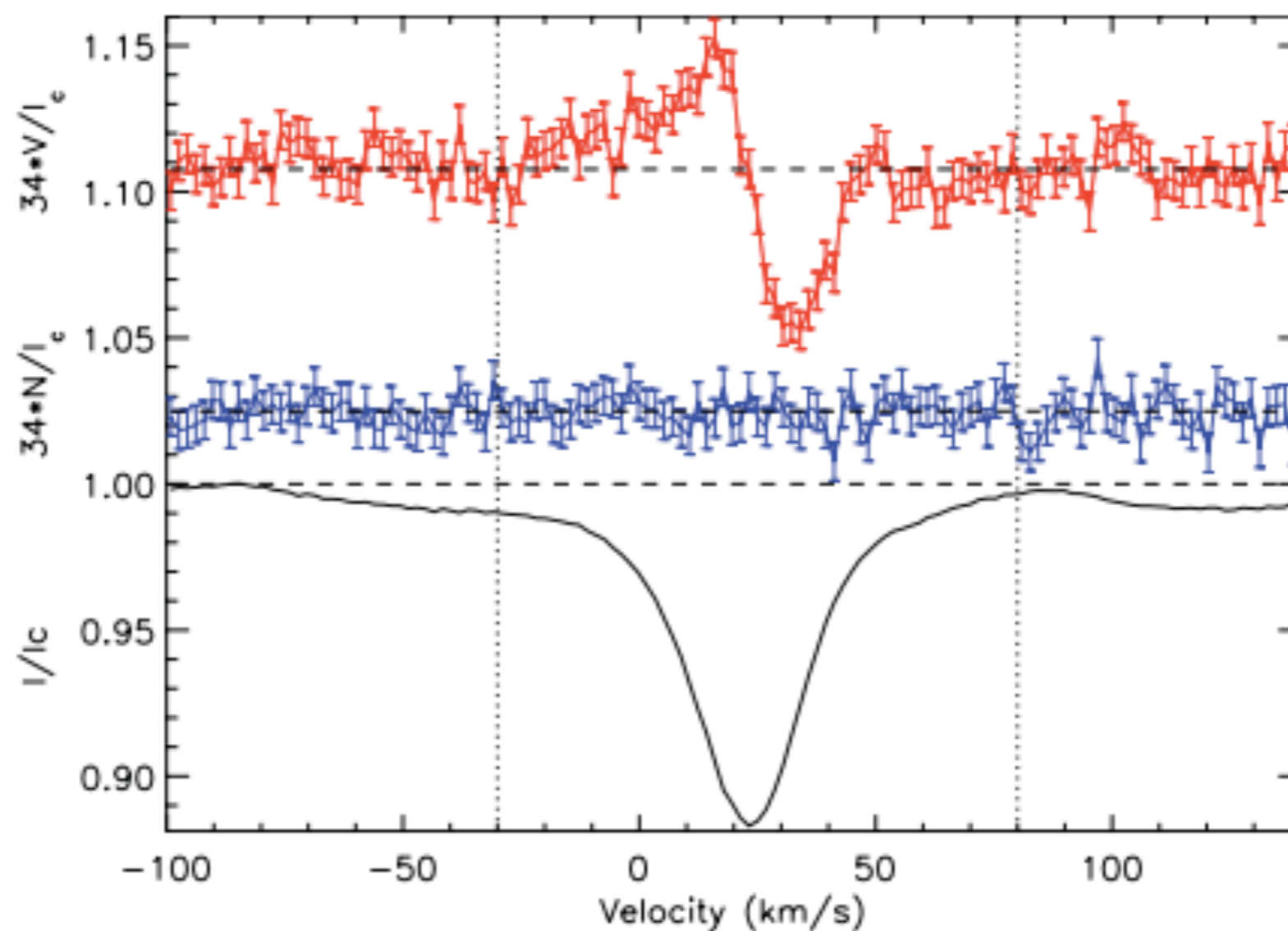
Abstract. The Magnetism in Massive Stars (MiMeS) Project is a consensus collaboration among many of the foremost international researchers of the physics of hot, massive stars, with the basic aim of understanding the origin, evolution and impact of magnetic fields in these objects. At the time of writing, MiMeS Large Programs have acquired over 950 high-resolution polarised spectra of about 150 individual stars with spectral types from B5-O4, discovering new magnetic fields in a dozen hot, massive stars. The quality of this spectral and magnetic matériel is very high, and the Collaboration is keen to connect with colleagues capable of exploiting the data in new or unforeseen ways. In this paper we review the structure of the MiMeS observing programs and report the status of observations, data modeling and development of related theory.

Zeeman splitting can be measured



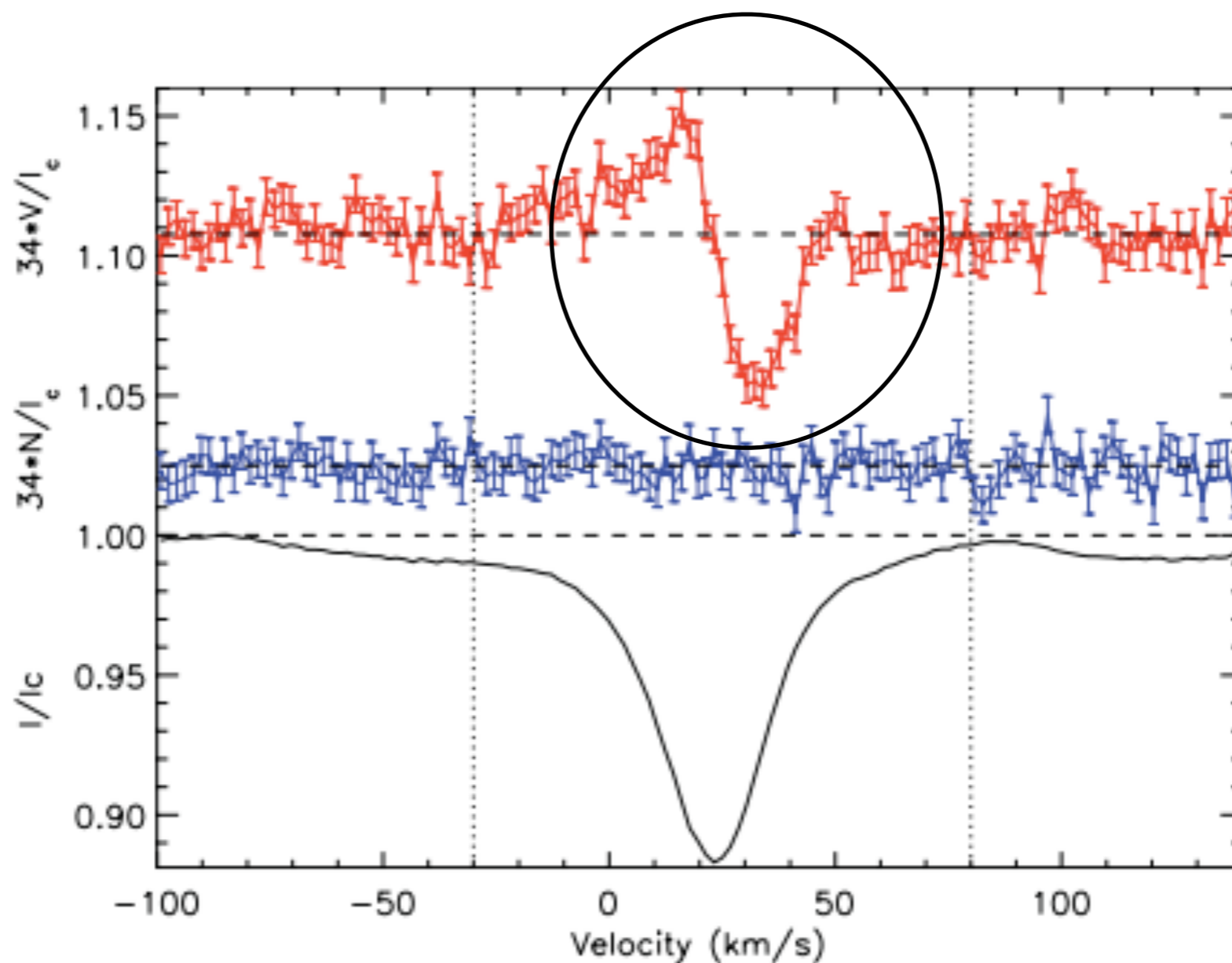
and for weaker magnetic fields, the Zeeman signal can be seen in circularly polarized light

G. A. Wade *et al.*



and for weaker magnetic fields, the Zeeman signal can be seen in circularly polarized light

G. A. Wade *et al.*



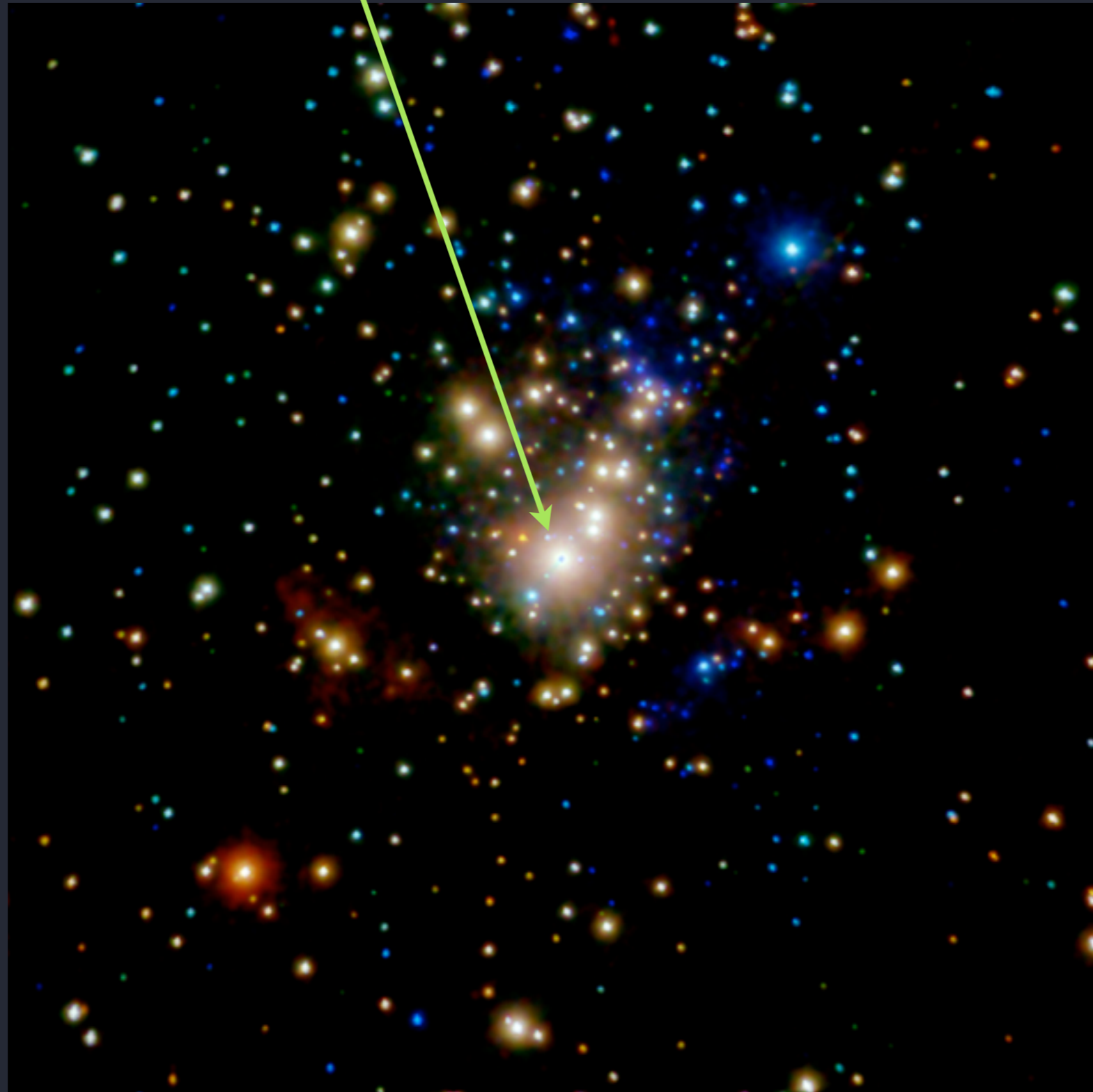
The O star that ionizes the Orion Nebula: ~ 1 kG tilted dipole



θ^1 Ori C

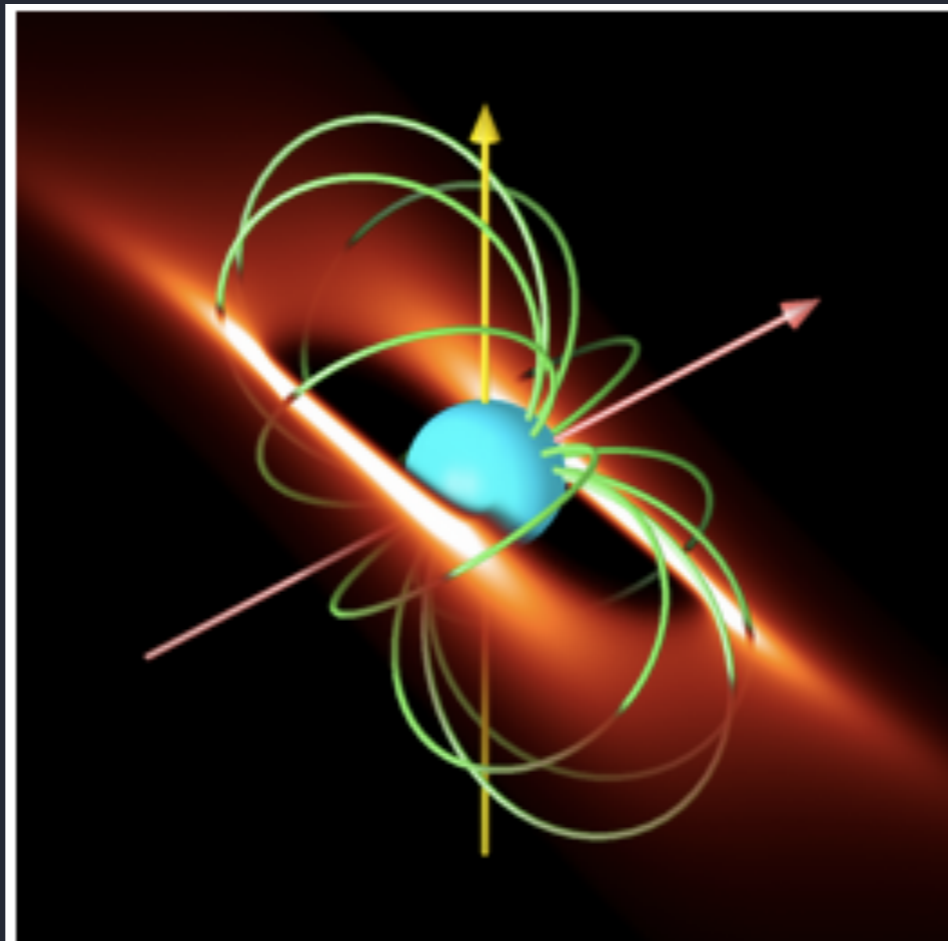
Chandra X-ray image of the Orion Nebula Cluster

θ^1 Ori C: very X-ray bright



Magnetic Wind Channeling

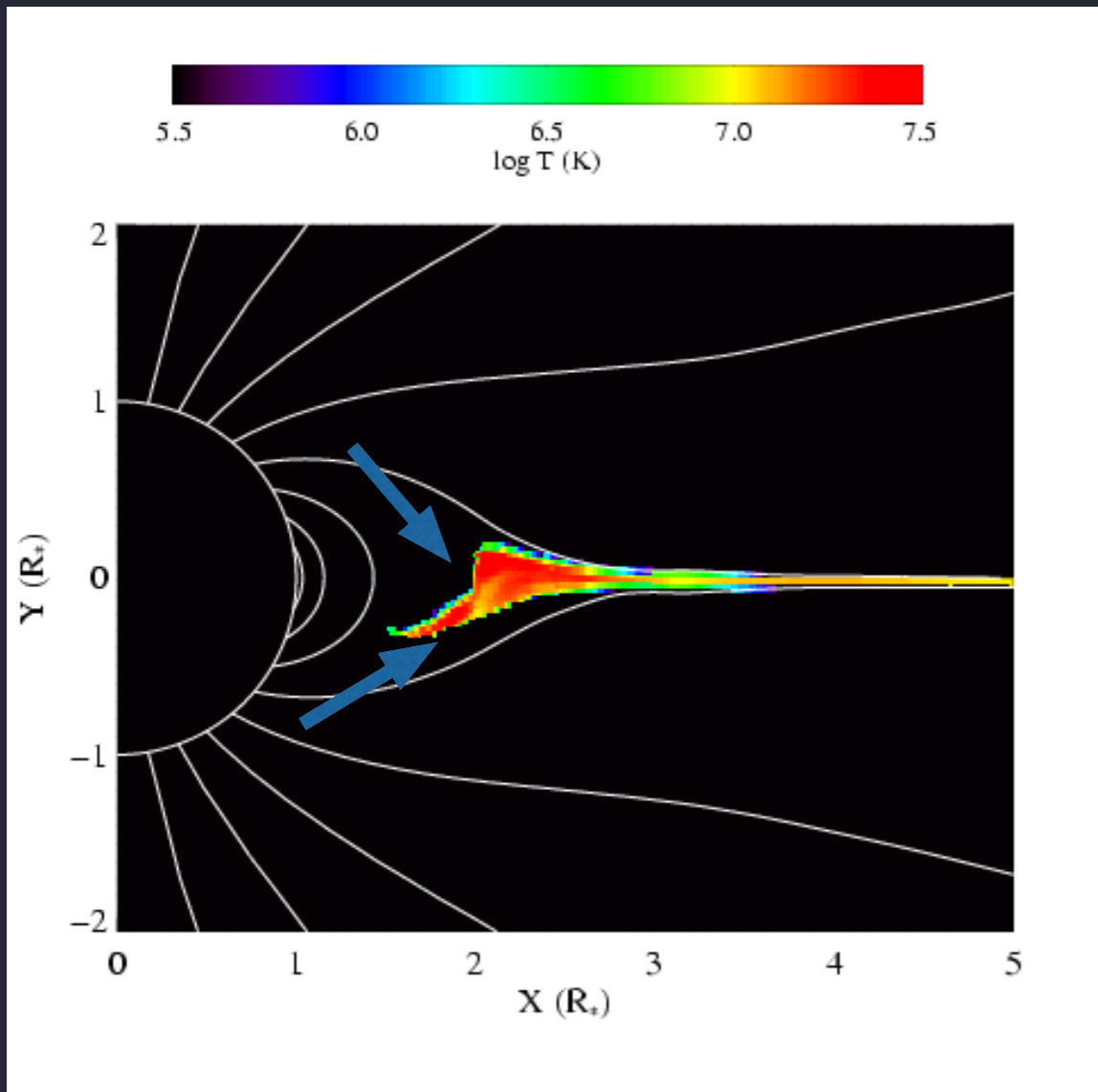
wind flows up magnetic footprints from each hemisphere and collides and is compressed in the magnetic equator



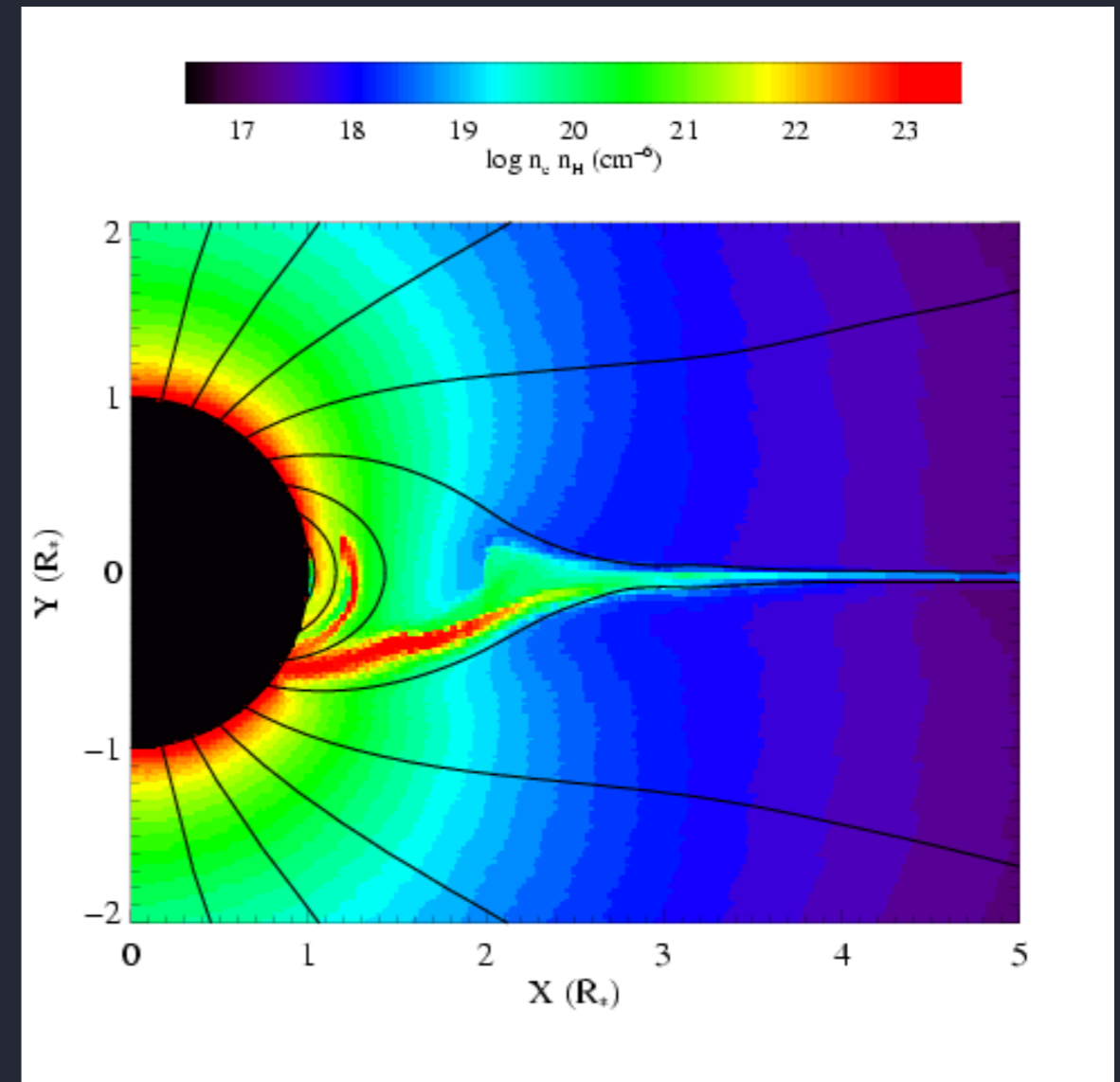
A simulation of the circumstellar matter distribution of σ Ori E, as predicted by the Rigidly Rotating Magnetosphere mode

MHD simulations of θ^1 Ori C: prototype magnetic O star

temperature

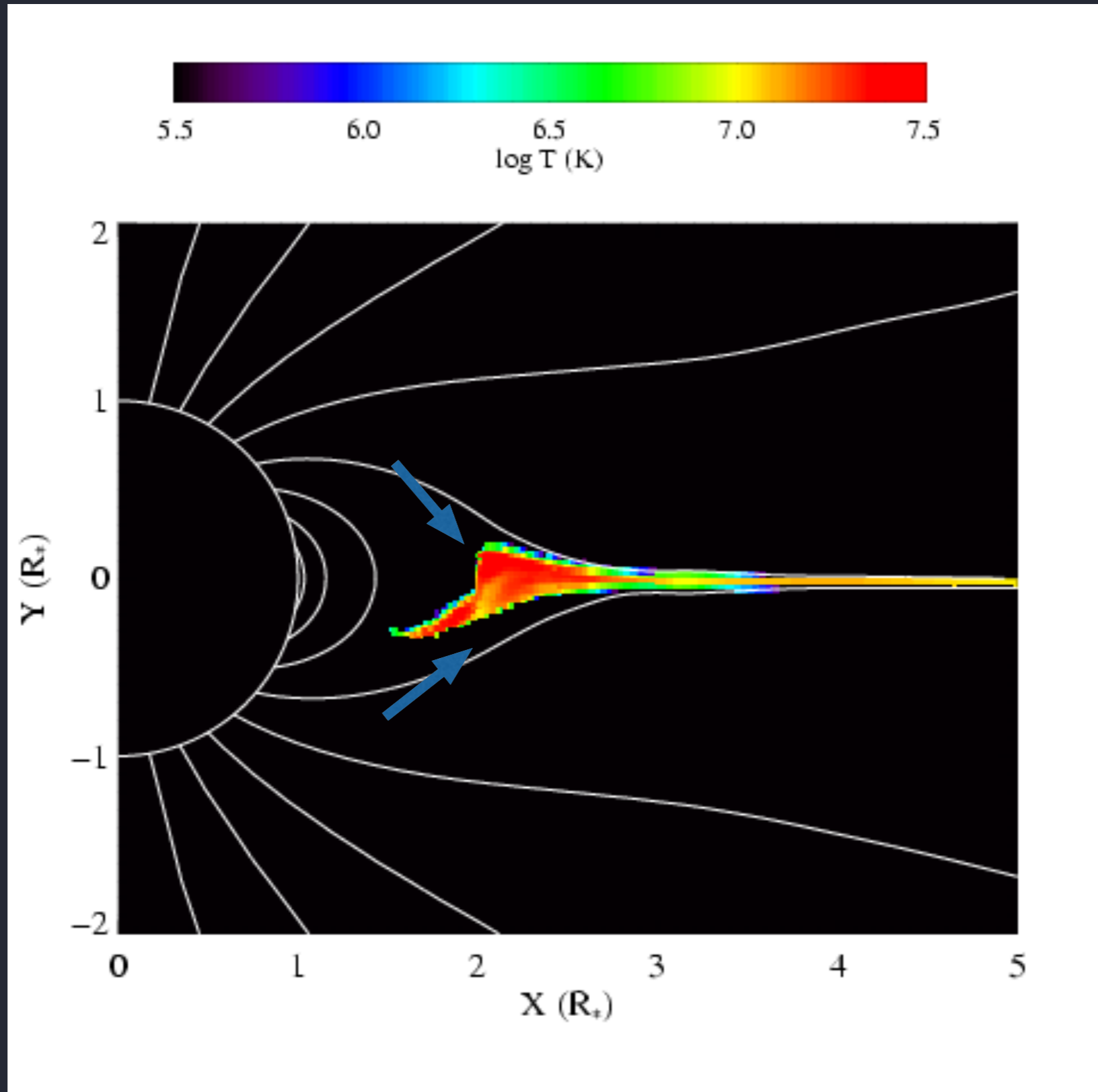


emission measure



simulations by A. ud-Doula; Gagné, Oksala, Cohen, et al. (2005)

opposite-directed flows along field lines collide
nearly head on at the magnetic equator



The line-deshadowing instability (LDI)

causes fast, rarefied wind plasma to slam into slower, denser wind plasma

the resulting shocks heat the plasma

the X-rays we see are the thermal emission from this hot wind plasma

general result from shock theory:

$$T \sim 10^6 (\Delta v_{\text{shock}} / 300 \text{ km/s})^2$$

Magnetically Channeled Wind Shock model

magnetic channeling causes wind flows from **opposite** hemispheres to collide in the magnetic equator

the resulting shocks heat the plasma

the X-rays we see are the thermal emission from this hot wind plasma

general result from shock theory:

$$T \sim 10^6 (\Delta v_{\text{shock}} / 300 \text{ km/s})^2$$

Magnetically Channeled Wind Shock model

magnetic channeling causes wind flows from **opposite** hemispheres to collide in the magnetic equator

the resulting shocks heat the plasma

the X-rays we see are the thermal emission from this hot wind plasma

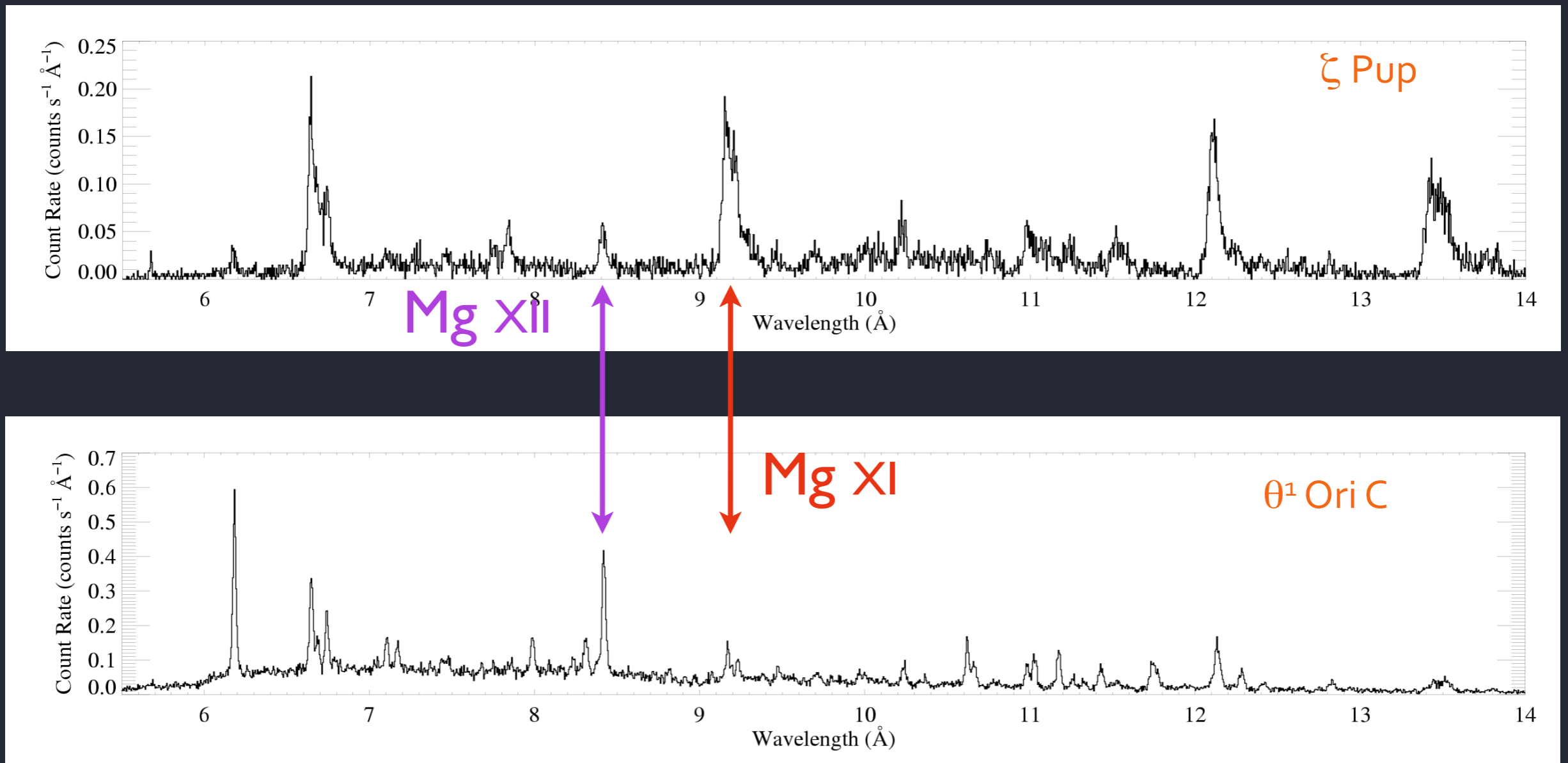
general result from shock theory:

$$T \sim 10^6 (\Delta v_{\text{shock}} / 300 \text{ km/s})^2$$

MCWS shocks have higher shock velocities because the magnetic channeling leads to more head-on collisions

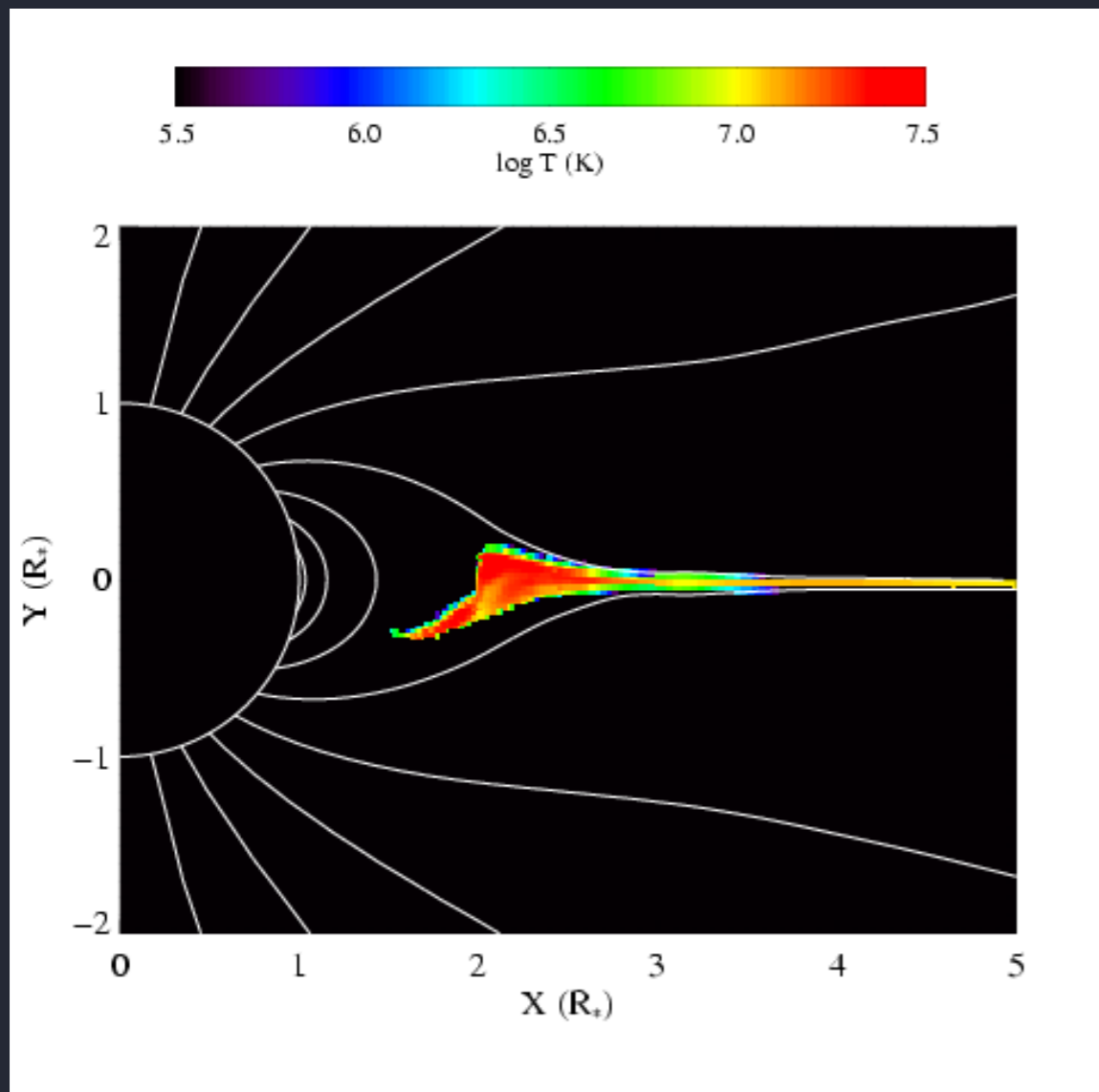
θ^1 Ori C: hotter plasma, narrower lines

Mg XII / Mg XI is proportional to temperature



θ^1 Ori C: prototype magnetic O star

temperature



magnetic channeling : strong shocks = hotter plasma

magnetic confinement : low post-shock velocity = narrower lines

simulations by A. ud-Doula; Gagné et al. (2005)

Conclusions

- Massive star X-ray emission is due to shocks embedded in their winds (LDI mechanism)
- Subset of massive stars with magnetic fields also emit wind-shock X-rays (MCWS mechanism)
- High-resolution X-ray spectroscopy is an excellent tool for studying the wind-shock physics

